

Technische Universität München

Lehrstuhl für Anorganische Chemie

*Rhenium in Biomass Refining – Catalyst
Development and Mechanistic Studies on the
Rhenium Oxide-Catalysed C–O Bond Cleavage of
Lignin Model Compounds*

Reentje Gerhard Harms

Vollständiger Abdruck der von der Fakultät für Chemie der Technischen Universität München zur Erlangung des akademischen Grades eines

Doktors der Naturwissenschaften

genehmigten Dissertation.

Vorsitzender:

Univ.-Prof. Dr. F. E. Kühn

Prüfer der Dissertation:

1. Univ.-Prof. Dr. Dr. h.c. mult. W. A. Herrmann
2. Univ.-Prof. Dr. V. Sieber

Die Dissertation wurde am 15.09.2014 bei der Technischen Universität München eingereicht und durch die Fakultät für Chemie am 13.10.2014 angenommen.

“More men are beaten than fail.”

Henry Ford — 1923

Meinen Eltern, Brüdern und Hilde.

Die vorliegende Arbeit entstand in der Zeit von Januar 2011 bis August 2014 an der Fakultät für Chemie, Lehrstuhl für Anorganische Chemie, der Technischen Universität München

Besonderer Dank gilt meinem verehrten Doktorvater

Herrn Professor Dr. Dr. h.c. mult. Wolfgang A. Herrmann

für die Aufnahme in den Arbeitskreis, das uneingeschränkte Vertrauen und die mir übertragene, große Freiheit zur Forschung, sowie für die Bereitstellung der dafür notwendigen Mittel und Infrastruktur.

Ferner gilt mein ganz herzlicher Dank

Herrn Professor Dr. Fritz E. Kühn

für die interessante Themenstellung, das meiner Arbeit entgegengebrachte uneingeschränkte Vertrauen, für die Betreuung meiner Arbeit und die damit verbundenen wertvollen Gespräche zur Wissenschaft und darüber hinaus, sowie die kontinuierlich positive Unterstützung während des Verfassens von Publikationen – All das hat maßgeblich zum Gelingen dieser Arbeit beigetragen

Acknowledgements

Eine Vielzahl von Personen hat einen Beitrag zu dieser Arbeit geleistet. Dafür möchte ich mich herzlich bedanken. Besonderer Dank gilt:

Herrn Dr. Markus Drees für die quantenmechanischen Berechnungen, die EDV Betreuung und die vielen Gesprächen;

Frau Dr. Gabriele Raudaschl-Sieber für die Leitung und tolle Atmosphäre während des anorganik Praktikums für Geowissenschaftler und ihre Großzügigkeit während der Korrektur und Aufsicht von Klausuren, ihre Authentizität und Integrität;

Herrn Jürgen Kudermann und Frau Maria Weindl für die Aufnahme zahlreicher NMR Spektren, für die fortwährende Unterstützung auch bei ungewöhnlichen Experimenten (verbunden mit so mancher Überstunde), und den vielen schönen Gesprächen und Diskussionen;

Den Damen von der Elementaranalyse Frau Ulrike Ammari und Frau Bircan Dilki für die Analysen und den freundlichen Kontakt;

Herrn Martin Scheller für das zuverlässige Bestellwesen und die angenehme Zeit als Mitbewohner in Singapur;

Den Sekretärinnen Frau Irmgard Grötsch, Frau Ulla Hifinger, Frau Renate Schuhbauer-Gerl und Frau Roswitha Kaufmann für die Übernahme bzw. Hilfestellung bei der Bewältigung lästiger Bürokratie;

Der Abteilung Ver- und Entsorgung, insbesondere Herrn Burghofer, sowie Herrn Wetzel für den guten Kontakt und etliche Leihgaben;

Kostas „dem Griechen“ für die Bereitstellung von Speisen und Kaffee zu später Stunde oder als Alternative bei schlechtem Angebot der Mensa;

Meinen studentischen Mitarbeitern „Knechte“ Alexandra Gerstle, Alex Lundberg, Daphne Cheung (DAAD exchange student), Gergana Nenova und Gregor Harzer sowie meiner studentischen Hilfskraft Leander Zimmermann für deren geleistete Arbeiten unter beachtlichen Einsatz;

Herrn Dr. Magnus Greiwe und Herrn Johannes Ostermann für die Korrektur von Kristallographie und Manuskripten;

Herrn Korbinian Riener, Herrn Andreaser Raba und Frau Olga Razskazovskaya für Korrekturen dieser Arbeit;

Meinen Laborkollegen Herr Mario Bitzer, Frau Claudia Hille, Herr Alex Pfaudler und Herr Dr. Daniel Betz für eine großartige gemeinsame Zeit mit viel Spaß, „supergeil“!

Frau Dr. Lilian Graser danke ich herzlich für die intensive und schöne Zusammenarbeit in Projekten;

Meinen guten Kollegen Herr Christian Münchmeyer, Herr Michael Anthofer, Herr Michael Wilhelm, Herr Dominik Höhne, Herr Robert Reich und Herr Zhong Rui (Dr. Billy Ray) sowie Frau Eva Hahn, Frau Sophie Jürgens, Frau Vesta Kohlmeier und Frau Julia Rieb und allen anderen nicht namentlich genannten wissenschaftlichen Mitarbeitern und Alumni der Arbeitsgruppen Kühn und Herrmann für die gute gemeinsame Zeit und die stete Hilfsbereitschaft;

Ferner möchte ich Herrn Dr. Stefan Reindl, Herrn Dr. Andreas Raba, Herrn Dr. Dominik Jantke, Herrn Dr. Thomas Wagner, Herrn Dr. Lars-Arne Schaper und Herrn Dr. Sebastian Hock für den Zusammenhalt, die Vielzahl an wissenschaftlichen und nicht wissenschaftlichen Diskussionen, gegenseitigen Hilfestellungen, Dienstreisen und Konferenzbesuche, ihr Vertrauen und die gemeinsame Freizeit.

Besonderers Danke ich an dieser Stelle Herrn Dr. Iulius Markovits, Herrn Korbinian Riener und Herrn Johannes Kreuzer für die vielen Korrekturen, Hilfen und Diskussionen, ihre Sportkameradschaft und den damit verbundenen Wettkämpfen, die Start-up Zeit, etlichen Taxi-Fahrten, Feierei und Freizeit.

Außerdem bedanke ich mich bei meinen Freunden außerhalb der Fakultät, mit denen ich eine großartige Zeit in München und Hamburg verbringen durfte, insbesondere Herrn Timm Böttger, die WG Hortensienstraße, Herrn Dr. Johannes Ostermann, Herrn Knut Peetz und Herrn Marco Bast.

Großen Dank und Anerkennung empfinde ich für Olga, welche mich insbesondere durch die schwersten und arbeitsaufwendigsten Zeiten mit viel Verständnis und Nachsicht begleitet.

Besonders herzlich bedanke ich mich an dieser Stelle bei meiner Familie, ohne dessen Rückhalt, Zuversicht und fortwährende Unterstützung die Anfertigung dieser Arbeit so nicht möglich gewesen wäre.

Danke.

Abstract

The manifold and captivating chemistry of organorhenium oxides has a long, more than 30 years lasting history in our work group. Behind the frontiers of the known the still continuing research interest facilitates discovery of novel chemistry.

Being faced with current and proposed ecological challenges of dwindling fossil resources, and, thus, depleting easily exploitable carbon feedstocks, motivates our investigation of sustainable approaches.

This thesis is divided in 7 chapters and devoted to the development of new catalysts for the refining of lignin based biomass which allows sustainable and economical access to renewable carbon feedstocks. In this research work, the catalysts screening, development, and reactivity studies were conducted on model compounds in order to enable comparison with known catalysts and to exclude technical (such as reactor setup, product separation, difficult analytics) and solubility issues.

Chapter 1 provides the reader with the broadened context of depleting fossil resources, the motivation why we use fossil resources, the challenge of increasing demands on petrochemical products, and the great opportunities that arise from application of biomass, particularly lignin within this thesis, as sustainable, renewable, and eco-friendly resource.

Chapter 2 discusses the coordination chemistry and catalytic application of methyltrioxorhenium (MTO), methyldioxorhenium (MDO), and rhenium heptoxide. As premiere, synthetic pathways and the chemistry of MDO is summarised comprehensively. Moreover, the so far underestimated oxygen atom transfer reactions are presented and the interplay of MTO and MDO is highlighted.

Chapter 3 defines the objective and possible approaches of this thesis.

In Chapter 4 the results of this research work are presented and discussed by providing short summaries of the work published during the dissertation. In here, MTO and rhenium heptoxide are presented as efficient catalysts for the cleavage of several lignin model compounds. The found reactivity was investigated and plausible mechanisms have been proposed. Moreover, the single X-ray crystal structure of MTO is discussed.

Chapter 5 summarises this work and provides the reader with a conclusion and outlook.

Bibliographic details and permissions of the publishers for the reuse of published articles within this thesis are contained in Chapter 6.

In Chapter 7 and 8 more details, a curriculum vitae, and an academic report about the author are given.

Table of Contents

Abbreviations.....	XV
1. Broader context of fossil resources and renewable biomass	3
1.1 Global challenges in fossil resource depletion	3
1.2 Biomass as renewable carbon feedstock	4
1.3 Lignin biomass as aromatic hydrocarbon feedstock.....	6
1.4 References in Chapter 1.....	11
2. Rhenium oxides – Reactivity and Catalysis.....	17
2.1 Preface	17
2.2 Methyltrioxorhenium (MTO).....	17
2.2.1 General chemistry.....	17
2.2.2 Reaction Pathways in the Presence of Alcohols	20
2.2.3 Application as oxidation catalyst in lignin refining.....	21
2.3 Methyl dioxorhenium (MDO).....	24
2.3.1 Broader context and importance of MDO	24
2.3.2 Synthesis of MDO	25
2.3.3 Oxygen atom transfer reactions	28
2.4 Excursus – MTO/MDO in refining of biomass derived sugar alcohols	31
2.5 Rhenium heptoxide	34
2.5.1 General and structural chemistry	34
2.5.2 Dissolution properties and coordination chemistry	34
2.5.3 Reactivity towards alcohols.....	36
2.6 References in Chapter 2.....	36
3. Objective.....	45
3.1 Topic of research.....	45
3.2 References in Chapter 3.....	46
4. Results and Discussion – Publication Summaries	53
4.1 Methyl dioxorhenium in the Cleavage of C–O Bonds in Lignin Model Compounds	53
4.2 Rhenium Heptoxide in the Cleavage of C–O Bonds in Lignin Model Compounds	57

4.3 Excursus: Single X-Ray Crystallographic Structure of MTO	60
4.4 References in Chapter 4.....	63
5. Summary and Conclusion	67
6. Bibliographic Details and Reprint Permissions	71
6.1 Bibliographic Details for Complete Publications	71
6.1.1 Organorhenium Dioxides as Oxygen Transfer Systems: Synthesis, Reactivity and Applications	71
6.1.2 Cleavage of C–O Bonds in Lignin Model Compounds Catalyzed by Methylidioxorhenium in Homogeneous Phase	71
6.1.3 Re_2O_7 in C–O bond cleavage of a β -O-4 lignin model linkage: A highly active Lewis acidic catalyst	72
6.2 Permissions for Reuse of Publications.....	73
6.2.1 Wiley Journals	73
6.2.2 Elsevier Journals	79
7. Appendix	85
7.1 Unpublished Manuscripts used within this Thesis	85
8. List of Publications, Talks and Poster Presentations.....	121

Abbreviations

Å	Ångström(s)
Atm	atmosphere = 1.01325 bar
ATR-IR	Attenuated Total Reflectance infra red
BTX	benzene, toluene, and xylene
δ	chemical shift
d	day(s)
DCM	dichloromethane
DHA	dihydroxyacetone
DODH	deoxydehydration
DMSO	dimethyl sulfoxide
Et	ethyl residue
Et ₂ O	diethylether
EtOH	ethanol
eq.	equation
equiv.	equivalents
h	hour(s)
HSQC	Heteronuclear Single Quantum Coherence
ⁱ Pr	<i>is</i> opropyl residue
L	ligand or coordination solvent molecule
M	molar
MDO	methyl dioxorhenium
Me	methyl residue
MeCN	acetonitrile
MHz	megahertz = 1 x 10 ⁶ Hz
min	minute(s)
mL	milliliter
MS	mass spectroscopy
mol%	mole fraction multiplied by factor 100
Mt	million tons
MTO	methyl trioxorhenium
pm	1 picometer = 1 x 10 ⁻¹² m
ppm	parts per million
r.t.	room temperature
^t Bu	<i>tert</i> butyl
THF	tetrahydrofurane
wt%	percentage by weight

*"I'd put my money on the sun and solar energy. What a source of power!
I hope we don't have to wait until oil and coal run out before we tackle
that."*

— **Thomas Edison**, 1931

1. Broader context of fossil resources and renewable biomass

1.1 Global challenges in fossil resource depletion

The exploitation of crude oil and coal during the past two centuries allowed the mankind a historically unique and remarkable advancement in technology, wealth, health and lifetime. Man- and horsepower driven fieldwork and factories became now boosted by efficient machines which consume copious amounts of energy – culled from fossil resources.¹

The constant growth in world population and level of industrialisation is concomitant with an incredibly increasing demand for energy and material sources which is depicted by the crude oil consumption in Figure 1-1.^{2,3} However, humankind's appetite for energy and materials is confronted seriously with dwindling petroleum resources. According to the most recent World Energy Outlooks of the International Energy Agency, only due to the extraction of unconventional oil sources the event of peak oil will be shifted past 2035.^{4,5} So far, the latter is announced by a sevenfold increase (inflation adjusted) in oil price during the last 15 years.⁶

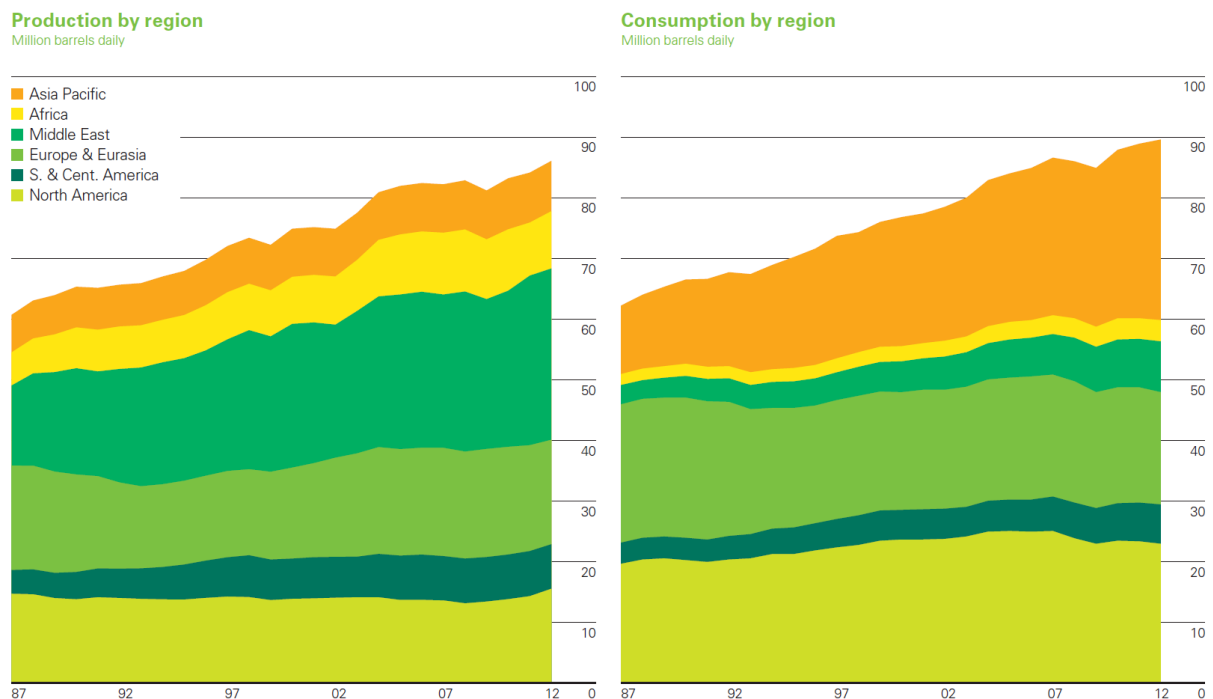


Figure 1-1. World oil production and consumption by region during the past 25 years, adapted from BP statistical review of world energy 2013.³

Hence, the upcoming economic, environmental, and political concerns about such a petroleum-based economy make it imperative to develop new strategies as either reducing

the oil consumption or creating sustainable value-added chains processing renewable resources.^{2,7-11}

1.2 Biomass as renewable carbon feedstock

For ages even before Christi biomass resources in form of wood were used as feasible material and energy sources. However, it was conveniently substituted by the advent of easily winnable fossil resources such as oil, coal, and natural gas since wood biomass bears major drawbacks as low energy density, poor local accessibility due to lack of lucrative natural deposits, and transportation issues (liquids or gas transports easier than stacks of wood).¹ Because of depleting fossil deposits, biomass as sustainable material and energy resource becomes more and more attractive. As renewable biomass is available in almost all parts of the world, its use became a focus of current research efforts of mainly industrial countries with concomitant high oil/energy consumption and expeditious depleting fossil deposits.¹² As perspective, the future energy demands might be complied by alternative power plants e.g. nuclear fusion, geothermal energy, solar and wind energy (hypothesising that efficient energy storage devices will have been developed).

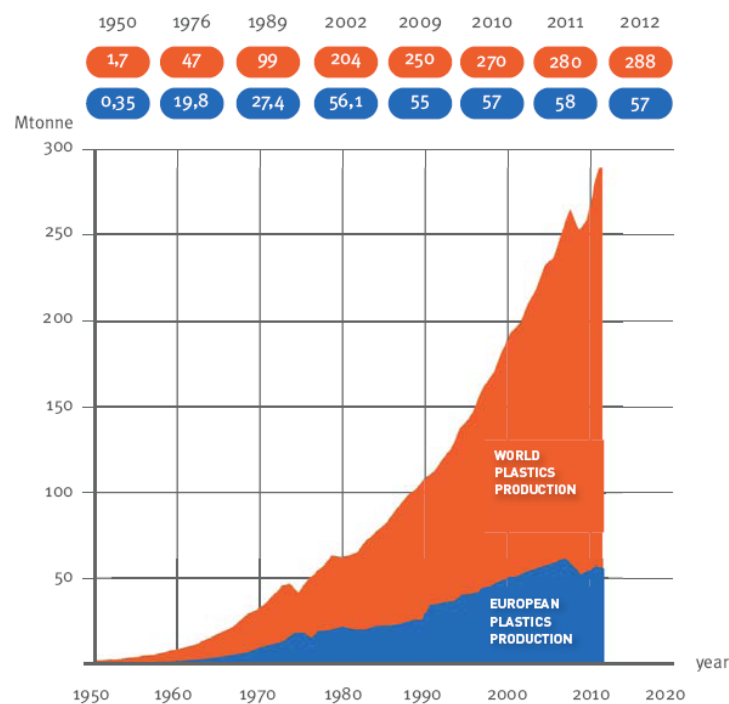


Figure 1-2. World plastic production from 1950–2012, adopted from *Plastics – the Facts 2013* by PlasticEuropes.¹³ Although the European production stagnates since early 2000s, the world production grows continuously for more than 50 years. Moreover, the volume produced is strongly related to the world's economy, as it can be read from the peaks and retracements.

Currently, worldwide 20% of the generated electricity is constituted by regenerative sources. Although more than 90% of the 7 billion tons annual extracted fossil carbon is “burned” for energy uses, the chemical industry requires as well impressive amounts for e.g. plastic production.¹⁴ As depicted in Figure 1-2 the world plastic production grows continuously and reached a volume of 288 million tons in 2012.¹³ We are living in the still young era of plastics, and many recent innovations were driven by the development of new polymeric materials. They allowed us a remarkable increase in wealth and lifestyle – just imagine your life without any. Hence, an abstinence of latter seems to be absolutely impossible emphasising the exigency for alternative non–crude oil based carbon resources, which might be provided by exhaust stream captured and liquefied carbon dioxide, methane, or biomass.^{2,8,15-17} Methane, predominantly as hydrate, presents the most abundant carbon source on earth, nevertheless, selective processing methods to value added hydrocarbons are in an early stage and the oxidation to methanol (precursor material for the MTO process) is difficult due to the thermodynamically favoured “over” oxidation to CO₂.¹⁸ Recently, Shell PLC started up the world largest gas-to-liquid Fischer–Tropsch plant refining methane to higher hydrocarbons;¹⁹ however, the extraction of methane hydrates is confronted with very high global environmental risks.^{20,21}

Direct recycling carbon dioxide would eliminate future carbon feedstock issues, but is rendered by the inefficient and thermodynamically highly disfavoured reduction of the CO₂ carbon atom. Serendipitously, this effort has already been done by nature in the process of photosynthesis, the biggest solar panel on earth; thus bio-renewables are considered as more reasonable carbon-feedstock. Although photosynthesis is inefficient with regards to photon energy to plant energy (sugars) conversion, the stunning amount of 107 billion tons of dried biomass grows annually ashore. Renewable biomass is easily available from agricultural crop residues which vast amount of 7 billion tons was estimated by Schöne *et al.*²² *Nota bene*, the entire area under cultivation does not produce sufficient amounts of biomass to satisfy the world’s energy demands! It probably allows solely substitution of fossil carbon feedstocks for the production of bulk chemicals.

Biomass is consisted mainly of cellulose, hemicellulose, and lignin which represents in total 94% of the entire biomass. The relative composition is depicted in Figure 1-3. The main components are found in cell walls and thus there are grouped as lignocellulose matter.^{7,11,23,24} Only marginal amounts of biomass are used as comestible good such as starch, proteins, sucrose, and plant oils.

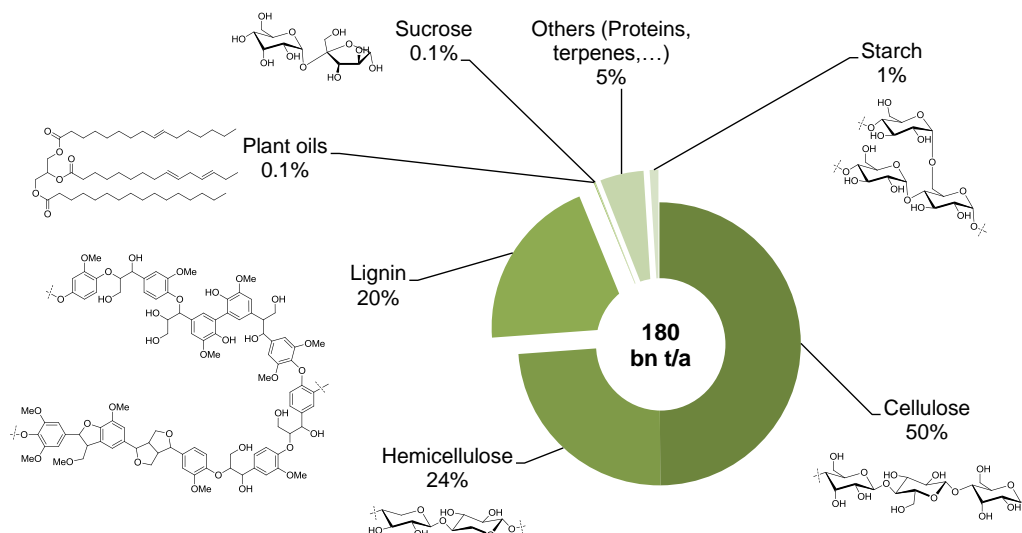


Figure 1-3. Composition of global (shore plus ashore) biomass per year.²⁴ 94% of all biomass consists of lignocellulose which is the largest material by volume produced in the world every year.^{7,24}

1.3 Lignin biomass as aromatic hydrocarbon feedstock

The manufacture and application of bio-based chemicals and polymers gains soaring ecological, economical and political significance. The actual amount produced per year was estimated by the International Energy Agency (IEA) to 50 million tons.²⁵

Although many routes have been developed for the refining of carbohydrate-derived feedstocks such as cellulose, starch, and sucrose, processing of lignin based biomass towards bulk chemicals is still in its early beginnings. However, lignin biomass represents tremendous opportunities to produce chemicals.^{7,10,11,25,26} For example, the food flavour and additive vanillin is synthesised from sulphite processed wood pulp.

Zakzeski *et al.* reviewed in 2010 catalytic refining processes of different lignins providing also an overview of the impressive variety of products which can be obtained. As depicted in Figure 1-4 the scope of potential products is grouped by either the processing type *exempli gratia* such as syngas products or oxidised products, or by the product compound type such as hydrocarbons and phenols. Lignosulphonate is the most abundant (commercially) lignin type (resource) and is available as waste product from paper mills. Yet, lignosulphonate is basically applied as fluxing agent for concrete, and industrial relevant bulk chemical products are rendered to DMSO and vanillin.

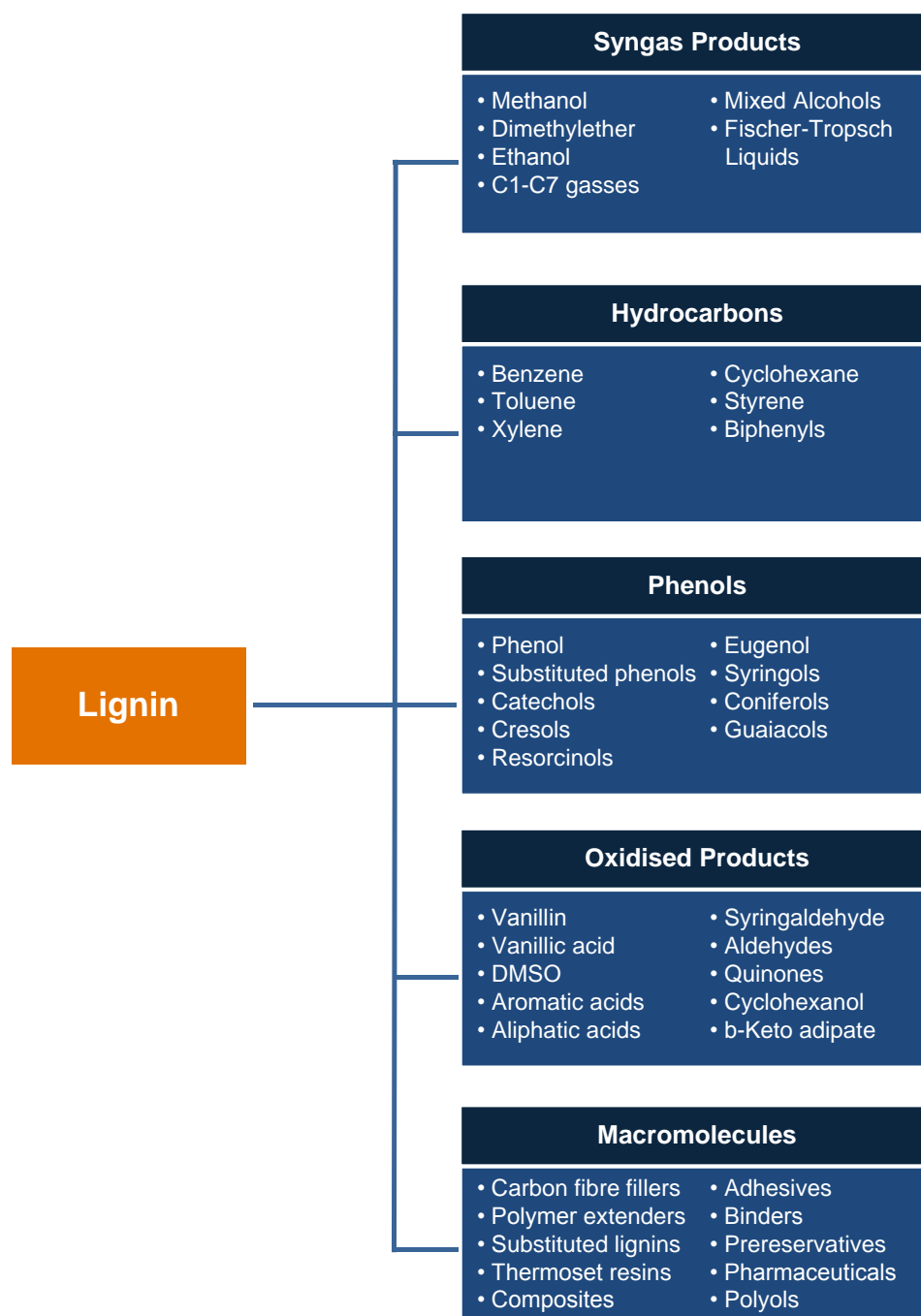


Figure 1-4. Potential products from Lignin categorised by its chemical class or applied the production route.

Since lignin represents next to naphtha the very only economical valuable feedstock for the production of bulk aromatic compounds such as BTX aromatics (benzene, toluene, xylene) and phenols, the development of new processes and efficient catalytic transformations needs to be in focus of future research efforts.

The global production of BTX aromatics is enormous and was published to amount 102.5 million metric tons (xylene 42.5 Mt, benzene 40.2 Mt, and toluene 19.8 Mt) in 2010 by the Global Chemical Outlook report of the United Nations Environment Programme.²⁷

Moreover, a continuing growth in global demand is proposed by several market research institutes.^{28,29}

In nature, lignin is found as three dimensional, amorphous, and polymeric framework stabilising the plant cell walls as depicted in Figure 1-5. In there, lignin is clinging the lignocellulosic matrix by filling the space between cellulose and hemicellulose together. Cross-linking to the carbohydrate strings (depicted as blue and green) warrants the rigidity and strength to the cell wall.

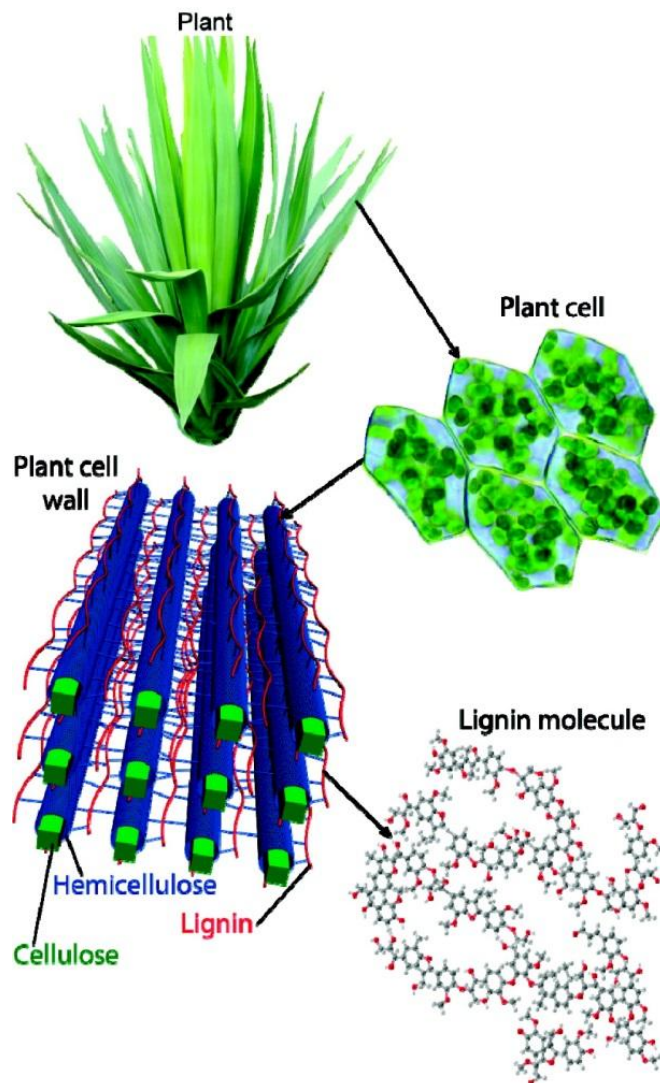


Figure 1-5. Schematic chart of the structure, function, and origin of lignin in plants. Adapted from a review article by Weckhuysen and co-workers.²⁶ The lignin fills the space between the cellulose/hemicelluloses strings and donates stability and rigidity to the cell wall.

Biosynthesis of the lignin polymer occurs exclusively from three very similar monomeric phenols, the monolignols *p*-coumaryl, coniferyl, and sinapyl alcohol (see Figure 1-6, A) which are synthesised in the cell cytosol by modification of phenylalanine. When transported

though the cell wall, oxidative enzymes such as laccase and peroxidase initiate a radical polymerisation. Since the phenol radical initiated polymerisation and the monomer feed is not controlled, always a heterogeneous structure is obtained. However, a limited chemical control is provided due to the involvement of enzymes as “dirigent” proteins and the relative amounts of monomer type produced by the cell. The composition, construct, and molecular weight strongly differs from plant to plant and also depends from environmental influences. The exact mechanism is still unknown and acutely discussed by the scientific community.³⁰⁻³⁴

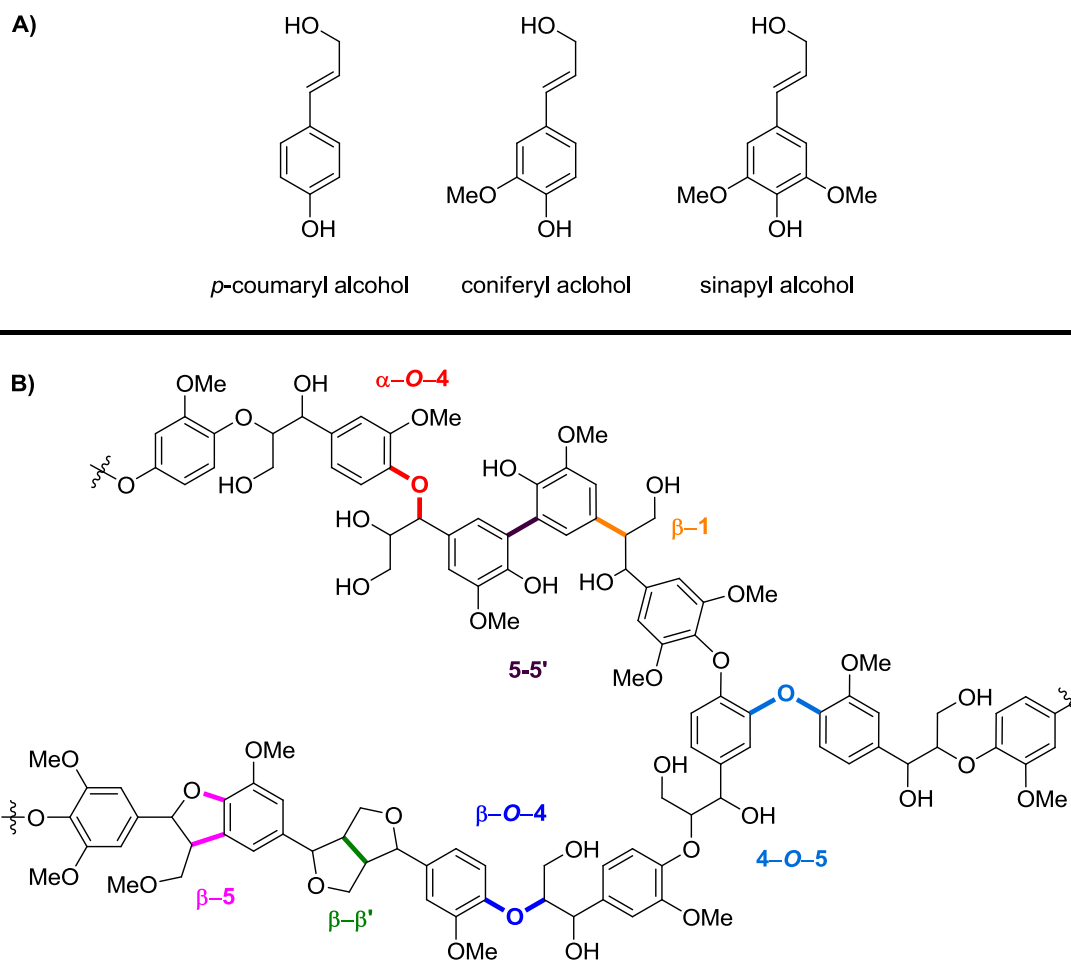


Figure 1-6. (A) The three lignin monomers (monolignols) are generated in the cell cytosol by chemical modification of glycosylated phenylalanine. Its radical polymerisation in the cell walls results in lignin. (B) Schematic structure of unmodified lignin including most natural occurring chemical linkages. Various linkage types are highlighted by different colours. Please note, the structure does not represent the natural abundance.^{26,35}

The polymeric structure of lignin is described by its contained chemical linkages between the aromatic building blocks, which schematic structure is depicted in Figure 1-6, B. The structure does not imply a particular sequence and is mere pictorial. The monolignols are connected by a β -O-4, β - β' , α -O-4, β -1, 4-O-5, and β -5 structural motifs as indicated by colour. The β -O-4 linkage is found as the dominant one in all plants, consisting of more than half of the linkages in hardwood.

The structure of the lignin polymer is influenced by the amount of contained methoxy groups. An increased content of coniferyl and sinapyl alcohol, and thus additional methoxy groups, prevent the formation of 5–5' and 4–O–5 linkages in the lignin polymer which results in a more linear structure as found in hardwood. Softwood, for example, is rather constituted by high amounts of coniferyl alcohol; hence a branched polymer is formed.²⁶

The systematic description of the linkages allows chemical discrimination of different lignin sources. In Table 1-1 the proportion of major linkages found in hardwood and softwood lignin are summarised.^{26,35}

Table 1-1. Approximate abundance of major linkage units found in softwood and hardwood lignin; adapted from Pandey and Weckhuysen.^{26,35}

Linkage type	Content in softwood (spruce) [%]	Content in hardwood (birch) [%]
β -O-4-aryl ether	45–50	60
α -O-4-aryl ether	6–8	6–8
4-O-5-diaryl ether	3.5–7	6.5
β -5-phenylcoumaran	9–12	6
5-5'-biphenyl	9.5–27	4.5–9
β -1-(1,2-diarylpropane)	7–9	7
β - β' -(resinol)	2–6	3
others	7–13	5

The chemical modification of lignin and most important its degradation by vast linkage bond cleavages is usually monitored by alteration of the ratio and total amount of contained linkage groups.³⁶⁻³⁹ For example, Zakzeski and Weckhuysen applied *in situ* ATR-IR spectroscopy to monitor the dissolution of organosolv lignin and product formation during the high-pressure water phase reforming process. Chan *et al.* and Galkin *et al.* revealed the extinction of β -O-4, β - β' , and β -5' (phenylcoumaran) by means of two-dimensional HSQC NMR spectroscopy.^{40,41}

In the course of investigating highly efficient and selective catalysts lignin is not used as substrate due to its complexness and structural variability, instead simple model compounds were used for the development of catalysts based on V,⁴¹⁻⁴⁴ Re,⁴⁵⁻⁴⁷ Fe,⁴⁸ Ru,⁴⁹⁻⁵¹ Ni,⁵²⁻⁵⁴ Pd,^{40,55,56} and sulphuric acid.^{57,58} Ordinary model compounds bear only a single linkage type between to aromatic building blocks, and additional methoxy and hydroxyl groups may be embellished as found in native lignin. The high substrate solubility, facile analytics during and after reaction, and the absence of additional disturbing functional groups and linkages are the main benefits of using simple models.

The application of model compounds allows the efficient investigation of suitable catalysts and optimal reaction conditions. Moreover, favourable catalytic systems are studied at model polymers whose monomers are connected by a single linkage. In Figure 1-7 commonly used β -O-4 linkage model compounds (dimers and polymers)^{49,56,59} are depicted; a comprehensive overview of all known model compounds can be found in a review article written by Zakzeski *et al.*²⁶ In this work compounds **1** and **10** were applied for all experiments, whereas 2-(2-methoxyphenoxy)phenylethanol (**1**) poses as “standard” substrate.

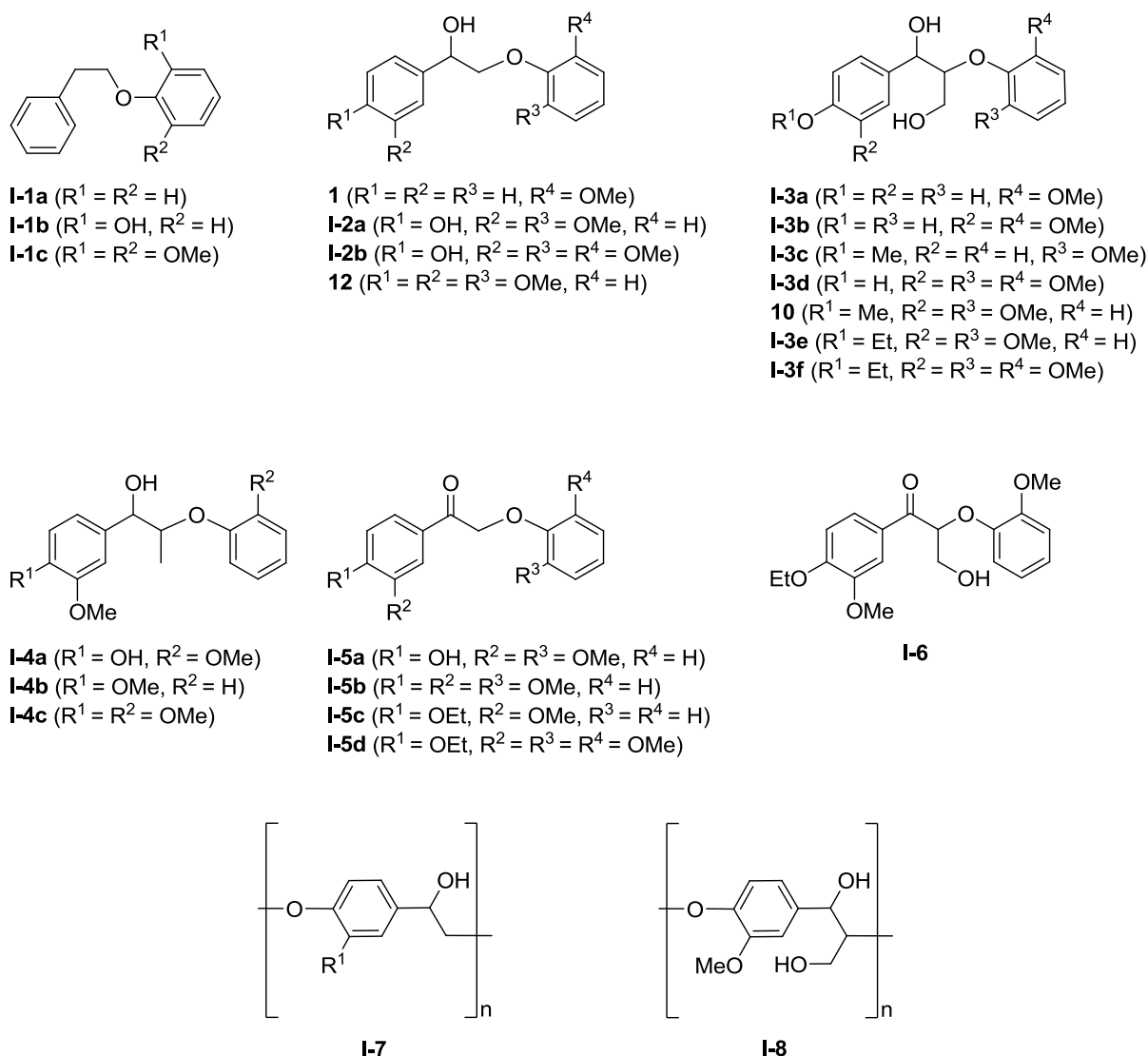


Figure 1-7. Dimeric and polymeric lignin model compounds commonly used in catalysis studies to mimic β -O-4 linkages contained in native lignin.^{26,49,56,59}

1.4 References in Chapter 1

1. P. O'Connor, in *The Role of Catalysis for the Sustainable Production of Bio-fuels and Bio-chemicals*, eds. K. S. Triantafyllidis, A. A. Lappas and M. Stöcker, Elsevier, Amsterdam, 2013, pp. 1-25.

2. C. K. James M. Tour, Vicki L. Colvin, *Nat. Mater.*, 2010, **9**, 871-874.
3. BP, *BP Statistical Review of World Energy June 2013*, 2013.
4. International Energy Agency, *World Energy Outlook 2013*, OECD, 2013.
5. International Energy Agency, *World Energy Outlook 2012*, OECD, 2012.
6. U.S. Energy Information Administration, monthly average Brent spot prices of 2004/Jan to 2014/Jan, conversion to February 2013 dollars uses US CPI for All Urban Consumers (CPI-U).
7. S. R. Collinson and W. Thielemans, *Coord. Chem. Rev.*, 2010, **254**, 1854-1870.
8. D. R. Dodds and R. A. Gross, *Science*, 2007, **318**, 1250-1251.
9. E. L. Kunkes, D. A. Simonetti, R. M. West, J. C. Serrano-Ruiz, C. A. Gärtner and J. A. Dumesic, *Science*, 2008, **322**, 417.
10. J. N. Chheda, G. W. Huber and J. A. Dumesic, *Angew. Chem.*, 2007, **119**, 7298-7318; *Angew. Chem. Int. Ed.*, 2007, **46**, 7164-7183.
11. I. T. Horváth and P. T. Anastas, *Chem. Rev.*, 2007, **107**, 2169-2173.
12. D. J. M. Hayes, in *The Role of Catalysis for the Sustainable Production of Bio-fuels and Bio-chemicals*, eds. K. S. Triantafyllidis, A. A. Lappas and M. Stöcker, Elsevier, Amsterdam, 2013, pp. 27-65.
13. PlasticsEurope, *Plastics - the Facts 2013*, 2013.
14. S. Kabasci, in *Bio-Based Plastics*, John Wiley & Sons Ltd, 2013, pp. 1-7.
15. H. Z. Tushar P. Vispute, Aimaro Sanna, Rui Xiao, George W. Huber, *Science*, 2010, **330**.
16. J. O. Metzger, *ChemCatChem*, 2013, **5**, 680-682.
17. S. Kabasci and C. Stevens, *Bio-Based Plastics: Materials and Applications*, Wiley, 2013.
18. G. A. Olah, A. Goeppert and G. K. S. Prakash, *Beyond Oil and Gas: The Methanol Economy*, Wiley, 2011.
19. Shell, Pearl GTL - an overview, <http://www.shell.com/global/aboutshell/major-projects-2/pearl/overview.html>, Accessed 28.04.2014.
20. J. Bohannon, *Science*, 2008, **319**, 1753.
21. C. Berndt, T. Feseker, T. Treude, S. Krastel, V. Liebetrau, H. Niemann, V. J. Bertics, I. Dumke, K. Dünnebier, B. Ferré, C. Graves, F. Gross, K. Hissmann, V. Hühnerbach, S. Krause, K. Lieser, J. Schauer and L. Steinle, *Science*, 2014, **343**, 284-287.
22. H. Schöne and M. R. gen. Klaas, *Chem. Ing. Tech.*, 2009, **81**, 901-908.
23. L. da Costa Sousa, S. P. S. Chundaway, V. Balan and B. E. Dale, *Curr. Opin. Biotechnol.*, 2009, **20**, 339.
24. M. Behrens and A. K. Datye, eds., *Catalysis for the Conversion of Biomass and Its Derivatives*, epubli, Berlin, 2013.

25. E. d. Jong, A. Higson, P. Walsh and M. Wellisch, Bioenergy Task 42, *Bio-based Chemicals, Value Added Products from Biorefineries*, International Energy Agency, 2012.
26. J. Zakzeski, P. C. A. Bruijninx, A. L. Jongerius and B. M. Weckhuysen, *Chem. Rev.*, 2010, **110**, 3552-3599.
27. R. Massey and M. Jacobs, Global Chemicals Outlook 2013, *Chapter I: Trends and Indicators*, United Nations Environment Programme, 2013.
28. Nexant, The Future Of Benzene And Para-Xylene After Unprecedented Growth In 2010,
<http://www.chemsystems.com/about/cs/news/items/PPE%20PCMD%20Aromatics%202011.cfm>, Accessed 01.05.2014.
29. L. Wood, Research and Markets: Xylenes Global Supply Dynamics to 2020 - Middle East and China Witnessing Huge Growth in Production,
<http://www.reuters.com/article/2011/01/13/idUS40276+13-Jan-2011+BW20110113>, Accessed 01.05.2014.
30. W. Boerjan, J. Ralph and M. Baucher, *Annual Review of Plant Biology*, 2003, **54**, 519-546.
31. F. S. Chakar and A. J. Ragauskas, *Ind. Crop. Prod.*, 2004, **20**, 131-141.
32. L. B. Davin and N. G. Lewis, *Curr. Opin. Biotechnol.*, 2005, **16**, 407-415.
33. J. Ralph, K. Lundquist, G. Brunow, F. Lu, H. Kim, P. Schatz, J. Marita, R. Hatfield, S. Ralph, J. Christensen and W. Boerjan, *Phytochem. Rev.*, 2004, **3**, 29-60.
34. A. Samuels, K. Rensing, C. Douglas, S. Mansfield, D. Dharmawardhana and B. Ellis, *Planta*, 2002, **216**, 72-82.
35. M. P. Pandey and C. S. Kim, *Chem. Eng. Technol.*, 2011, **34**, 29-41.
36. C. G. Boeriu, D. Bravo, R. J. A. Gosselink and J. E. G. van Dam, *Ind. Crop. Prod.*, 2004, **20**, 205-218.
37. Z. Xue-Fei and L. Jing, *Hem. Ind.*, 2012, **66**, 685-692.
38. J. Zakzeski, P. C. A. Bruijninx and B. M. Weckhuysen, *Green Chem.*, 2011, **13**, 671-680.
39. J. Zakzeski and B. M. Weckhuysen, *ChemSusChem*, 2011, **4**, 369-378.
40. M. V. Galkin, S. Sawadjoon, V. Rohde, M. Dawange and J. S. M. Samec, *ChemCatChem*, 2014, **6**, 179-184.
41. J. M. W. Chan, S. Bauer, H. Sorek, S. Sreekumar, K. Wang and F. D. Toste, *ACS Catal.*, 2013, **3**, 1369-1377.
42. S. K. Hanson, R. Wu and L. A. P. Silks, *Angew. Chem.*, 2012, **124**, 3332-3332; *Angew. Chem. Int. Ed.*, 2012, **51**, 3410-3413.

43. B. Sedai, C. Díaz-Urrutia, R. T. Baker, R. Wu, L. A. P. Silks and S. K. Hanson, *ACS Catal.*, 2011, **1**, 794-804.
44. S. Son and F. D. Toste, *Angew. Chem.*, 2010, **122**, 3879-3882; *Angew. Chem. Int. Ed.*, 2010, **49**, 3791-3794.
45. C. Crestini, M. C. Caponi, D. S. Argyropoulos and R. Saladino, *Biorg. Med. Chem.*, 2006, **14**, 5292-5302.
46. C. Crestini, P. Pro, V. Neri and R. Saladino, *Biorg. Med. Chem.*, 2005, **13**, 2569-2578.
47. R. G. Harms, I. I. E. Markovits, M. Drees, W. A. Herrmann, M. Cokoja and F. E. Kühn, *ChemSusChem*, 2014, **7**, 429-434.
48. Y. Ren, M. Yan, J. Wang, Z. C. Zhang and K. Yao, *Angew. Chem.*, 2013, **125**, 12906-12910; *Angew. Chem. Int. Ed.*, 2013, **52**, 12674-12678.
49. J. M. Nichols, L. M. Bishop, R. G. Bergman and J. A. Ellman, *J. Am. Chem. Soc.*, 2010, **132**, 12554-12555.
50. T. vom Stein, T. Weigand, C. Merckens, J. Klankermayer and W. Leitner, *ChemCatChem*, 2013, **5**, 439-441.
51. A. Wu, B. O. Patrick, E. Chung and B. R. James, *Dalton Trans.*, 2012, **41**, 11093-11106.
52. A. G. Sergeev and J. F. Hartwig, *Science*, 2011, **332**, 439-443.
53. A. G. Sergeev, J. D. Webb and J. F. Hartwig, *J. Am. Chem. Soc.*, 2012, **134**, 20226-20229.
54. M. R. Sturgeon, M. H. O'Brien, P. N. Ciesielski, R. Katahira, J. S. Kruger, S. C. Chmely, J. Hamlin, K. Lawrence, G. B. Hunsinger, T. D. Foust, R. M. Baldwin, M. J. Bidy and G. T. Beckham, *Green Chem.*, 2014, **16**, 824-835.
55. X. Zhou, J. Mitra and T. B. Rauchfuss, *ChemSusChem*, 2014, **7**, 1623–1626.
56. T. H. Parsell, B. C. Owen, I. Klein, T. M. Jarrell, C. L. Marcum, L. J. Hauptert, L. M. Amundson, H. I. Kenttamaa, F. Ribeiro, J. T. Miller and M. M. Abu-Omar, *Chem. Sci.*, 2013, **4**, 806-813.
57. M. R. Sturgeon, S. Kim, K. Lawrence, R. S. Paton, S. C. Chmely, M. Nimlos, T. D. Foust and G. T. Beckham, *ACS Sus. Chem. Eng.*, 2014, **2**, 472-485.
58. K. Lundquist and R. Lundgren, *Acta Chem. Scand.*, 1972, **26**, 2005-2023.
59. T. Kishimoto, Y. Uraki and M. Ubukata, *Org. Biomol. Chem.*, 2006, **4**, 1343-1347.

“New catalysts, new enzymes, new processing systems, and new plant hybrids may all be part of the future solutions to the use of biobased building blocks that will be built on the Green Chemistry research starting to be engaged today.”

— Paul T. Anastas, 2007

2. Rhenium oxides – Reactivity and Catalysis

2.1 Preface

Rhenium oxides exhibit a rich chemistry in their oxidation states Re(V), Re(VI), and Re(VII). Especially some organorhenium oxides exhibit diverse coordination chemistry,¹ and are well known for their high catalytic activity in many reactions.² Out of all, methyltrioxorhenium (MTO) – a comparatively small and stable 14 VE organometallic compound – emerges outstanding in homogeneous catalysis, as in olefin metathesis,³ aldehyde olefination,^{4,5} and versatile oxidation catalysis.⁶⁻⁹

In this chapter, the reactivity and catalytic application of MTO, methyldioxorhenium (MDO) and rhenium heptoxide is presented. Remarkably, MTO is the only rhenium compound which was applied in the field of lignin refining.^{10,11} Moreover, biomass derived (poly)alcohols were also upgraded by latter rhenium oxides. MTO and rhenium heptoxide are known to catalyse efficiently the dehydration of secondary alcohols,¹²⁻¹⁴ and MDO is known deoxydehydrate (DODH, removal of O + H₂O) vicinal diols in homogeneous phase.^{15,16}

2.2 Methyltrioxorhenium (MTO)

2.2.1 General chemistry

MTO was serendipitously isolated in microscale amounts by Beattie and Jones in 1979 due to a slow, inadvertent, air oxidation of tetramethylrhenium(VI) oxide Me₄ReO.^{1,2}

Decades later MTO emerged as one of the best examined organometallic compounds. The transition was facilitated by the development of a straight-forward synthetic route, based on the reaction of rhenium heptoxide and methyl stannanes, which was reported by Herrmann and co-workers in 1988.³ Because MTO is conveniently purified by sublimation, stable under aerobic atmosphere, and a highly active and selective catalyst for olefin metathesis and oxidation chemistry,^{3,17} it has become very attractive for a broad community of chemists, which devoted much research efforts to demonstrate its full chemical and catalytic potential.^{1,2,6,18}

Due to the high oxidation state at the transition metal centre, MTO behaves strongly Lewis acidic. Furthermore, the ligand sphere donates 14 valence electrons to rhenium(VII), thus MTO is an electron deficient coordination compound. As consequence the coordination chemistry is decisively determined by its aspiration to reach a stable 18 electron configuration.¹⁹ In presence of Lewis bases such as electron donating *N*-compounds MTO readily forms Lewis acid/base adducts in the type of CH₃ReO₃ · L or CH₃ReO₃ · L₂ (L =

electron pair donor) in trigonal bipyramidal and octahedral molecular geometry, respectively (Figure 2-1).

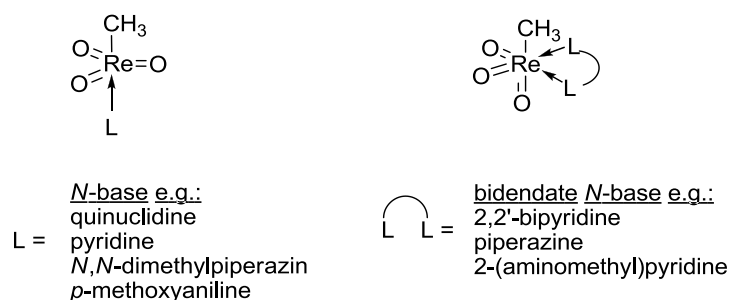


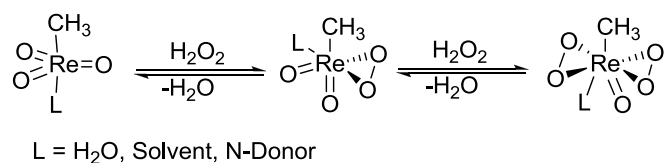
Figure 2-1. Lewis base adducts of MTO and *N*-donor compounds. Assembled from Ramão *et al.*¹ In coordinating solvents L is in equilibrium with the solvent.

Many octahedral Lewis base adducts are very stable and isolable, in particular when L_2 is a bidentate ligand, however, the adducts are more sensitive towards hydrolysis in undried solvents and thermal treatment than MTO itself due to an weakening of the Re–C bond. In ^1H and ^{13}C NMR spectroscopic experiments the signal of the methyl group is shifted upfield compared to MTO. This effect is referred to the electron donor capability of the bidentate *N*-bases and correlates with the pK_a value; higher values result in an increased electron donation. An analogue behaviour of MTO is observed in alcoholic solution; the more stable the coordination, the higher the relative NMR upfield shift. Although alcohols bear higher pK_a values than *N*-compounds such as 2,2'-bipyridine and pyridine, they are weaker ligands, thus no MTO alcohol adducts have ever been isolated. The latter antagonism is probably explained by the spectrochemical series discovered by Tsuchida *et al.* which reveals alcohols being comparable but weaker ligands than water ($\text{H}_2\text{O} > \text{CH}_3\text{OH} > \text{CH}_3\text{CH}_2\text{OH}$).²⁰ Known examples of *S*- and *O*-coordination are very rare and limited to either intramolecular coordination or to formation of condensates the type of $\text{CH}_3\text{ReO}[(\eta^1\text{-X})_2\text{L}]$ ($\text{X} = \text{S}, \text{O}$).^{1,2}

MTO's chemistry is well known for oxygen atom transfer reactions and is applied as oxidation catalyst. Its catalytic activity in oxidation of olefins to epoxides using hydrogen peroxide as oxygen source is unparalleled so far.^{2,6,7,9}

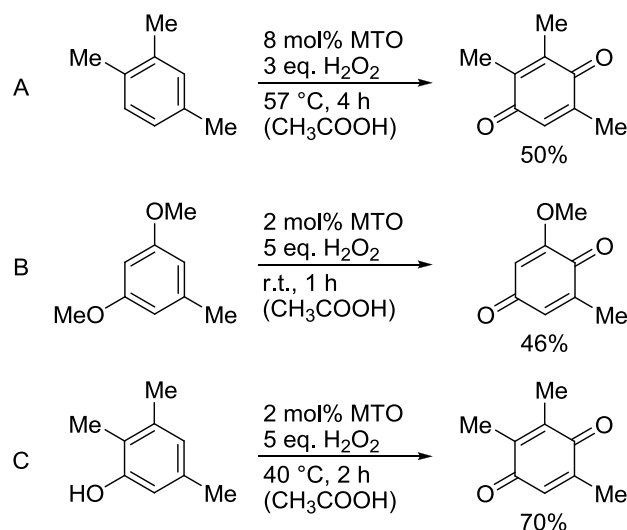
In a standard catalytic reaction the olefin oxidation is started by addition of MTO to a cooled emulsion (vigorously stirring of a two-phasic system) of neat substrate and a aqueous solution of hydrogen peroxide. However, the reaction may also be conducted in organic solvents such as DCM or MeCN. In order to suppress the acid-catalysed hydrolysis of product oxiranes to vicinal *trans*-diols, frequently an *N*-donor base is added to reduce MTO's high Lewis acidity.^{21,22}

Because of the remarkable high activity and simple experimental setup and reaction conditions the olefin oxidation emerged to the very most investigated and best understood reaction of MTO. As the initial mechanistic step, a distorted octahedral monooxomethylrhenium peroxo complex is formed in the presence of hydrogen peroxide as oxygen donor (see Scheme 2-1).



Scheme 2-1. Oxidation of MTO forms first a methylrhenium monoperoxo species, and subsequently the methylrhenium bisperoxo species (butterfly complex) using perhydrol as oxygen source.^{17,23,24}

If the oxidation is conducted in an excess of oxidation agent, formation of a monooxomethylrhenium bisperoxo butterfly complex is observed due to a subsequent second oxidation step. The butterfly complex is stable in presence of excess perhydrol and a preparative isolation is possible at a low temperature. Both, the mono- and bisperoxo species are capable and involved in oxygen transfer reaction accompanied with reformation of MTO.^{17,23,24} Beside the rather prominent olefin epoxidation, MTO is also able to catalyse various oxidation reactions such as the Baeyer-Villiger- and the Dakin oxidation,²⁵⁻²⁷ oxidation of alcohols,²⁸ alkynes,²⁷ anilines,²⁹ amines,^{30,31} sulphuric compounds,³² C–H and Si–H bond oxidation,³³⁻³⁵ and also oxidation of aromatic rings which is depicted in Scheme 2-2.^{9,36,37}

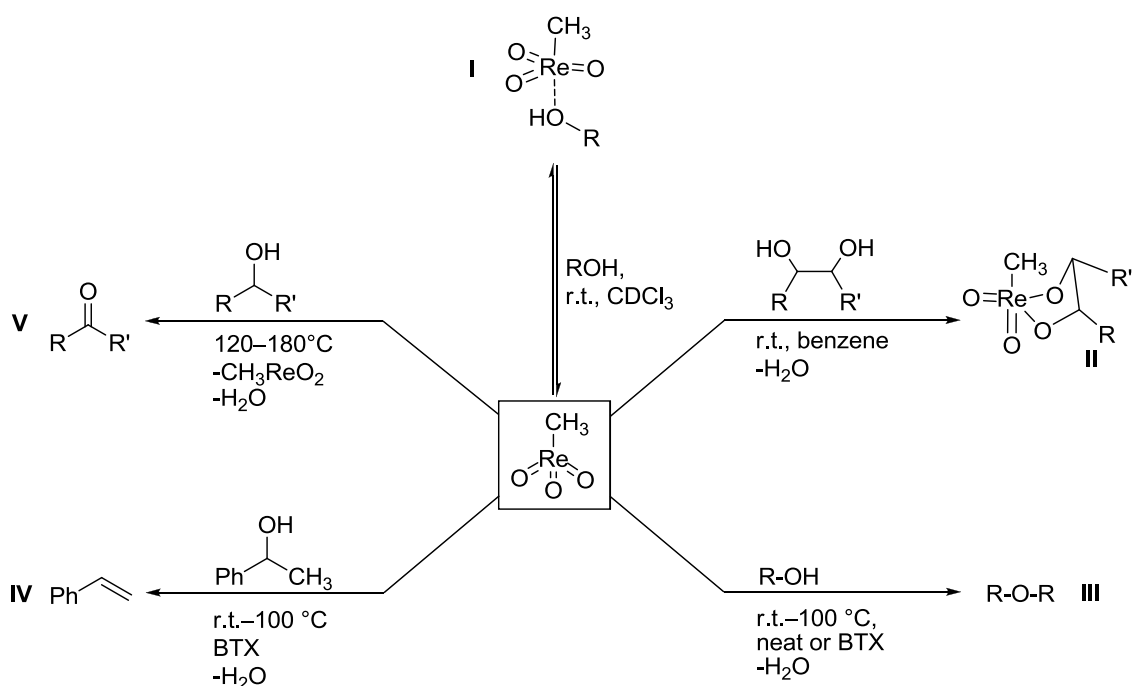


Scheme 2-2. The MTO-catalysed oxidation of xylenes, anisoles, and phenols under mild conditions yields in 1,4-benzoquinones.³⁷

A variety of aromatic hydrocarbons such as xylenes, anisoles, and phenols are oxidised to 1,4-benzoquinones using excess hydrogen peroxide in acetic acid at mild reaction conditions.³⁷ As expected, the more electron rich the aromatic system, the easier the oxidation proceeds. In presence of adjacent methoxy substituents which exert a positive mesomeric effect the reaction finishes within one hour even at room temperature (see Scheme 2-2, B). In the case of aryl-alkyl ether bonds partial C–O degradation takes place to generate the quinoid system.³⁸ If cresols are used as substrate, oxidation of the phenol OH-group results in benzoquinone formation in good yields (see Scheme 2-2, C).³⁹

2.2.2 Reaction Pathways in the Presence of Alcohols

Depending on the reaction conditions, MTO exhibits different chemical behaviour towards alcohols as depicted in Scheme 2-3. Thus, MTO coordinates alcohols weakly,⁴⁰ catalyses its etherification and dehydration,⁴¹ and oxidises alcohols.²⁸



Scheme 2-3. Possible reaction pathways of MTO subjected to alcohols depending on the applied reaction parameters and alcohol type.^{14,15,23,41-43}

The coordination of an alcohol to rhenium is indicated by a yellow colour which forms when alcohol is added to a benzene solution of MTO (path I).⁴¹ In NMR spectroscopy, the ROH–Re coordination becomes visible by shifting the ¹⁷O signal,⁴³ however, formation of a stable coordination compound is not known (*vide infra*). Noteworthy, treatment of MTO with glycols results in condensation to stable MTO-diolates (path II).^{41,42} In alcoholic solutions (neat or in

BTX), catalytic formation of ethers is observed (path **III**). Using an asymmetric mixture of aliphatic and benzylic alcohols improves the etherification efficiency. In case when the alcohol contains a saturated β -carbon atom, dehydration to olefins is the preferred pathway (path **IV**). Since CH_3^+ -group rearrangement occurs when the β -carbon atom is quaternary, an ionic dehydration mechanism is most probably.⁴⁴

Benzylic alcohols react more easily and give dehydration products in higher yields. At elevated temperatures of 100 °C efficient MTO-catalysed (applying 1 mol%) dehydration of benzylic alcohols is observed, with symmetric ethers as side product.¹⁴ Further elevation of the reaction temperature will not increase the reaction rate, but results in alcohol oxidation/MTO reduction (path **V**, see also chapter 2.3 for detailed information).¹⁵

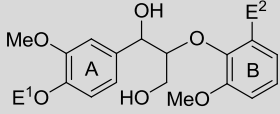
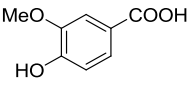
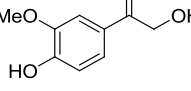
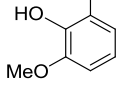
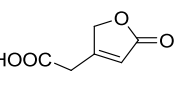
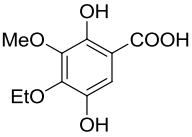
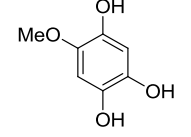
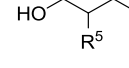
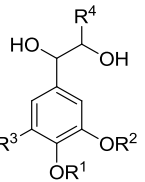
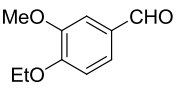
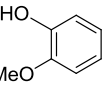
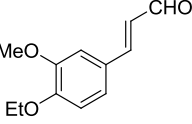
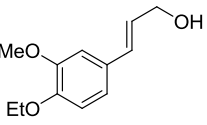
2.2.3 Application as oxidation catalyst in lignin refining

In 2005 the research groups of Crestini and Saladino reported the first example of a rhenium catalyst degrading lignin model compounds and hydrolysis/organosolvent lignin.^{10,45-47}

Treatment of simple dimeric model compounds e.g. β -O-4 ether (**I-3d**, **I-3e**, and **I-3f**) with substoichiometric amounts of MTO (20 mol%) in presence of excess hydrogen peroxide in acetic acidic media at room temperature yields in degradation to mixture of numerous monomeric units as depicted in Table 2-1. The composition of the obtained product mixture depends strongly on the used substrate type and whether it is equipped with phenolic or methoxy groups. Moreover, small structural alterations were found to provoke huge changes in the product pattern.¹³ Oxidative cleavage of phenolic hardwood model compound **I-3d** yields in derivatives of benzoic acid **I-9**, ketol **I-10**, and lactone **I-12** derived from the aromatic "A-ring", and syringol (**I-11**) originating from the aromatic "B-ring" (see Table 2-1, Entry 1). A relative low cumulative product yield of 26% (based on the mass balance given by the reactivity $A \rightarrow B+C$) is the major drawback.

If the non-phenolic hardwood model compound **I-3f** is used instead, the selectivity drops drastically (see Entry 2). As it can be read from the substitution pattern the products are primarily derived from the "A-ring" and are subjected to miscellaneous advanced levels of oxidation. The "B-ring" apparently undergoes severe decomposition since only small amounts of initial aromatic systems were isolated, and the low overall mass-balance of 43% found renders the usability.

Table 2-1. Oxidative MTO-catalysed cleavage of various β -O-4 hardwood and softwood lignin model compounds, yields are given in brackets.⁴⁸

				20 mol% MTO 1.5 eq. H ₂ O ₂ r.t., 24 h (CH ₃ COOH)		oxidative cleavage products	
Entry	Model compound/ type	E ¹	E ²	Isolated products (yield %)			
1	phenolic hardwood I-3d	H	OMe	 I-9 (16%)	 I-10 (15%)	 I-11 (12%)	 I-12 (9%)
2	hardwood I-3f	Et	OMe	 I-13 (5%)	 I-14 (6%)	 I-15 R ⁵ = CH=CHCOOH (3%) I-16 R ⁵ = CH ₂ CH ₂ COOEt (4%)	 I-17 R ¹ = Et, R ² = Me, R ³ = H, R ⁴ = CH ₂ OH (6%) I-18 R ¹ = R ² = R ³ = H, R ⁴ = CH ₂ OH (2%) I-19 R ¹ = R ⁴ = H, R ² = Me, R ³ = OH (4%) I-20 R ¹ = R ² = R ³ = H, R ⁴ = (=O) (2%)
3	softwood I-3e	Et	H	 I-21 (3%)	 3 (24%)	 I-22 (6%)	 I-23 (7%)

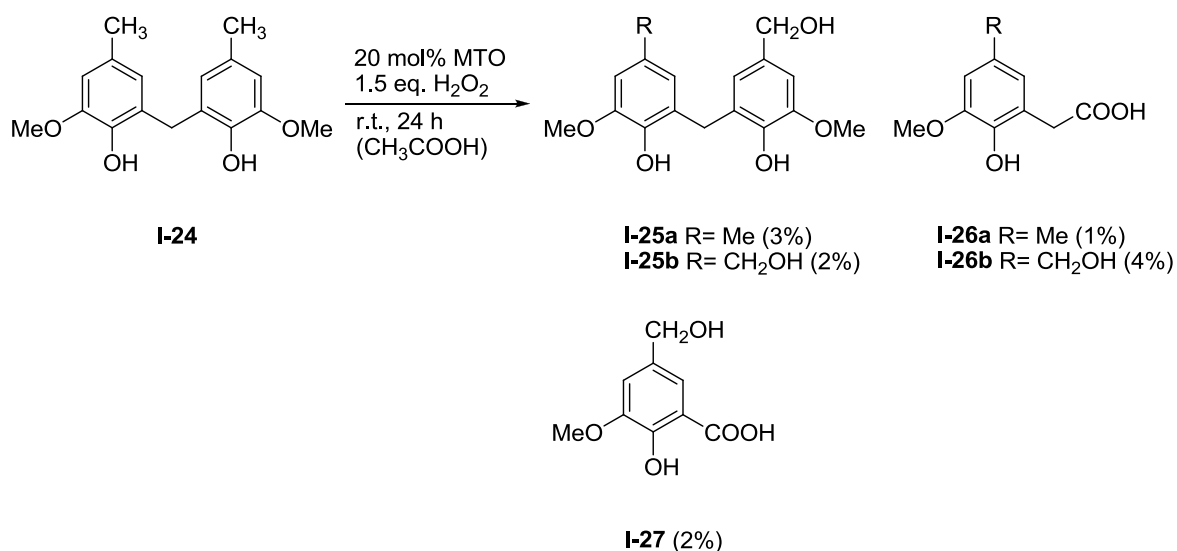
If a softwood model compound containing less aryl methoxy groups is subjected to oxidation the selectivity increases significantly and formation of four main products is observed (see Entry 3). Notably, the cleavage products are similar to the monolignols observed in nature, and the aldehydic derivatives and guaiacol present the main fragments. The unanticipated increase in selectivity indicates an alternative reaction pathway. Thus, the cleavage probably occurs not due to oxidation, but to acidolysis. Subsequent oxidative modification of the cleavage products yields then the observed products. The conducted reaction conditions are very acidic because glacial acetic acid was used as the reaction medium and the strong Lewis acid “catalyst” MTO is added in a rather high loading of 0.2 equivalents. It has been mentioned that the acidic cleavage of similar β -O-4 model compounds was reported previously.⁴⁹⁻⁵¹ Hardwood seems to be stable under those acidic conditions (as read by product distribution and constitution) also emphasizing an oxidative cleavage pathway.

Oxidative treatment of simple aryl alkyl ethers such as derivatives of vanillyl alcohol results in formation of umpteen oxidation products. In particular, oxidation of the alcoholic groups but

not of the desired cleavage of aryl alkyl ethers occurs. Moreover, abolishment of the aromaticity yields derivatives of unsaturated lactones and 1,4-benzoquinones.

On the other hand, the oxidative cleavage of very stable 5-5' linkages is possible as depicted in Scheme 2-4. This linkage type and structural motif is present in Kraft processed lignin highlighting the industrial potential of the MTO-catalysed oxidative lignin refining.⁵²

Reaction of the methylene bridged diphenol **I-24** gives the monomers as aromatic, carbonic acids. Therefore, the cleavage proceeds at the expense of one aromatic ring and not of the methylene bridge. As a drawback, non-phenolic 5-5' model compounds are stable under the applied reaction conditions, resulting exclusively in alkyl side chain oxidation. The contrary reaction outcome points out the oxidation of phenol-OH groups essentially and thus the abolishment of the aromaticity. A protective group such as a methyl ether is satisfactory sufficient to inhibit the cleavage.



Scheme 2-4. Oxidative MTO-catalysed cleavage of the phenolic 5-5' diphenylmethylene linked Kraft lignin model compound **I-24**.⁴⁸

2.3 Methyldioxorhenium (MDO)

This chapter mainly originates from the following publication:

Reentje G. Harms, Wolfgang A. Herrmann, Fritz E. Kühn, “Organorhenium Dioxides – Promising Oxygen Transfer Systems in Biomass Conversion: Synthesis, Reactivity and Applications”, *Manuscript in preparation*
(refer to 6.1.1)

2.3.1 Broader context and importance of MDO

It has been shown that methyldioxorhenium is the key compound for many “MTO”-catalysed transformation. Once generated *in situ* by reductive MTO deoxygenation MDO catalyses the formation of olefins via deoxydehydration of diols and deoxygenation of epoxides,^{23,40,53,54} olefination of aldehydes and ketones,^{7,8,55,56} hydrogenation,^{54,57} and hydrosilylation.⁵⁸

In the context of sustainable chemical feedstocks, MTO/MDO has proven to be an efficient deoxygenation catalyst for the refining of lignocellulosic biomass such as carbohydrates and polyols in homogeneous phase.^{13,15,59,60} So far, the wide substrate scope under mild reaction conditions is unequalled by other catalysts. Although the reactivity of Re(V) compounds has already been studied since the late 1980s, possible applications in catalysis particularly in biomass conversion have only been investigated very recently.

The progress of organorhenium dioxide chemistry over the last 25 years is illustrated by the number of corresponding publications and their cumulative impact factor is presented in Figure 2-2.

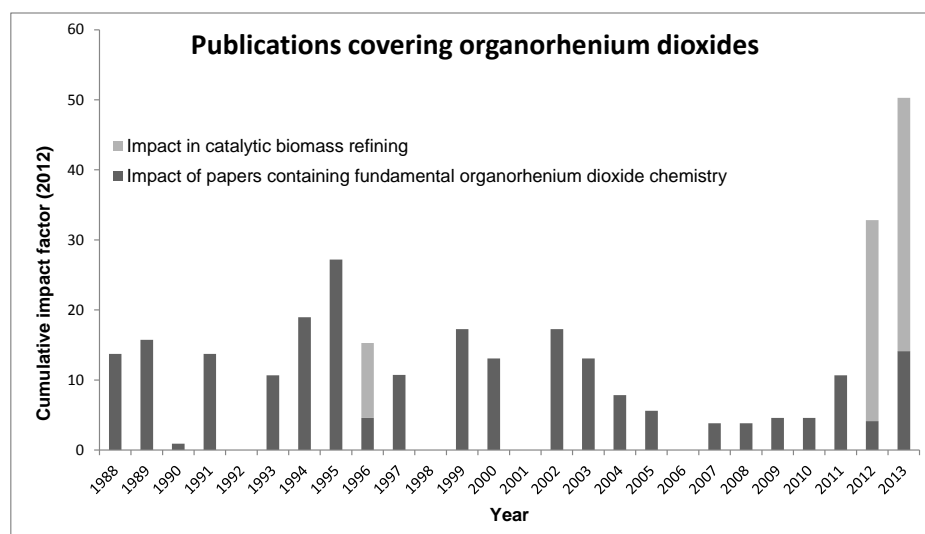
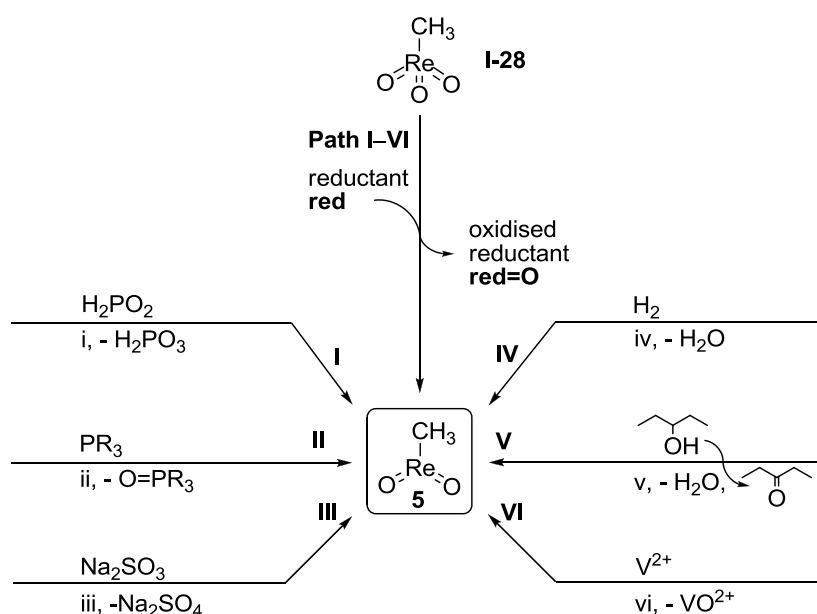


Figure 2-2. Development of the impact of publications containing organorhenium dioxide chemistry as indicated by dark grey bars. Impact of papers discussing an application in biomass refining is indicated by pale grey bars.

2.3.2 Synthesis of MDO

MDO covers only a very narrow field of the manifold organorhenium chemistry. Hence, all known synthetic procedures are not well developed and are entirely based on reduction steps, and thus on the oxygen atom abstraction of MTO. Other low oxidation state methyl rhenium precursor complexes have not sustained due to their instability.^{1,2}

Typically, MDO is generated *in situ* from MTO, and at present, six synthetic routes are known (Figure 2-5). Organic phosphines and phosphonic oxides have emerged as easily accomplishable and efficient reagents for *in situ* MTO deoxygenation. Espenson *et al.* have developed a procedure treating MTO with hypophosphorous acid in aqueous solution at room temperature (path I, Scheme 2-5). To prevent polymerisation of MTO to rhenium bronzes (layer-structure of corner-sharing $\text{ReO}_5(\text{CH}_3)$ octahedra and intercalated water) a strong acidic condition of $\text{pH} = 0$ is necessary.⁶¹⁻⁶³ Moreover, application of triaryl- or trialkylphosphines allow the synthesis in organic solvents as benzene at room temperature (path II).⁵³ The clean formation of MDO can be achieved by the use of immobilised triphenylphosphine, which allows an easy removal of the phosphine oxide waste by-product by filtration.^{64,65} In a similar manner sodium sulphite generates MDO by oxygen abstraction in aprotic solvents (see path III), however, the observed conversion is rather low.^{66,67}



Scheme 2-5. *In situ* formation of MDO by oxygen abstraction of MTO. Reaction conditions: i) r.t., aqueous sol., 0.1-0.7 M hypophosphorous acid, 1.0 M trifluoromethanesulfonic acid;⁶¹ ii) r.t., benzene, 1 equiv. triaryl or trialkyl phosphine;⁵³ iii) 150 °C, benzene, 1.5 equiv. Na_2SO_3 ;^{66,67} iv) 150 °C, THF, 20.4 atm H_2 ,⁵⁴ or 80 °C, toluene, 24 h, 8 atm H_2 ;⁵⁷ v) 155 °C, CHCl_3 or neat in alcohol, 5 equiv. 3-pentanol;^{15,16} vi) r.t., aqueous sol., 12–160 equiv. V^{2+} , $\text{pH} = 0$.⁶¹

More benign MDO generation is achieved by hydrogenation as depicted in path **IV**.⁵⁴ Treatment with moderate hydrogen pressures up to 20 atm at elevated temperatures (150 °C) generates MDO with water as the only side product. Furthermore, the groups of Bergman and Toste reported that transfer hydration of secondary alcohols at elevated temperatures also yields in MDO, water, and ketone (see path **V**).^{15,16} *Nota bene*, the use of low oxidation state transition metals such as V^{2+} as oxygen abstraction agent in aqueous solutions was also reported (see path **VI**).⁶¹

Once MDO has formed it tends to dimerization and oligomerisation to stabilise its 12 VE electron deficiency, which can be monitored by colour change in absorption UV/Vis spectroscopy. During that process, the colourless molecular MDO becomes yellow upon dimerisation, and further oligomerisation leads to an intense blue colour.^{68,69} With growing chain lengths the oligomer becomes insoluble and precipitates as a black solid. Details on colour and absorption maximum for each form are given in Figure 2-3.

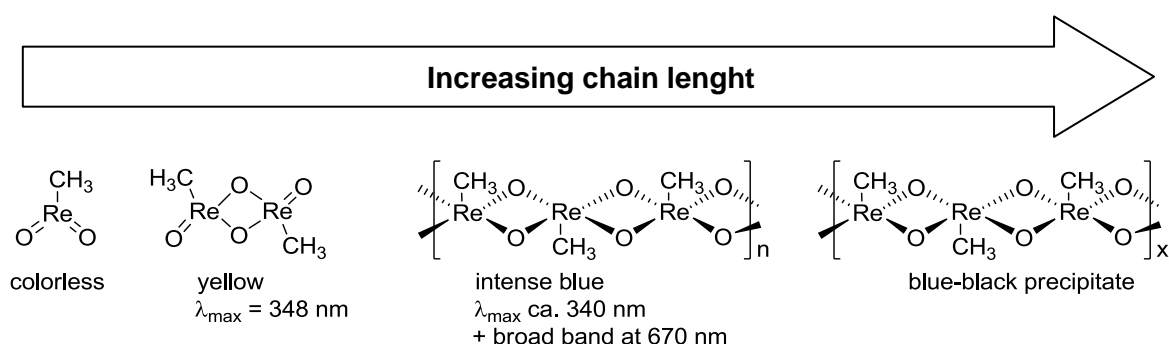
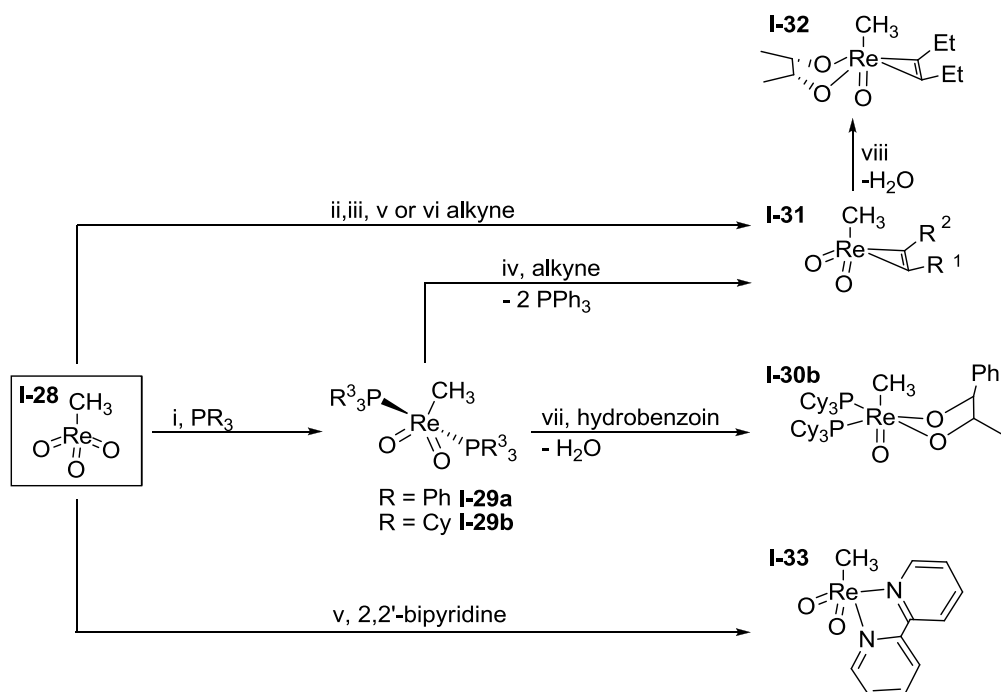


Figure 2-3. Dimerisation and oligomerisation of MDO. Although MDO is colourless and not visible, the oligomerisation can be monitored by change of colour over yellow to intense blue, and by absorption UV/Vis spectroscopy. While smaller oligomers ($n = 3\text{--}30$) are soluble in aqueous solution, long polymers ($x > 30$) are insoluble and precipitate.^{68,69}

To prevent MDO from oligomerisation the monomer complex needs to be stabilised by auxiliary ligands (see Scheme 2-6). Thus, synthetic strategies using phosphine and alkyne ligands were developed by the groups of Herrmann and Espenson.^{64,65,69,70} Reduction of MTO with an excess of organophosphines PR_3 ($R = \text{Ph}, \text{Cy}$) in aprotic solvents results in formation of MDO phosphine adducts **I-29** which bear two *trans*-aligned phosphine ligands in trigonal bipyramidal geometry.⁴⁰ PPh_3 is coordinated weakly to MDO, since liberation of free PPh_3 is observed in solution; however, for PCy_3 not. Recently, the single X-ray crystal structure of **I-29a** and **I-29b** were published by Liu *et al.*, but they differ from those previously reported by Roesky *et al.*,⁷⁰ who crystallised MDO as the dinuclear and mixed valent complex $\text{CH}_3\text{ReO}_2(\text{PR}_3)_2 \cdot \text{MTO}$ ($R = \text{Ph}, \text{Cy}$) where the oxogroup of MDO coordinates to MTO's

rhenium centre.⁷⁰ This example suggests that by reduction MTO's Lewis acidic characteristics became such Lewis basic. Those contradicting results are possibly explained due to an alteration of the original synthetic procedure – Liu *et al.* used 6 equivalents of phosphine, whereas Roesky *et al.* used only 2 equivalents.



Scheme 2-6. Stabilisation of MDO by auxiliary ligands. Published reaction conditions: i) r.t., Et₂O, 24 h;^{40,70} ii) r.t., toluene, 16 h, 1.1 equiv. polymer supported PPh₃;^{64,65} iii) 155 °C, CHCl₃, 5 h 5 equiv. 3-pentanol;¹⁵ iv) r.t., toluene, 24 h;^{54, 61} v) r.t., MeCN, H₃PO₂;⁶¹ vi) 80 °C, toluene, 24 h, 8 atm H₂;⁵⁷ vii) r.t., CDCl₃ + molecular sieve;⁴⁰ viii) r.t., benzene, R¹ = R² = CH₃CH₂, *meso*-2,3-butylenglycol.¹⁵

In analogy to MTO's chemistry treatment of **I-29** with glycols yields CH₃ReO-diolates accompanied with condensation of water. The rhenium-diolate complex may be chaperoned and stabilised by the phosphines used in excess for MDO generation. Using (*r,r*)-(+)-hydrobenzoin and MDO·(PCy)₂ (**I-29b**), formation of deep blue coloured diolate complex **I-30b** was observed in an *in situ* experiment.⁴⁰

In contrast, when an excess of alkyne is used complete ligand exchange to CH₃ReO₂(R¹C≡CR²) **I-31** is observed.⁷⁰ The capability of stronger coordination is also shown by **I-31**'s stability under aerobic atmosphere. Thus, easy preparative synthetic routes from MTO, PPh₃ and alkyne were developed by Herrmann and co-workers.^{64,65}

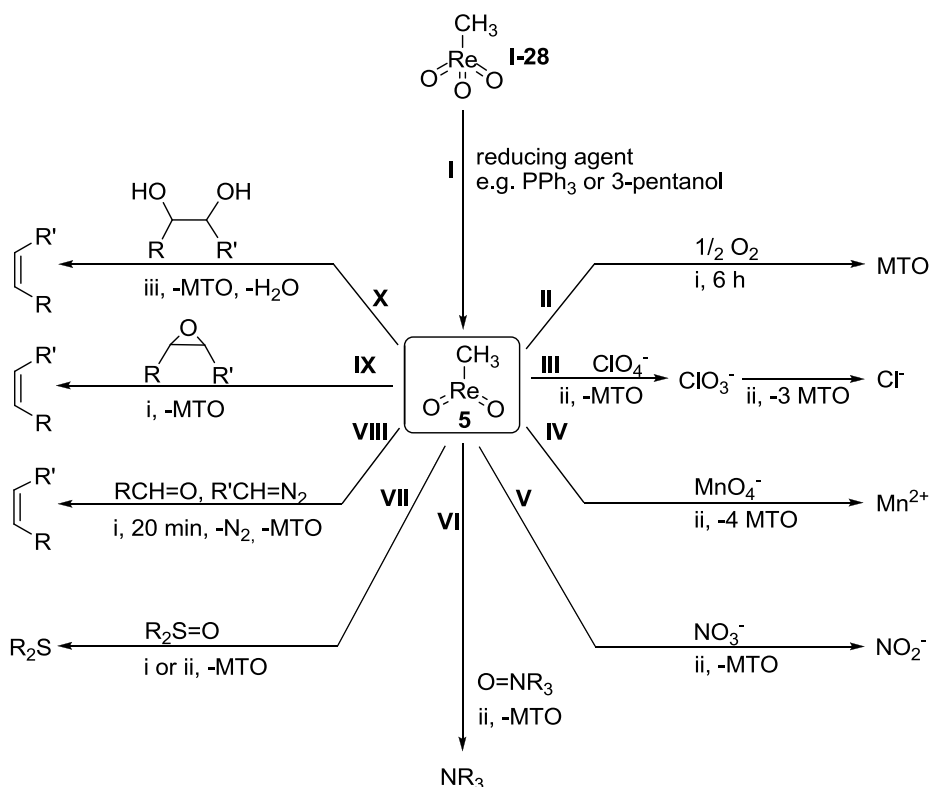
MDO-alkyne complexes **I-31** exhibit a chemical behaviour similar to CH₃ReO₂(PR₃)₂ **I-29** and the condensation with glycols succeeds starting from **I-31** yielding CH₃ReO-diolate alkyne adducts **I-32**. Hence, the alkyne stabilises MDO and allows preparative condensation

chemistry similar to MTO. However, a *cis*-configuration of the vicinal diol is mandatory; a reaction of *trans*-diols has never been observed.¹⁵

Not only alkynes and phosphine, but also *N*-donor compounds are capable stabilising highly reactive MDO. For example, addition of 2,2'-bipyridine whilst treatment of MTO with hypophosphorous acid in acetonitrile results in formation of MDO-bipyridine complex **I-33**.⁶¹

2.3.3 Oxygen atom transfer reactions

MDO is a strong two-electron reducing agent and capable to abstract an oxygen from manifold inorganic and organic oxides, which actually represents the formal reverse reaction of its formation. The reaction is driven by the oxidation of Re(V) to Re(VII) and formation of stable rhenium oxo double bonds, thus resulting in a more electron rich (14 VE) environment. A comprehensive overview which highlights the substrate variety is depicted in Scheme 2-7. Due to the pronounced instability and preparative unavailability of MDO usually oxygen atom transfer reactions are conducted applying catalytic amounts of MTO and stoichiometric amounts of a reducing agent (path I, Scheme 2-7, see also Scheme 2-5).



Scheme 2-7. Portfolio of oxygen atom transfer reactions catalysed by MDO. Various inorganic group 15–17 oxides,^{53,61,71} group 5–7 transition metal oxides,⁶¹ and organic oxides undergo oxygen abstraction.^{8,59,72-76} Reaction conditions: i) r.t., benzene; ii) r.t., aqueous sol. 1.0 M trifluoromethanesulfonic acid; iii) 140–170 °C, neat, 0.5–3.5 h.

Molecular oxygen is activated from ambient aerobic atmosphere when tertiary phosphine is added to benzene solution of MTO (see Scheme 2-7, path **II**). Under the latter conditions the oxidation of phosphine to phosphine oxide is catalysed, however, under inert gas atmosphere no quantitative oxidation but instead formation of rhenium(V) phosphine adducts **I-29** (*vide supra*) is observed, pointing this complex as intermediate.^{53,77}

A bound oxide O-atoms is also abstracted by treatment with MDO. For example, reaction with perchlorate anion yields in chlorate, and a continued reaction to chloride consuming three additional equivalents of MDO (if available) is observed, as well (see path **III**).⁷¹ Analogue reaction occurs also with the remaining halogen oxides as perbromate, bromate and iodate.⁶⁹ Furthermore, some examples of group 5–7 metal oxide reduction are known, thus an aqueous solutions of purple MnO_4^- is achromatised by formation of Mn^{2+} (path **IV**), molybdenum(VI) oxide $[\text{HOMoO}_2(\text{OH}_2)]^+$ yields the Mo(V) dimer $[\text{MoO}(\text{OH}_2)_3(\mu\text{-O})_2]_2$ (probably due to comproportionation of Mo(IV) and Mo(VI) after initial oxygen abstraction), and the vanadates VO_2^+ and VO^{2+} dispense an oxygen atom yielding VO^+ and V^{2+} , respectively.⁶⁹

Furthermore, oxygen atom abstraction from non-metal oxides is observed, too. Treatment of nitrates at strong acidic conditions gives nitrous acid which subsequently reacts to hyponitrous acid HON (see path **V**). In general, MTO/MDO catalyses the oxygen transfer reaction of group 15 tertiary organooxides to PPh_3 , thus tertiary amine oxides (pyridine oxide and in *para*-position modified *N,N*-dimethyl aniline derivatives, see path **VI**), triphenylarsine oxide and triphenylstibine oxide are converted to the corresponding amines, arsines and stibines, which is indeed a quick reaction and occurs within 30 min at room temperature.⁵³ Since no reverse-reaction has ever been observed, the formation of phosphine oxide double bonds is suggested to drive thermodynamically the reaction forward.

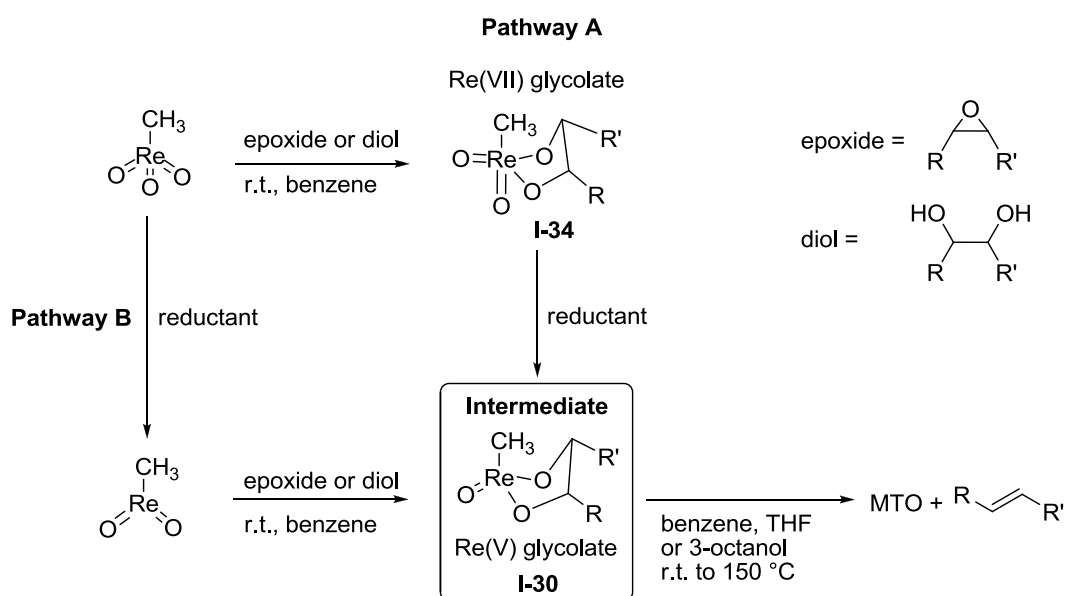
Moreover, organic sulphoxides are reduced to the organic sulphides (path **VII**). The latter synthetic useful catalytic transformation was studied thoroughly with various compounds in benzene solution at room temperature.⁵³

By far, the most important application of the MTO/MDO system is the deoxygenation of organic substrates such as aldehydes, epoxides, and vicinal diols forming olefins.^{8,59,72-76} The aldehyde olefination (path **VIII**) is a catalysed C–C coupling reaction similar to the Wittig reaction,⁷⁸⁻⁸⁰ however, in alteration an aldehyde and azide is coupled consuming stoichiometric amounts of organophosphines.⁵ The reaction allows the coupling of very electron deficient aldehydes and ketones and thus preferable to classical and catalysed Wittig reactions.^{55,56} Noteworthy, not ylide but phosphazine formation is observed. The mechanism was intensively discussed by Santos, Kühn, and Chen *et al.* and is proposed to proceed via cycloreversion of rhenaoxetane which is formed by [2+2] addition of the

aldehyde and methyloxorhenium carbene.^{1,6-8,55,56,75,81} The intermediate carbene is generated by reaction of MDO and phosphazine accompanied by N₂ gas liberation.⁸²

The abstraction of an oxygen atom from epoxides (see path **IX**) by MDO leads to the formation of olefins. If instead a vicinal diol (glycol) is subjected as substrate, again an olefin is formed under liberation of water (see path **X**). The combination of deoxygenation and dehydration reaction steps leads to olefinic dehydration products under formal loss of one oxygen atom which is abstracted first by MDO, and subsequently by the reductant in the course of MDO regeneration. Both latter transformations bear a similar reaction mechanism since they pass through the same glycolate intermediate.

In general, two mechanistic reaction pathways towards Re(V) glycolate intermediate **I-30** are discussed in literature (see Scheme 2-8).²³ MTO is known to form Re(VII)-glycolates **I-34** by condensation with glycols or addition of oxirans, and subsequent oxygen abstraction which leads to the formation of Re(V)-diolate **I-30** seems plausible (pathway A).^{41,53,64,83} Due to thermodynamical reasons oxirane ring opening and addition is preferred over O-coordination,⁸⁴ thus formation of **I-34** is already observed at room temperature. However, MTO reduction may precede Re-diolate formation (pathway B). Upon thermal treatment of **I-34**, no olefin extrusion but decomposition is observed,⁸³ and once PPh₃ is added to **I-34** olefin extrusion starts immediately already at room temperature, probably due to the formation of intermediate **I-29**.^{23,53,83} Recently, Re(V)-glycolates were evidenced spectroscopically by Abu-Omar and co-workers using ¹H NMR.⁴⁰



Scheme 2-8. Proposed mechanism for the deoxygenation and deoxydehydration of epoxides and vicinal diols, respectively. Either diolate formation precedes reduction of Re(VII)→Re(V) (pathway A) or the Re(V)-diolate forms after MDO generation (pathway B).²³ H₂O in the reaction equations is omitted for clarity.

In a computational study Bi *et al.* discusses whether the deoxygenation proceeds via pathway A or pathway B (Scheme 2-8).^{54,84}

Energies barriers for each reduction step of MTO→MDO and Re(VII)-diolate→Re(V)-diolate were calculated and compared. The model system used hydrogen as oxygen acceptor, which demands under real experimental conditions temperatures of >80 °C for MTO reduction (usually 150 °C are applied to keep the reaction within a convenient time frame).^{54,57} As result the reductive [3+2] addition of hydrogen to **I-34** is favoured to the [3+2] addition to MTO, due to both thermodynamic and kinetic reasons, hence, the formation of glycolates facilitates oxygen abstraction. Noteworthy, since MDO forms from MTO/PPh₃ mixtures readily at room temperature, no distinct reaction pathway can be concluded (*vide supra*).

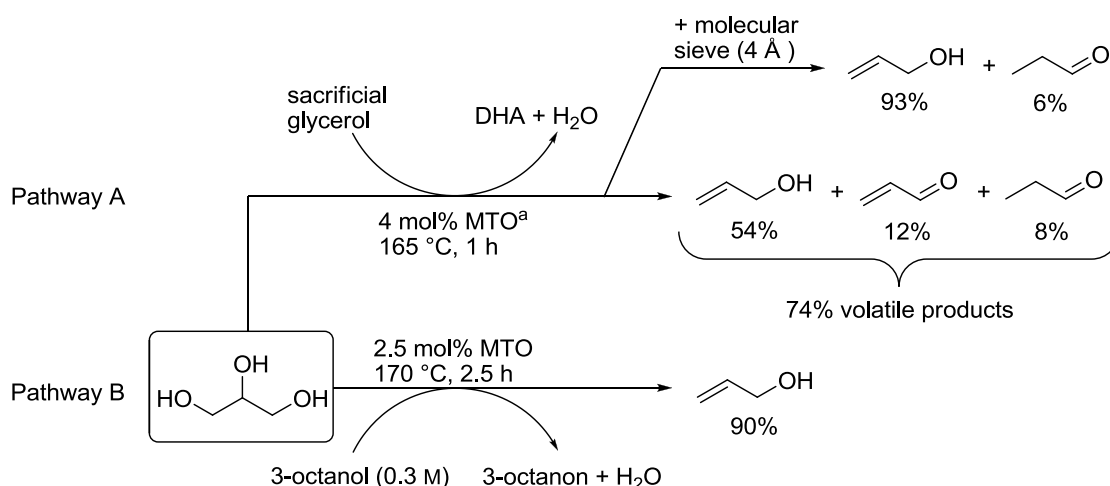
The final olefin extrusion step is commonly understood to occur from Re(V)-diolate **I-30**, which could be proven by mass spectrometry and NMR spectroscopy.⁴⁰ As mechanism a concerted [3+2] cycloreversion step was proposed, supported by theoretical considerations and experiments of Gable and co-workers.⁸⁵⁻⁹⁰

In the last five years, intensive research efforts on the MTO-catalysed DODH reaction were undertaken by the groups of Nicholas, Abu-Omar, Toste, Bergman, and recently the application of the DODH reaction upgrading biomass derived sugars and sugar alcohols have been investigated.^{15,40,54,60,67,91} Previous year, Shiramizu and Toste reported in a follow-up work the tandem DODH reaction of allylic 1,4- and 1,6-diols, realised due to a MTO-catalysed [1,3-OH] shift expanding the substrate scope by sugar acids.⁵⁹ In excursus 2.4 (*vide infra*) some examples on the refining of sugar alcohols are presented.

2.4 Excursus – MTO/MDO in refining of biomass derived sugar alcohols

Although lignocellulosic biomass presents the most abundant sustainable material on earth its chemical-industrial account is limited. The high oxygen content lowers the energy density and does not allow for example an efficient combustion.⁹² Moreover, most commodity chemicals also bear low oxygen content.⁹³ As state of the art, deoxygenation is conducted via high-temperature pyrolysis,^{94,95} Fischer-Tropsch synthesis approaches,⁹⁶ or hydrodeoxygenation.⁷³ However, the ecological worthwhile application of natural's pool of organic compounds, avoiding an energy intensive build-up of higher hydrocarbons, desires selective deoxygenative transformations such as the acid-catalysed dehydration,⁹⁷⁻⁹⁹ hydrogenolysis,⁹³ and DODH reaction.^{72,73} The rhenium-catalysed DODH reaction (see section 2.3.3) was investigated during the past 5 years and applied upgrading biomass

derived polyols.^{15,16,59,60,72,73} In the following, refining of biomass derived polyols is illustrated by the DODH reaction of glycerol and the C₆ hydrocarbons sorbitol, mannitol and inositol. Glycerol is a C₃-triol and easily available in high amounts as waste material from biodiesel production. The low market price makes glycerol very attractive as green carbon feedstock. In 2009 the price per metric ton was 820 US\$ for refined, and 120 US\$ for crude glycerol.¹⁰⁰ Applying the DODH reaction on glycerol, allyl alcohol is obtained as major product, acryloin and propaldehyde as side product. (Scheme 2-9).

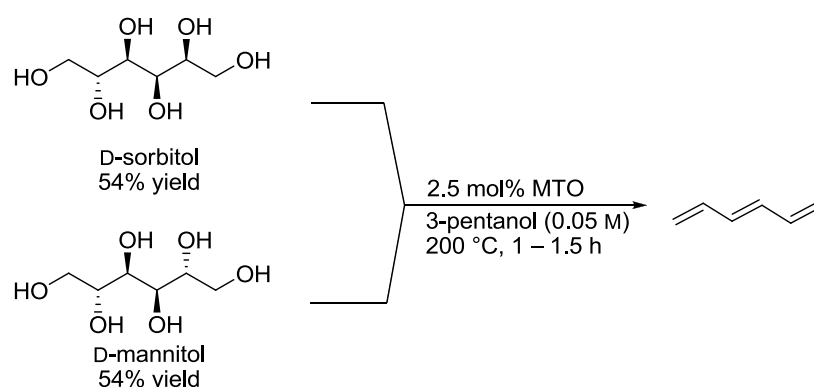


Scheme 2-9. DODH reaction of glycerol yields in allyl alcohol in high yields, acryloin and propaldehyde are observed as side products; a) 2 mol% related to total amount of glycerol in reaction vessel.

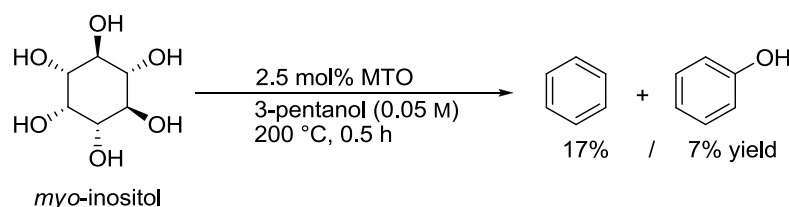
The reactor design for neat conditions (MTO is added to glycerine) allows separation of the volatile reaction products by operando distillation at 165 °C to give an oil of 74% of the theoretical yield within 1 h (see pathway A). The oil yield corresponds to 0.5 equivalent of glycerol since stoichiometric amounts of glycerol react to dihydroxyacetone (DHA) reducing MTO to MDO. An isolation of DHA at the applied reaction conditions is not possible due to its polymerisation. Addition of sacrificial alcohols (3-octanol or 1-heptanol) increases significantly the selectivity, and a ratio of allyl alcohol/propaldehyde (10:1) is obtained, however, the overall oil yield decreases to 52–55%. Noteworthy, if the reaction water is removed due to the presence of 4 Å molecular sieve a high selectivity (100:6) and excellent yield of volatiles is obtained after prolonged reaction time (2.5 h). When 3-octanol is used as both solvent and reductant under similar reaction conditions, an excellent allyl alcohol yield, and no glycerine loss due to DHA formation is obtained (pathway B).

Sorbitol is an important sugar alcohol and is applied as sweetener; mannitol is used as sweetener for diabetics. Both sweeteners are produced in industrial scale by hydrogenation of sucrose. The DODH reaction of D-sorbitol and D-mannitol is conducted at 200 °C and

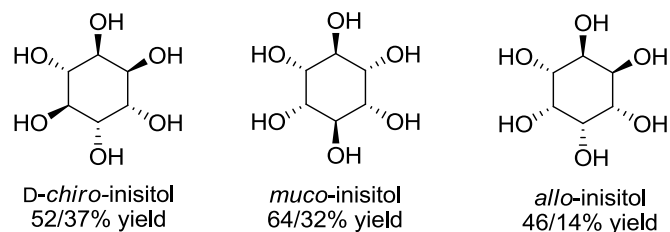
yields the conjugated polyene *E*-hexatriene in moderate yields (see Scheme 2-10), which possibly can be used as polymer precursor.¹⁰¹ In analogy, polyenes (butadiene) are observed when C₄-polyols are used instead. Since sorbitol and mannitol gave the same hexatriene yields, the stereochemistry is not decisive for the product selectivity and overall yields. Moreover, no product mixture containing monoenes, dienes and trienes, originating from 1, 2, or 3 DODH steps respectively, was obtained. This is probably explained by the recently published MTO-catalysed [1,3]-OH shift allowing also 1,4-DODH and 1,6-DODH reactions to take place.⁵⁹



Scheme 2-10. Three consecutive DODH reactions of the sweeteners D-sorbitol and D-mannitol yield *E*-hexatriene in moderate yields, which possibly can be used as polymer precursor.¹⁵



Product yields of other inositols:



Scheme 2-11. The combination of several consecutive DODH and dehydration reactions on inositols produces benzene and phenol, expanding the scope of possible biomass feedstocks for aromates production.

Inositols are sixfold cyclic polyols. Nature's most abundant inositol is the *myo*-isomer and is industrially produced by hydrolysis of the phytate salts which is consisted in e.g. sesame seed flour, tofu, linseed, and corn by a few percentage of weight.

Benzene and phenol is obtained when inositols are treated with MTO at 200 °C (see Scheme 2-11). Therefore, benzene is formed by three consecutive DODH reactions, and phenol is formed by a combination of two DODH and a single dehydration reaction.

Good to very good mass balances of $\approx 90\%$ and good yields are obtained for upgrading D-*chiro*- and *muco*-inisol, the *allo*-inisol isomer still exhibits a mass balance of 60%. Unfortunately, the natural abundant *myo*-form is the less suitable isomer which gives benzene and phenol in 17% and 7% yield, respectively. This is a rare example which expands the scope of biomass derived carbon feedstocks suitable for the production of aromates. In future works isomerisation of the *myo*-isomer needs to be developed to gain higher efficiency.

2.5 Rhenium heptoxide

2.5.1 General and structural chemistry

In the group of rhenium oxides the lemon yellow coloured rhenium(VII) heptoxide (**I-35**) is the highest possible oxide, the key compound in Re(VII) chemistry, and used as the very initiate precursor compound.¹

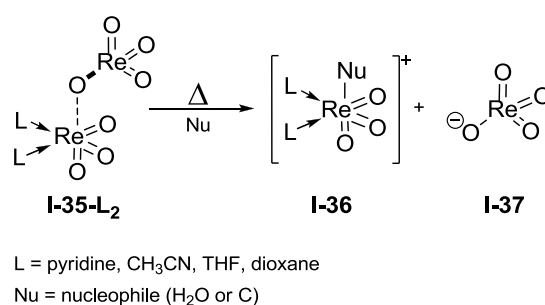
I-35 is produced by roasting of elemental rhenium metal or lower oxides in an oxygen stream at 400 °C, purification and crystallisation succeeds by sublimation. Re_2O_7 melts readily at 220 °C to a colourless cast, boils at 363 °C and shows high vapour pressure.¹⁰² In solid state the binary oxide is consisted of an equal number of nearly regular ReO_4 tetrahedra and highly distorted ReO_6 octahedra which are linked by shared oxide corners. The structure was first determined by Krebs and Beyer in 1968 using X-ray crystallography, in which the bridging Re–O bonds found longer (172.5–216 pm) than the terminal ones (165–174.2 pm).¹⁰³⁻¹⁰⁵ In the gas phase, however, electron diffraction exhibits rhenium(VII) oxide as molecular dimer of equivalent Re atoms tetrahedrally enclosed by oxygen atoms. The $\text{ReO}_3\text{--O--ReO}_3$ centres are linked by a bent oxygen bridge with a Re–O–Re angle of 143.6(9)°. The distances of the Re– μO are identical for both rhenium atoms. **I-35** is applied as catalyst in the olefin metathesis,¹⁰⁶ hydrogenation,^{107,108} and dehydration reaction of secondary alcohols.^{12-14,44}

2.5.2 Dissolution properties and coordination chemistry

Rhenium heptoxide dissolves in coordinating solvents but is insoluble in non-polar hydrocarbon or weakly coordinating solvents. To allow dissolution the solvent needs to break down the polymeric structure existent in the solid state. In a seminal study concerning the dissolution behaviour Krebs and Müller stated that dissolution in alcohols, ethers, and

amines (ethanol, *t*-butanol, cyclohexanol, diethylether, 1,4-dioxane, THF, piperidine, pyridine, *n*-dibutylamine) results in reductive decomposition.^{109,110} In other solvents/media such as benzene, carbon tetrachloride, DMSO, and nitromethane, reduction is observed upon thermal treatment. If **I-35** is dissolved in water the oxidation state Re(VII) is maintained due to the formation of perrhenic acid HReO_4 . In concentrated aqueous solutions containing >80 wt% Re_2O_7 not hydrolysis but coordination of two molecules water is observed. The bis-aqua $\text{ReO}_3(\text{H}_2\text{O})_2\text{OReO}_3$ (**I-35-aq**) complex is consisted of an unsymmetrical oxygen bridged $\text{ReO}_3-\mu\text{O}$ tetrahedron and a $(\text{H}_2\text{O})_2\text{ReO}_3-\mu\text{O}$ octahedron. From latter concentrated solutions **I-35-aq** can be crystallised, however, dilution to rhenium content <70% results in complete dissociation to perrhenate ReO_4^- and H_3O^+ .^{1,103}

Analogue coordination chemistry is observed with coordinating Lewis basic solvents such as THF, 1,4-dioxane, and acetonitrile. Evaporation/saturation of a solution of THF/**I-35** yields THF adduct as colourless crystals/white powder (see Scheme 2-12, **I-35-L₂**).¹⁰³



Scheme 2-12. Lewis base coordination to Re_2O_7 weakens the Re–O bond and preforms a ReO_4^- fragment. The perrhenyl fragment becomes extremely sensitive to nucleophiles.^{111,112}

In common, the presence of Lewis base O- or N-donor compounds (THF, 1,4-dioxane, CH_3CN) results in formation of Lewis acid-base pairs in the type of $\text{L}_2\text{ReO}_3[\text{ReO}_4]$ (**I-35-L₂**). Again, two octahedral aligned ligands coordinate a single rhenium centre generating a perrhenyl and perrhenate centre, which in consequence loses the Re–O–Re intramolecular bond. However, pyridine represents an exception of this general reactivity, and coordination of three molecules pyridine to $\text{py}_2\text{ReO}_3(\mu\text{-O})\text{ReO}_3\text{py}$ is observed. As known for MTO monodendating ligands are easily replaced by bidentating ligands e.g. dimethoxyethane and 2,2'-bipyridine.¹¹² As a consequence of the Lewis base/acid adduct formation the Re–O–Re bonds become unsymmetrical. The $\text{L}_2\text{ReO}_3\text{-O}$ bond weakens, in contrast the $\text{ReO}_3\text{-O}$ bond distance decreases (see Scheme 2-12, dashed and bold bond, respectively), which adumbrates the formation of perrhenate (**I-37**) and perrhenyl fragments **I-36**.¹¹¹ Thus, a high sensitivity towards moisture and temperature is observed. Stable perrhenyl cations are obtained when **I-35** is treated with tridendate N-base ligands such as L = *N,N,N'*-trimethyl-1,4,7-triazacyclononane.

2.5.3 Reactivity towards alcohols

Rhenium heptoxide is known to decompose as soon dissolved in alcohols. Emel'yanov *et al.* reported the formation of Re(VI) oxide,¹¹⁰ and a patent of Hiromitsu and Hiroko describes the formation of ReO₃ particles with a size ranging from 10–100 nm.¹¹³ The thermal decomposition of rhenium heptoxide–dioxane adduct to metallic ReO₃ nanoparticles was reported by Biswas *et al.*¹¹⁴ However, when a secondary alcohol is added to a mixture of **I-35** and toluene at 100 °C, catalytic dehydration is observed.

The dehydration of a broad scope of alcohols was exhaustively studied by Espenson *et al.* and Korstanje *et al.* applying the Brønsted acids *p*-toluenesulphonic acid, sulphuric acid, perrhenic acid, and the Lewis acids MTO and rhenium heptoxide.^{12,14,41,44} Noteworthy, additions of *N*-bases deactivates the catalyst, either by lowering the Lewis acidity as applied for MTO (*vide supra*) or by occupying free coordination sites. Based on kinetic isotope effect and DFT calculations the mechanism is proposed to follow an ionic pathway exactly as known for Brønsted acid-catalysed dehydration reactions.⁴⁴

The dehydration occurs more easily from benzylic alcohols, but the scope extends aliphatic and terpeneols. If a primary alcohol is subjected to Re₂O₇ under the latter reaction conditions, catalytic oxidation to an aldehyde is observed in aerobic atmosphere. In contrast, under exclusion of air neither dehydration nor oxidation occurs.¹²

2.6 References in Chapter 2

1. C. C. Romão, F. E. Kühn and W. A. Herrmann, *Chem. Rev.*, 1997, **97**, 3197-3246.
2. W. A. Herrmann and F. E. Kühn, *Acc. Chem. Res.*, 1997, **30**, 169-180.
3. W. A. Herrmann, J. G. Kuchler, J. K. Felixberger, E. Herdtweck and W. Wagner, *Angew. Chem.*, 1988, **100**, 420-422; *Angew. Chem. Int. Ed.*, 1988, **27**, 394-396.
4. W. A. Herrmann and M. Wang, *Angew. Chem. Int. Ed.*, 1991, **30**, 1641-1643.
5. W. A. Herrmann and M. Wang, *Angew. Chem.*, 1991, **103**, 1709-1711; *Angew. Chem. Int. Ed.*, 1991, **30**, 1641-1643.
6. F. E. Kühn, A. Scherbaum and W. A. Herrmann, *J. Organomet. Chem.*, 2004, **689**, 4149-4164.
7. F. E. Kühn and A. M. Santos, *Mini-Rev. Org. Chem.*, 2004, **1**, 55-64.
8. A. M. Santos, C. C. Romão and F. E. Kühn, *J. Am. Chem. Soc.*, 2003, **125**, 2414-2415.
9. F. E. Kühn, A. M. Santos, I. S. Gonçalves, C. C. Romão and A. D. Lopes, *Appl. Organomet. Chem.*, 2001, **15**, 43-50.

10. C. Crestini, M. Crucianelli, M. Orlandi and R. Saladino, *Catal. Today*, 2010, **156**, 8-22.
11. S. R. Collinson and W. Thielemans, *Coord. Chem. Rev.*, 2010, **254**, 1854-1870.
12. T. J. Korstanje, E. F. de Waard, J. T. B. H. Jastrzebski and R. J. M. K. Gebbink, *ACS Catal.*, 2012, **2**, 2173-2181.
13. T. Korstanje and R. M. K. Gebbink, in *Organometallics and Renewables*, eds. M. A. R. Meier, B. M. Weckhuysen and P. C. A. Bruijninx, Springer Berlin Heidelberg, 2012, vol. 39, ch. 4, pp. 129-174.
14. T. J. Korstanje, J. T. B. H. Jastrzebski and R. J. M. K. Gebbink, *ChemSusChem*, 2010, **3**, 695-697.
15. M. Shiramizu and F. D. Toste, *Angew. Chem.*, 2012, **124**, 8206-8210; *Angew. Chem. Int. Ed.*, 2012, **51**, 8082-8086.
16. E. Arceo, J. A. Ellman and R. G. Bergman, *J. Am. Chem. Soc.*, 2010, **132**, 11408-11409.
17. W. A. Herrmann, R. W. Fischer, W. Scherer and M. U. Rauch, *Angew. Chem.*, 1993, **105**, 1209-1212; *Angew. Chem. Int. Ed.*, 1993, **32**, 1157-1160.
18. B. Cornils and W. A. Herrmann, *Applied homogeneous catalysis with organometallic compounds: Developments*, Wiley-VCH, 2002.
19. F. E. Kühn, R. W. Fischer and W. A. Herrmann, *Chem. unserer Zeit*, 1999, **33**, 192-198.
20. R. Tsuchida, *Bull. Chem. Soc. Jpn.*, 1938, **13**, 388-400.
21. W. A. Herrmann, J. G. Kuchler, G. Weischselbaumer, E. Herdtweck and P. Kiprof, *J. Organomet. Chem.*, 1989, **372**, 351-370.
22. W. A. Herrmann, G. Weischselbaumer and E. Herdtweck, *J. Organomet. Chem.*, 1989, **372**, 371-389.
23. J. H. Espenson, *Chem. Commun.*, 1999, 479-488.
24. W. A. Herrmann, R. W. Fischer, M. U. Rauch and W. Scherer, *J. Mol. Catal.*, 1994, **86**, 243-266.
25. W. A. Herrmann, R. W. Fischer and J. D. G. Correia, *J. Mol. Catal.*, 1994, **94**, 213-223.
26. R. Bernini, A. Coratti, G. Fabrizi and A. Goggiamani, *Tetrahedron Lett.*, 2003, **44**, 8991-8994.
27. M. M. Abu-Omar and J. H. Espenson, *Organometallics*, 1996, **15**, 3543-3549.
28. T. H. Zauche and J. H. Espenson, *Inorg. Chem.*, 1998, **37**, 6827-6831.
29. Z. Zhu and J. H. Espenson, *J. Org. Chem.*, 1995, **60**, 1326-1332.
30. S. Yamazaki, *Bull. Chem. Soc. Jpn.*, 1997, **70**, 877-883.
31. R. W. Murray, K. Iyanar, J. Chen and J. T. Wearing, *J. Org. Chem.*, 1996, **61**, 8099-8102.

32. W. Adam, C. M. Mitchell and C. R. Saha-Möller, *Tetrahedron*, 1994, **50**, 13121-13124.
33. W. Adam, C. M. Mitchell, C. R. Saha-Möller and O. Weichold, *J. Am. Chem. Soc.*, 1999, **121**, 2097-2103.
34. U. Schuchardt, D. Mandelli and G. B. Shul'pin, *Tetrahedron Lett.*, 1996, **37**, 6487-6490.
35. R. W. Murray, K. Iyanar, J. Chen and J. T. Wearing, *Tetrahedron Lett.*, 1995, **36**, 6415-6418.
36. G. S. Owens, J. Arias and M. M. Abu-Omar, *Catal. Today*, 2000, **55**, 317-363.
37. J. Jacob and J. H. Espenson, *Inorg. Chim. Acta*, 1998, **270**, 55-59.
38. W. Adam, W. A. Herrmann, C. R. Saha-Möller and M. Shimizu, *J. Mol. Catal. A: Chem.*, 1995, **97**, 15-20.
39. W. Adam, W. A. Herrmann, J. Lin and C. R. Saha-Moeller, *J. Org. Chem.*, 1994, **59**, 8281-8283.
40. S. Liu, A. Senocak, J. L. Smeltz, L. Yang, B. Wegenhart, J. Yi, H. I. Kenttämä, E. A. Ison and M. M. Abu-Omar, *Organometallics*, 2013, **32**, 3210-3219.
41. Z. L. Zhu and J. H. Espenson, *J. Org. Chem.*, 1996, **61**, 324-328.
42. J. Takacs, P. Kiprof, J. Riede and W. A. Herrmann, *Organometallics*, 1990, **9**, 782-787.
43. W. A. Herrmann, F. E. Kühn and P. W. Roesky, *J. Organomet. Chem.*, 1995, **485**, 243-251.
44. T. J. Korstanje, J. T. B. H. Jastrzebski and R. J. M. Klein Gebbink, *Chem. Eur. J.*, 2013, **19**, 13224-13234.
45. H. Lange, S. Decina and C. Crestini, *Eur. Polym. J.*, 2013, **49**, 1151-1173.
46. C. Crestini, M. C. Caponi, D. S. Argyropoulos and R. Saladino, *Biorg. Med. Chem.*, 2006, **14**, 5292-5302.
47. C. Crestini, P. Pro, V. Neri and R. Saladino, *Bioorg. Med. Chem. Lett.*, 2005, **13**, 2569.
48. C. Crestini, P. Pro, V. Neri and R. Saladino, *Biorg. Med. Chem.*, 2005, **13**, 2569-2578.
49. K. Lundquist and R. Lundgren, *Acta Chem. Scand.*, 1972, **26**, 2005-2023.
50. M. Aoyama, C.-L. Chen and D. Robert, *J. Chin. Chem. Soc.*, 1991, **38**, 77-84.
51. M. R. Sturgeon, S. Kim, K. Lawrence, R. S. Paton, S. C. Chmely, M. Nimlos, T. D. Foust and G. T. Beckham, *ACS Sus. Chem. Eng.*, 2014, **2**, 472-485.
52. J. Zakzeski, P. C. A. Bruijninx, A. L. Jongerius and B. M. Weckhuysen, *Chem. Rev.*, 2010, **110**, 3552-3599.
53. Z. Zhu and J. H. Espenson, *J. Mol. Catal. A: Chem.*, 1995, **103**, 87-94.

54. J. E. Ziegler, M. J. Zdilla, A. J. Evans and M. M. Abu-Omar, *Inorg. Chem.*, 2009, **48**, 9998-10000.
55. F. M. Pedro, S. Hirner and F. E. Kühn, *Tetrahedron Lett.*, 2005, **46**, 7777-7779.
56. A. M. Santos, F. M. Pedro, A. A. Yogalekar, I. S. Lucas, C. C. Romão and F. E. Kühn, *Chem. Eur. J.*, 2004, **10**, 6313-6321.
57. P. M. Reis, P. J. Costa, C. C. Romao, J. A. Fernandes, M. J. Calhorda and B. Royo, *Dalton Trans.*, 2008, 1727-1733.
58. B. Royo and C. C. Romão, *J. Mol. Catal. A: Chem.*, 2005, **236**, 107-112.
59. M. Shiramizu and F. D. Toste, *Angew. Chem.*, 2013, **125**, 13143-13147; *Angew. Chem. Int. Ed.*, 2013, **52**, 12905-12909.
60. J. Yi, S. Liu and M. M. Abu-Omar, *ChemSusChem*, 2012, **5**, 1401-1404.
61. M. M. Abu-Omar, E. H. Appelman and J. H. Espenson, *Inorg. Chem.*, 1996, **35**, 7751-7757.
62. W. A. Herrmann, R. W. Fischer and W. Scherer, *Adv. Mater.*, 1992, **4**, 653-658.
63. W. A. Hermann and R. W. Fischer, *J. Am. Chem. Soc.*, 1995, **117**, 3223-3230.
64. W. A. Herrmann, J. K. Felixberger, J. G. Kuchler and E. Herdtweck, *Z. Naturforsch.*, 1990, **45b**, 876-886.
65. J. K. Felixberger, J. G. Kuchler, E. Herdtweck, R. A. Paciello and W. A. Herrmann, *Angew. Chem.*, 1988, **100**, 975-978; *Angew. Chem. Int. Ed.*, 1988, **27**, 946-948.
66. I. Ahmad, G. Chapman and K. M. Nicholas, *Organometallics*, 2011, **30**, 2810-2818.
67. S. Vkuturi, G. Chapman, I. Ahmad and K. M. Nicholas, *Inorg. Chem.*, 2010, **49**, 4744-4746.
68. J. H. Espenson and D. T. Y. Yiu, *Inorg. Chem.*, 2000, **39**, 4113-4118.
69. M. M. AbuOmar, E. H. Appelman and J. H. Espenson, *Inorg. Chem.*, 1996, **35**, 7751-7757.
70. W. A. Herrmann, P. W. Roesky, M. Wang and W. Scherer, *Organometallics*, 1994, **13**, 4531-4535.
71. M. M. Abu-Omar and J. H. Espenson, *Inorg. Chem.*, 1995, **34**, 6239-6240.
72. J. O. Metzger, *ChemCatChem*, 2013, **5**, 680-682.
73. S. Dutta, *ChemSusChem*, 2012, **5**, 2125-2127.
74. S. C. A. Sousa and A. C. Fernandes, *Tetrahedron Lett.*, 2011, **52**, 6960-6962.
75. X. Zhang and P. Chen, *Chem. Eur. J.*, 2003, **9**, 1852-1859.
76. K. P. Gable, F. A. Zhuravlev and A. F. T. Yokochi, *Chem. Commun.*, 1998, 799-800.
77. M. D. Eager and J. H. Espenson, *Inorg. Chem.*, 1999, **38**, 2533-2535.
78. E. W. Abel, F. G. A. Stone and G. Wilkinson, eds., *Comprehensive Organometallic Chemistry II: A Review of the Literature 1982-1994*, Pergamon, Oxford, UK, 1995.
79. B. E. Maryanoff and A. B. Reitz, *Chem. Rev.*, 1989, **89**, 863-927.

80. J. E. McMurry, *Chem. Rev.*, 1989, **89**, 1513-1524.
81. X. Chen, X. Zhang and P. Chen, *Angew. Chem.*, 2003, **115**, 3928-3931; *Angew. Chem. Int. Ed.*, 2003, **42**, 3798-3801.
82. For a comprehensive literature overview and mechanistic discussion please refer to the manuscript version on which this chapter is based.
83. Z. Zhu, A. M. Al-Ajlouni and J. H. Espenson, *Inorg. Chem.*, 1996, **35**, 1408-1409.
84. S. Bi, J. Wang, L. Liu, P. Li and Z. Lin, *Organometallics*, 2012, **31**, 6139-6147.
85. K. P. Gable, A. AbuBaker, K. Zientara and A. M. Wainwright, *Organometallics*, 1999, **18**, 173-179.
86. K. P. Gable and J. J. J. Juliette, *J. Am. Chem. Soc.*, 1995, **117**, 955-962.
87. K. P. Gable and J. J. J. Juliette, *J. Am. Chem. Soc.*, 1996, **118**, 2625-2633.
88. K. P. Gable and T. N. Phan, *J. Am. Chem. Soc.*, 1993, **115**, 3036-3037.
89. K. P. Gable and T. N. Phan, *J. Am. Chem. Soc.*, 1994, **116**, 833-839.
90. K. P. Gable and F. A. Zhuravlev, *J. Am. Chem. Soc.*, 2002, **124**, 3970-3979.
91. C. Boucher-Jacobs and K. M. Nicholas, *ChemSusChem*, 2013, **6**, 597-599.
92. G. W. Huber and A. Corma, *Angew. Chem.*, 2007, **119**, 7320-7338; *Angew. Chem. Int. Ed.*, 2007, **46**, 7184-7201.
93. A. Corma, S. Iborra and A. Velty, *Chem. Rev.*, 2007, **107**, 2411-2502.
94. D. Mohan, C. U. Pittman and P. H. Steele, *Energy & Fuels*, 2006, **20**, 848-889.
95. Q. Zhang, J. Chang, T. Wang and Y. Xu, *Energy Convers. Manage.*, 2007, **48**, 87-92.
96. G. W. Huber, S. Iborra and A. Corma, *Chem. Rev.*, 2006, **106**, 4044-4098.
97. F. Jin and H. Enomoto, *Energy Environ. Sci.*, 2011, **4**, 382-397.
98. X. Tong, Y. Ma and Y. Li, *Appl. Catal., A*, 2010, **385**, 1-13.
99. R. Rinaldi and F. Schuth, *Energy Environ. Sci.*, 2009, **2**, 610-626.
100. M. Ayoub and A. Z. Abdullah, *Renewable and Sustainable Energy Reviews*, 2012, **16**, 2671-2686.
101. V. L. Bell, *J. Polym. Sci., Part A: Gen. Pap.*, 1964, **2**, 5291-5303.
102. M. KGaA, Safety Data Sheet Rhenium(VII) oxide,
http://www.merckmillipore.com/germany/chemicals/rheniumvii-oxid-77-prozent-re/MDA_CHEM-812309/p_YFKb.s1L6pIAAAEWpOefVhTI, Accessed 27.05.2014.
103. F. E. Kühn, Ph.D. thesis, Technische Universität München, 1994.
104. B. Krebs, A. Muller and H. Beyer, *Chem. Commun.*, 1968, 263-264.
105. B. Krebs, *Angew. Chem.*, 1968, **80**, 291-291; *Angew. Chem. Int. Ed.*, 1968, **7**, 308-308.
106. J. C. Mol, *Catal. Today*, 1999, **51**, 289-299.

107. W. J. Bartley, *Rhenium Trioxide, Rhenium Heptoxide and Rhenium Trichloride as Hydrogenation Catalysts*, United States Air Force, Office of Scientific Research, Brigham Young University. Department of Chemistry, 1958.
108. H. S. Broadbent, G. C. Campbell, W. J. Bartley and J. H. Johnson, *J. Org. Chem.*, 1959, **24**, 1847-1854.
109. B. Krebs and A. Müller, *Z. Naturforsch., B: Chem. Sci.*, 1968, **23b**, 415.
110. D. E. Emel'yanov, Y. Y. Gukova, Y. V. Karyakin and M. I. Ermolaev, *Russ. J. Inorg. Chem.*, 1968, **13**, 89-90.
111. W. A. Herrmann, P. W. Roesky, F. E. Kuehn, M. Elison, G. Artus, W. Scherer, C. C. Romao, A. Lopes and J.-M. Basset, *Inorg. Chem.*, 1995, **34**, 4701-4707.
112. W. A. Herrmann, P. W. Roesky, F. E. Kühn, W. Scherer and M. Kleine, *Angew. Chem.*, 1993, **105**, 1768-1770; *Angew. Chem. Int. Ed.*, 1993, **32**, 1714-1716.
113. T. Hiromitsu and I. Hiroko, Japan Patent, JP 09142846 and JP 3956400, 1997.
114. K. Biswas and C. N. R. Rao, *J. Phys. Chem. B*, 2006, **110**, 842-845.

“Green carbon will help to reduce the loss of our precious carbon resources and it will ensure that those hydrocarbons used for fuels will minimize carbon emissions”

— Vicki L. Colvin, 2010

3. Objective

3.1 Topic of research

The chemistry and application of organorhenium oxides, in particular MTO, has a long tradition in the Herrmann group.¹⁻¹⁸ Since all rhenium(VII) precursors originate from rhenium heptoxide, rhenium oxides were also significant research topic of the group.

Nowadays, the research focus of natural sciences is strongly modulated by the modern society challenges such as environmental issues, depletion of resources, energy supply and storage, and development of new materials.¹⁹⁻²⁵ As the outcome of ecological concerns the field of “green” science emerged, and principles of green chemistry were expressed and discussed. They include catalysis as the key technology for realising a “greener” world.²⁶ Being faced by rapid depletion of easy exploitable carbon feedstocks, such as crude oil, biomass is currently considered as the most eligible renewable carbon feedstock. In this context, much research efforts have been concentrated on establishing the chemistry and technology of the cellulose refining, however, lignin remains to be difficult for exploitation as feedstock.^{20,23,24,27,28} In order to cope with the growing demand on BTX chemicals, the usage of lignin appears to be the only direct and economical reasonable feedstock.²⁹

Despite the high importance, only very few examples on the rhenium-catalysed refining of biomass derived compounds are known. For example, MTO is used as catalyst for dehydration of alcohols (neutral conditions),³⁰⁻³⁴ deoxydehydration of polyols (reductive conditions),³⁵⁻³⁹ oxidative degradation of lignin model compounds and lignin (acidic and oxidative conditions),⁴⁰⁻⁴³ and oxidative upgrade of natural products.⁴⁴⁻⁴⁹

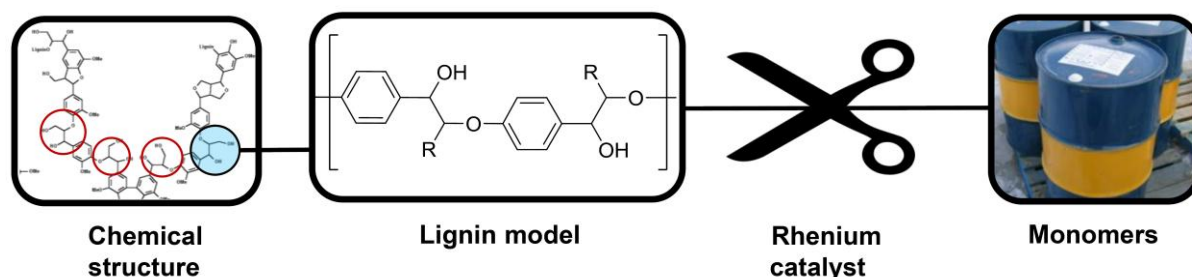


Figure 3-1. Development of new rhenium catalysts (depicted as scissors) active in the cleavage of β -hydroxy aryl ether linkages (also denoted as β -O-4 linkage type), the most abundant ones found in native lignin.

Aim of this research work is the development of a rhenium based catalytic system that is capable of degrading native lignin, in which the monomers are linked irregularly.^{28,50} Hence, to obtain sufficient depolymerisation the catalyst of choice must be suitable for cleaving the

most abundant linkage type, the β -hydroxy aryl ether group in native lignin (see Figure 3-1, please also refer to Chapter 1 for further information about lignin and model compounds).

Furthermore, all catalysts are required to be tested on model compounds thus enabling comparison with known benchmarking catalysts and excluding solubility, product separation, analytical, and reactor setup issues.

Known catalysts for the selective cleavage of β -hydroxy aryl ethers bear major drawbacks. Although many catalysts are based on less expensive precious metals or inexpensive transition metals, such as nickel or iron, they lack in activity, require high efforts for preparation, are difficult to handle under ambient conditions and demand unpractical reaction conditions, which limit an industrial application.^{40,51-55} Thus, there is still a high demand for the development of novel, easily manageable and applicable, and more active catalysts.

3.2 References in Chapter 3

1. W. A. Herrmann, A. M. J. Rost, J. K. M. Mitterpleininger, N. Szesni, S. Sturm, R. W. Fischer and F. E. Kühn, *Angew. Chem.*, 2007, **119**, 7440-7442; *Angew. Chem. Int. Ed.*, 2007, **46**, 7301-7303.
2. B. Cornils and W. A. Herrmann, *Applied homogeneous catalysis with organometallic compounds: Developments*, Wiley-VCH, 2002.
3. F. E. Kühn, R. W. Fischer and W. A. Herrmann, *Chem. unserer Zeit*, 1999, **33**, 192-198.
4. C. C. Romão, F. E. Kühn and W. A. Herrmann, *Chem. Rev.*, 1997, **97**, 3197-3246.
5. W. A. Herrmann and F. E. Kühn, *Acc. Chem. Res.*, 1997, **30**, 169-180.
6. W. A. Herrmann, P. W. Roesky, M. Wang and W. Scherer, *Organometallics*, 1994, **13**, 4531-4535.
7. W. A. Herrmann, P. W. Roesky, F. E. Kühn, W. Scherer and M. Kleine, *Angew. Chem.*, 1993, **105**, 1768-1770; *Angew. Chem. Int. Ed.*, 1993, **32**, 1714-1716.
8. W. A. Herrmann, F. E. Kühn, C. C. Romão, H. T. Huy, M. Wang, R. W. Fischer, P. Kiprof and W. Scherer, *Chem. Ber.*, 1993, **126**, 45-50.
9. W. A. Herrmann, R. W. Fischer, W. Scherer and M. U. Rauch, *Angew. Chem.*, 1993, **105**, 1209-1212; *Angew. Chem. Int. Ed.*, 1993, **32**, 1157-1160.
10. W. A. Herrmann, R. W. Fischer and W. Scherer, *Adv. Mater.*, 1992, **4**, 653-658.
11. W. A. Herrmann and M. Wang, *Angew. Chem.*, 1991, **103**, 1709-1711; *Angew. Chem. Int. Ed.*, 1991, **30**, 1641-1643.
12. W. A. Herrmann, W. Wagner, U. N. Flessner, U. Volkhardt and H. Komber, *Angew. Chem.*, 1991, **103**, 1704-1706; *Angew. Chem. Int. Ed.*, 1991, **30**, 1636-1638.

13. W. A. Herrmann, J. G. Kuchler, J. K. Felixberger, E. Herdtweck and W. Wagner, *Angew. Chem.*, 1988, **100**, 420-422; *Angew. Chem. Int. Ed.*, 1988, **27**, 394-396.
14. W. A. Herrmann, *Angew. Chem.*, 1988, **100**, 1269-1286; *Angew. Chem. Int. Ed.*, 1988, **27**, 1297-1313.
15. J. K. Felixberger, J. G. Kuchler, E. Herdtweck, R. A. Paciello and W. A. Herrmann, *Angew. Chem.*, 1988, **100**, 975-978; *Angew. Chem. Int. Ed.*, 1988, **27**, 946-948.
16. W. A. Herrmann and J. Okuda, *J. Mol. Catal.*, 1987, **41**, 109-122.
17. W. A. Herrmann, D. Marz, E. Herdtweck, A. Schäfer, W. Wagner and H.-J. Kneuper, *Angew. Chem.*, 1987, **99**, 462-464; *Angew. Chem. Int. Ed.*, 1987, **26**, 462-464.
18. W. A. Herrmann, R. Serrano and H. Bock, *Angew. Chem.*, 1984, **96**, 364-365; *Angew. Chem. Int. Ed.*, 1984, **23**, 383-385.
19. International Energy Agency, *World Energy Outlook 2013*, OECD, 2013.
20. E. d. Jong, A. Higson, P. Walsh and M. Wellisch, Bioenergy Task 42, *Bio-based Chemicals, Value Added Products from Biorefineries*, International Energy Agency, 2012.
21. T. P. Vispute, H. Zhang, A. Sanna, R. Xiao and G. W. Huber, *Science*, 2010, **330**, 1222-1227.
22. E. L. Kunkes, D. A. Simonetti, R. M. West, J. C. Serrano-Ruiz, C. A. Gärtner and J. A. Dumesic, *Science*, 2008, **322**, 417.
23. I. T. Horváth and P. T. Anastas, *Chem. Rev.*, 2007, **107**, 2169-2173.
24. J. N. Chheda, G. W. Huber and J. A. Dumesic, *Angew. Chem.*, 2007, **119**, 7298-7318; *Angew. Chem. Int. Ed.*, 2007, **46**, 7164-7183.
25. G. W. Huber, S. Iborra and A. Corma, *Chem. Rev.*, 2006, **106**, 4044-4098.
26. P. T. Anastas and J. C. Warner, *Green Chemistry: Theory and Practice*, Oxford University Press, Incorporated, 1998.
27. S. R. Collinson and W. Thielemans, *Coord. Chem. Rev.*, 2010, **254**, 1854-1870.
28. J. Zakzeski, P. C. A. Bruijninx, A. L. Jongerius and B. M. Weckhuysen, *Chem. Rev.*, 2010, **110**, 3552-3599.
29. R. Massey and M. Jacobs, Global Chemicals Outlook 2013, *Chapter I: Trends and Indicators*, United Nations Environment Programme, 2013.
30. T. J. Korstanje, J. T. B. H. Jastrzebski and R. J. M. Klein Gebbink, *Chem. Eur. J.*, 2013, **19**, 13224-13234.
31. T. J. Korstanje, E. F. de Waard, J. T. B. H. Jastrzebski and R. J. M. K. Gebbink, *ACS Catal.*, 2012, **2**, 2173-2181.
32. T. Korstanje and R. M. K. Gebbink, in *Organometallics and Renewables*, eds. M. A. R. Meier, B. M. Weckhuysen and P. C. A. Bruijninx, Springer Berlin Heidelberg, 2012, vol. 39, ch. 4, pp. 129-174.

33. T. J. Korstanje, J. T. B. H. Jastrzebski and R. J. M. K. Gebbink, *ChemSusChem*, 2010, **3**, 695-697.
34. M. M. Abu-Omar, E. H. Appelman and J. H. Espenson, *Inorg. Chem.*, 1996, **35**, 7751-7757.
35. M. Shiramizu and F. D. Toste, *Angew. Chem.*, 2013, **125**, 13143-13147; *Angew. Chem. Int. Ed.*, 2013, **52**, 12905-12909.
36. S. Liu, A. Senocak, J. L. Smeltz, L. Yang, B. Wegenhart, J. Yi, H. I. Kenttämä, E. A. Ison and M. M. Abu-Omar, *Organometallics*, 2013, **32**, 3210-3219.
37. J. Yi, S. Liu and M. M. Abu-Omar, *ChemSusChem*, 2012, **5**, 1401-1404.
38. M. Shiramizu and F. D. Toste, *Angew. Chem.*, 2012, **124**, 8206-8210; *Angew. Chem. Int. Ed.*, 2012, **51**, 8082-8086.
39. J. E. Ziegler, M. J. Zdilla, A. J. Evans and M. M. Abu-Omar, *Inorg. Chem.*, 2009, **48**, 9998-10000.
40. H. Lange, S. Decina and C. Crestini, *Eur. Polym. J.*, 2013, **49**, 1151-1173.
41. C. Crestini, M. Crucianelli, M. Orlandi and R. Saladino, *Catal. Today*, 2010, **156**, 8-22.
42. C. Crestini, M. C. Caponi, D. S. Argyropoulos and R. Saladino, *Biorg. Med. Chem.*, 2006, **14**, 5292-5302.
43. C. Crestini, P. Pro, V. Neri and R. Saladino, *Biorg. Med. Chem.*, 2005, **13**, 2569-2578.
44. T. Michel, M. Cokoja and F. E. Kühn, *J. Mol. Catal. A: Chem.*, 2013, **368–369**, 145-151.
45. S. A. Hauser, M. Cokoja and F. E. Kühn, *Catal. Sci. Technol.*, 2013, **3**, 552-561.
46. T. Michel, M. Cokoja, V. Sieber and F. E. Kühn, *J. Mol. Catal. A: Chem.*, 2012, **358**, 159-165.
47. M. Carril, P. Altmann, W. Bonrath, T. Netscher, J. Schutz and F. E. Kühn, *Catal. Sci. Technol.*, 2012, **2**, 722-724.
48. T. Michel, D. Betz, M. Cokoja, V. Sieber and F. E. Kühn, *J. Mol. Catal. A: Chem.*, 2011, **340**, 9-14.
49. M. Carril, P. Altmann, M. Drees, W. Bonrath, T. Netscher, J. Schütz and F. E. Kühn, *J. Catal.*, 2011, **283**, 55-67.
50. L. B. Davin and N. G. Lewis, *Curr. Opin. Biotechnol.*, 2005, **16**, 407-415.
51. M. R. Sturgeon, M. H. O'Brien, P. N. Ciesielski, R. Katahira, J. S. Kruger, S. C. Chmely, J. Hamlin, K. Lawrence, G. B. Hunsinger, T. D. Foust, R. M. Baldwin, M. J. Bidy and G. T. Beckham, *Green Chem.*, 2014, **16**, 824-835.
52. Y. Ren, M. Yan, J. Wang, Z. C. Zhang and K. Yao, *Angew. Chem.*, 2013, **125**, 12906-12910; *Angew. Chem. Int. Ed.*, 2013, **52**, 12674-12678.

53. A. G. Sergeev, J. D. Webb and J. F. Hartwig, *J. Am. Chem. Soc.*, 2012, **134**, 20226-20229.
54. A. G. Sergeev and J. F. Hartwig, *Science*, 2011, **332**, 439.
55. A. G. Sergeev and J. F. Hartwig, *Science*, 2011, **332**, 439-443.

“Biomass energy in the form of wood had fuelled the world’s economy for thousands of years before the advent of more easily winnable coal and subsequently oil, gas, and uranium.”

— Paul O’Connor, 2013

4. Results and Discussion – Publication Summaries

In this chapter, short summaries of the publications submitted during the course of this dissertation are presented. The full manuscripts can be found in the appendix of the thesis. Moreover, also non-published results are included.

4.1 Methyldioxorhenium in the Cleavage of C–O Bonds in Lignin Model Compounds

This chapter originates from the following publication:¹

Reentje G. Harms, Iulius I. E. Markovits, Markus Drees, Wolfgang A. Herrmann, Mirza Cokoja and Fritz E. Kühn, “Cleavage of C–O Bonds in Lignin Model Compounds Catalyzed by Methyldioxorhenium in Homogeneous Phase”,

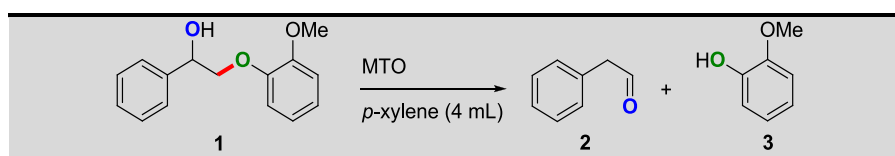
ChemSusChem **2014**, 7, 429–434.

(refer to 6.1.2)

In this manuscript, the first example of a C–O bond cleavage catalysed by methyldioxorhenium (MDO) is described. Furthermore, this is the first example on the non-oxidative rhenium-catalysed refining of a wide range of lignin model compounds. An entirely new reactivity of MDO was discovered which now became well understood due to detailed mechanistic studies conducted in this work.

The treatment of the simple, but commonly applied, lignin β -O-4 model compound **1** with catalytic amounts of MTO in *p*-xylene at 135 °C in homogeneous phase yields into quantitative and redox-neutral cleavage to phenylacetaldehyde (**2**) and guaiacol (**3**) as depicted in the head of Table 4-1. For this reaction, a catalyst concentration of 5 mol%, a reaction temperature of 135 °C, and 12 h reaction time were elucidated as optimal reaction parameters (Entry 1). Shorter reaction time resulted in worse conversion (Entry 2), however, prolonged reaction time decreases the yield of **2** (Entry 3) due to decomposition of **2** caused by its temperature and acid sensitivity (MTO is Lewis acidic). Lower catalyst loadings gave incomplete conversions even after prolonged reaction times (Entry 4). At elevated temperature, complete conversion is obtained after only 10 h, but decomposition of **2** also takes place faster (Entry 5). The catalytic system itself is very stable and the same catalyst loading can be used for at least five consecutive runs (substrate is re-added after full conversion of **1** and quantitative cumulative yield of **3** is observed).

Table 4-1. Influence of the reaction parameters temperature, catalyst concentration, and reaction time on the C–O cleavage of 2-(2-methoxyphenoxy)phenylethanol (**1**) to phenylacetaldehyde (**2**) and guaiacol (**3**).



Entry	Cat. conc. [mol%]	Temp. [°C]	t [h]	Conv. [%] ^a	Yield 2 [%] ^a	Yield 3 [%] ^a
1	5	135	12	>99	95	>98
2	5	135	4	8	-	-
3	5	120	24	35	18	19
4	2.5	135	24	65	40	46
5	5	155	10	>99	80	>98
6	0	135	12	0	-	-

a) Determined by GC FID and ¹H NMR spectroscopy versus an internal standard.

The catalytic active species MDO is generated *in situ* by reduction upon oxygen abstraction. Reaction of the air-stable precursor MTO with the secondary alcohol group of the substrate **1** molecule gives MDO and ketone **1a** (see Scheme 4-1). The kinetic reaction profile underlines the relevance of MDO. Whereas application of MTO shows a long induction period up to three hours, the MDO-hexyne complex exhibits none.

Nota bene, DFT calculations revealed that in MDO, rhenium exhibits a free electron pair in the σ -symmetric HOMO with a graphical expression depicted in Figure 4-1. Hence, MDO is acting rather as Lewis base and not like MTO as Lewis acid – its constitutive chemistry changes by oxygen abstraction and 2 electron reduction.² It is known that MDO forms stable Lewis acid/base pairs with e.g. MTO or π -acceptors such as alkynes.³⁻⁵ Thus, the appearance of MDO could be proven by “trapping” it as 3-hexyne complex which, is sufficiently stable at room temperature to be detected on NMR time scale.

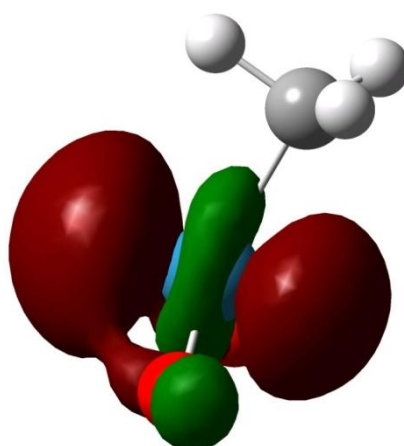
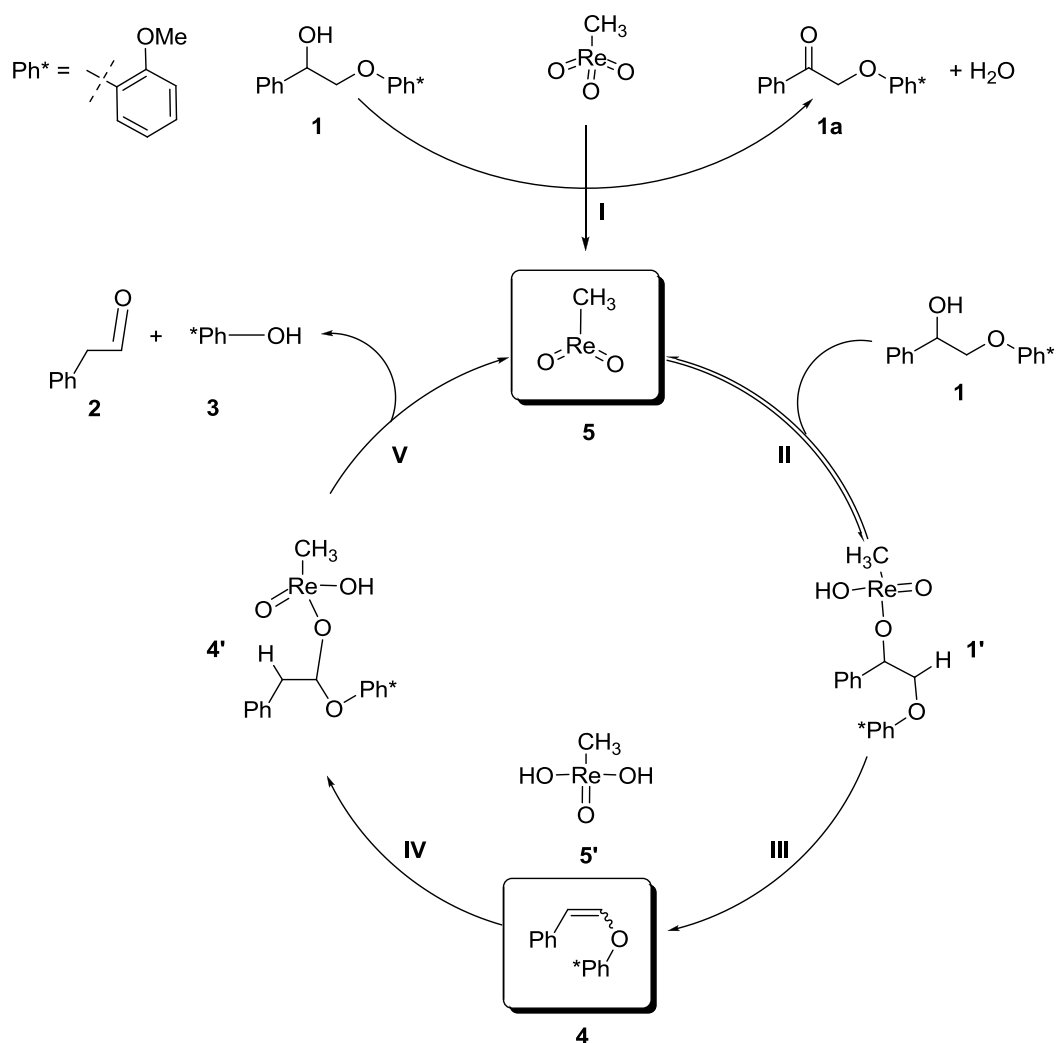


Figure 4-1. Graphical expression of the HOMO of MDO – taken from Mulliken population analysis and cubegen as implemented in Gaussian09.



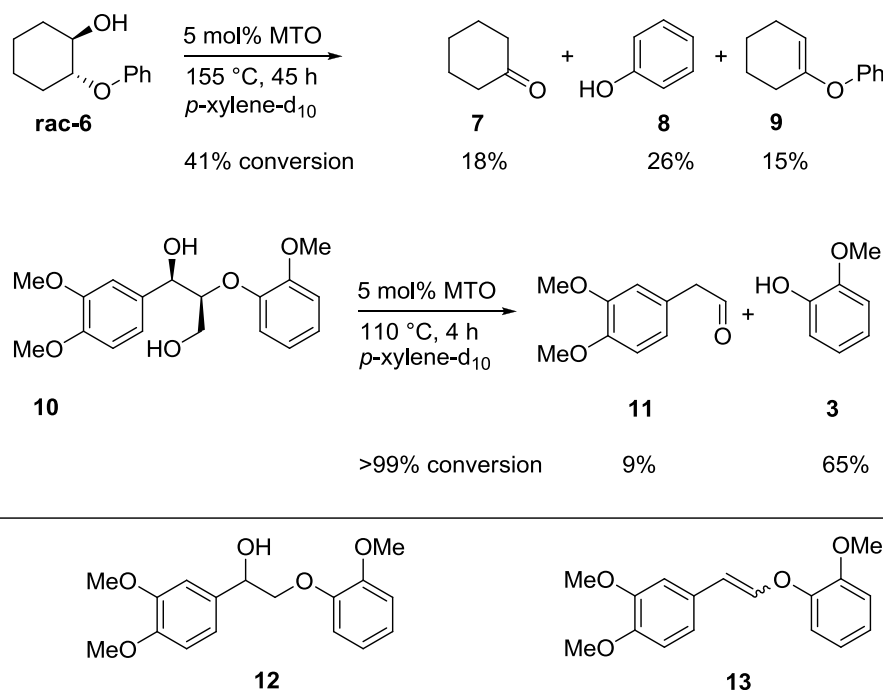
Scheme 4-1. Proposed mechanism of the MTO/MDO-catalysed C–O bond cleavage of **1** over the observed intermediate **4**. Possible intermediates **1'** (–13.7 kcal/mol) and **4'** (1.4 kcal/mol) are based on DFT calculations, the respective ΔG values (zero-point energy refers to **5**) are given in brackets.

During the reaction, the appearance of enol-ether **4** is observed. The enol-ether **4** was found to be a stable and isolable intermediate, which forms readily prior to C–O bond cleavage to the products **2** and **3**. In deuterium- and ^{17}O -labelling and *in situ* ^1H , ^2H , ^{13}C , and ^{17}O NMR experiments it could be shown that 1) the carbon backbone of **1** remains unchained, 2) that **2** and **3** are originating from cleavage of **4**, 3) that oxygen transfer reaction from the catalyst and the substrate are involved, 4) and that labelled oxygen is only found in phenylacetaldehyde (**2**), thus no aryl–O bond cleavage occurs at all.

Taking into consideration all experimental results, DFT calculations allowed to propose a possible mechanism which is depicted in Scheme 4-1. Once MDO forms (step I), it reacts with a second molecule of **1** forming an alcoholate adduct **1'** (step II). Subsequent dehydration forms enol ether **4** (step III) due to the exergonic elimination of the rhenium(V) bis(hydroxo) species **5'**. Then, **5'** (formally) adds an O and H atom to the double bond forming acetal **4'** (step IV) consisting a phenoxy group and a rhenium alcoholate. However,

in contrast to **1'** formation of **4'** is endergonic. Liberation of MDO and guaiacol (**3**) results in the C–O bond scission (step **V**). Noteworthy, the energy levels of the reaction pathway generating MDO from MTO due to the alcohol oxidation **1** to **1a** were also determined by DFT calculations. Here, the key transition states were found to have 8.4–11.9 kcal/mol higher ΔG energy values than calculated for **1'** and **4'**. The observed remarkable difference in the reactivity of MTO and MDO is also reflected by the ΔG energy values of their respective alcoholates. Whereas addition of **1** to MTO is endergonic, an exergonic reaction of **1** and MDO to **1'** was revealed.

The C–O bond cleavage was also successfully applied on the β -O-4 linkage model compounds **rac-6** and **10**, which show an identical reaction mechanism via the enol ether intermediates **9** and **13** (see Scheme 4-2). As a drawback, **10** is very sensitive under the applied reaction conditions and undergoes decarbonylation to **12**. Moreover, the yield of aldehyde **11** is decreased due to the formation of several side products which were identified to a certain extent by means of gas chromatography/mass spectrometry.



Scheme 4-2. MDO-catalysed C–O bond cleavage of non-benzylic β -hydroxy aryl ether **rac-6** and lignin model compound **10**, which cleavage gave several side products such as 4-propenyl-1,2-dimethoxybenzene, 3,4-dimethoxybenzaldehyde, (3,4-dimethoxyphenyl)acetone, (3,4-dimethoxyphenyl)ethanone, 3,4-dimethoxybenzoic acid methyl ester, 3,4-dimethoxymandelic acid methyl ester, (3,4-dimethoxyphenyl)-2-propenal).

In summary, an efficient and selective method for the cleavage of C–O bonds of several β -hydroxy aryl ethers with catalytic amounts of MTO is presented. As the catalyst system requires no additional reagents, is remarkably stable under the applied reaction conditions, and can be reused without loss of activity, it appears to be superior to other homogeneous

Re,^{6,7} Ni,⁸ Fe,^{9,10} or Ru catalysts.¹¹⁻¹³ It could be shown that the catalyst is able to cleave a broad scope of substrates. With perspective to degrade even polymeric β -O-4 linkages, and thus native lignin or epoxy resins, these results are promising for plastic recycling and biomass refining issues.

4.2 Rhenium Heptoxide in the Cleavage of C–O Bonds in Lignin Model Compounds

This chapter originates from the following publication:

Reentje G. Harms, Lilian Graser, S. Schwaminger, Wolfgang A. Herrmann and Fritz E. Kühn,
“Re₂O₇ in C–O bond cleavage of a β -O-4 lignin model linkage: A highly active Lewis acidic
catalyst in heterogeneous phase”,

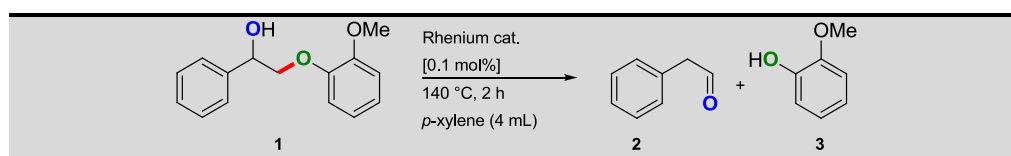
In preparation

(refer to 6.1.3)

In this research work, the most active and thus benchmarking catalyst for the C–O bond cleavage of 2-(2-methoxyphenoxy)phenylethanol (**1**), a commonly used and the most stable β -O-4 lignin model compound, has been investigated (see Table 4-2). The linkage in compounds similar to **1** was previously reported to be labile towards treatment with both Brønsted and Lewis acids such as sulphuric acid or ferric chloride.¹⁴⁻¹⁶ Re₂O₇ and MTO are published to efficiently catalyse the dehydration of benzylic alcohols similar to **1** in aromatic media.^{17,18} Based on the reported reactivity, Lewis acids and rhenium oxides were studied in their catalytic activity.

The systematic screening of various Lewis acids revealed rhenium heptoxide (see Table 4-2) as the most active catalyst which yields in quantitative substrate conversion, excellent mass balance, and selectivity towards two cleavage products as phenylacetaldehyde (**2**) and guaiacol (**3**). Although less pricy Lewis acids as scandium triflate also gave full conversion, the usability is limited due to the pronounced acid sensitivity of **2**. Furthermore, the capability of rhenium to catalyse the cleavage of **1** has been evaluated with several commercially available rhenium compounds, from rhenium(0) to ordinary rhenium oxides.

Table 4-2. Overview on the catalytic activity of different rhenium(0) and rhenium oxide compounds ranging from Re(IV), Re(VI), to Re(VII) under optimised catalytic reaction conditions.



Entry	Rhenium compound	Conv. 1 [%] ^a	Yield 2 [%] ^a	Yield 3 [%] ^a
1	none	0	-	-
2	Re powder (325 mesh)	7	2	3
3	Re ₂ (CO) ₁₀	24	11	13
4	ReO ₂ ^b	0	0	0
5	ReO ₃ ^b	0	0	0
6	AgReO ₄	6	2	4
7	NH ₄ ReO ₄ ^c	15	4	6
8	HReO ₄	91	42	44
9	Re ₂ O ₇	>99	96	97

Reaction conditions: 0.1 mol% rhenium-compound, 4 mL *p*-xylene, 140°C, 2 h; a) conversions and yields were determined by GC FID; b) conducted under argon atmosphere c) aqueous stock solution precluded solubility issues.

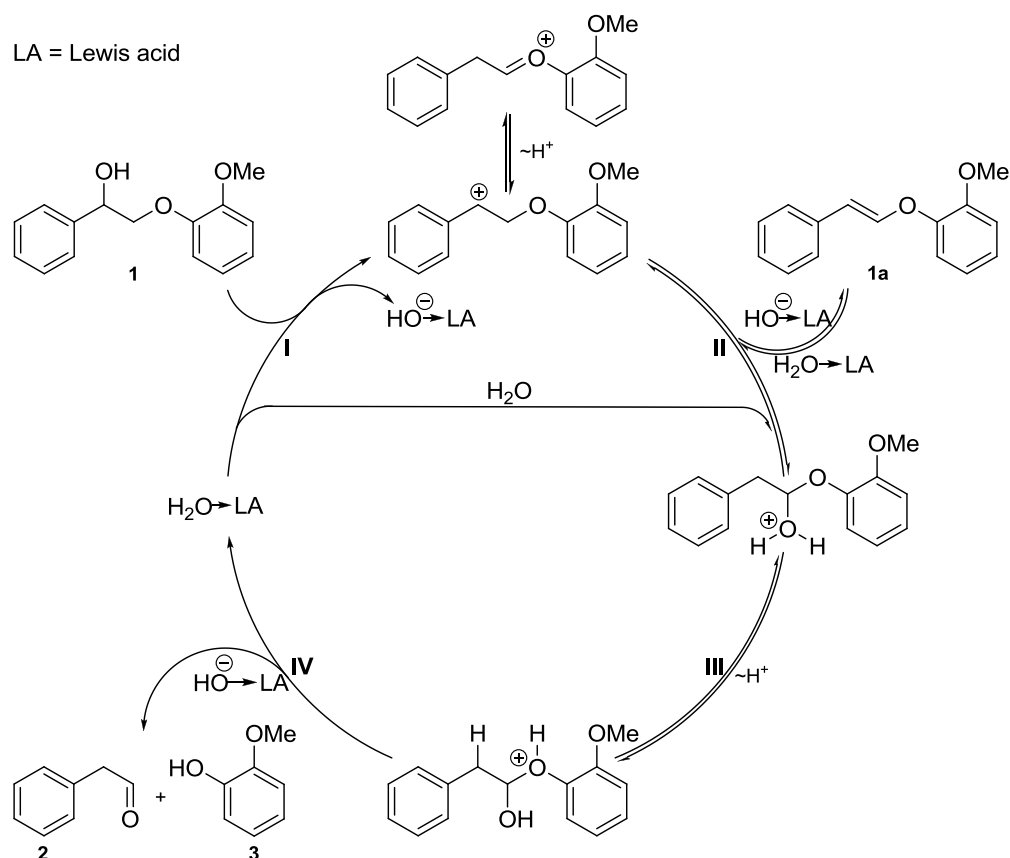
Whereas Re(IV) and Re(VI) oxides exhibit no catalytic activity, Re(VII) oxides do. Re₂O₇ shows an outstanding activity reflected by a turnover frequency of TOF = 2400 h⁻¹ (at 20% conversion, reaches full conversion after 2 h) and a turnover number of TON = 2200. Due to the nature of Re(0) compounds being easily oxidised (to Lewis acidic oxides), the observed but low activity of Re(0) is probably explained.

Re₂O₇ was identified as the actual catalyst which stays in form of fine particle in heterogeneous phase. Filtration of the reaction solution after 50% conversion of **1** through a layer of diatomaceous earth showed no further conversion in the filtrate, however, when filtered through a syringe filter with 0.45 μm pore size an unchanged activity is observed.

After complete conversion, intact Re₂O₇ could be identified by aqueous extraction (hydrolysis to two equivalents HReO₄) and subsequent precipitation as AgReO₄. Furthermore, the pH value of the aqueous extract indicated a residual amount of 55% Re₂O₇.

However, as a major drawback, the formation of a black, insoluble decomposition product is observed. An isolated and washed sample exhibits no residual catalytic activity. Elemental analysis revealed high contents of rhenium (56%) and carbon (19%). In a blind test heating a suspension of Re₂O₇ and *p*-xylene, again the black decomposition product appears. X-ray photoelectron spectroscopy revealed the formation of rhenium(0) and graphite. Furthermore, graphitic carbon, carbon nanotubes and ReO₂ are identified by means of Raman spectroscopy; however, elemental rhenium is not Raman active.

Based on the observed intermediate enol ether **4**, a first order behaviour in the kinetic profile, and the absence of an induction period, a mechanism is proposed as depicted in Scheme 4-3 (*vide supra*), which was adapted from similar work previously published on the acid-catalysed C–O bond cleavage of various β-hydroxy aryl ether.^{14-16,19}



Scheme 4-3. Mechanistic proposal of the Lewis acid-catalysed C–O bond cleavage of β -O-4 lignin model compound **1**. The proposal is adapted from both the Brønsted acid-catalysed C–O bond cleavage reaction of **1**, and the MTO-catalysed dehydration reaction of benzylic alcohols according to Aoyama *et al.* and Korstanje *et al.*^{14,19}

In summary, an outstandingly efficient and selective catalytic system for the C–O bond cleavage of a very stable and commonly used β -O-4 lignin model compound has been developed. For the cleavage of **1**, rhenium heptoxide is so far the most active catalyst which has been reported. Moreover, the active catalyst remains as fine particle in heterogeneous phase and the observed remarkable activity is based on its pronounced Lewis acidity. These promising results disclose Lewis acids are very efficient catalysts for the cleavage of C–O bonds as found in native lignin. In future applications Lewis acids may assist the paper and pulp industry to develop more environmentally benign processes.

4.3 Excursus: Single X-Ray Crystallographic Structure of MTO

This chapter contains unpublished results:

Reentje G. Harms, Alexandra P. Gerstle, Alexander Pöthig, Wolfgang A. Herrmann and Fritz E. Kühn, "Single X-Ray Crystallographic Structure of MTO".

Since in the late 80s when Herrmann *et al.* developed an elegant and versatile synthetic route for preparing MTO in large scale,²⁰ much research has been conducted in this field of organometallic chemistry. When the extraordinary catalytic activity of MTO in homogeneous olefin metathesis and olefin epoxidation was discovered, a large community became interested in investigating the coordination chemistry of organorhenium compounds, as well as in the synthesis of additional derivatives.²¹⁻²³ Although many organorhenium trioxides R–ReO₃ could be synthesised, their role in catalysis is limited because higher alkyl-homologues decompose easily due to their pronounced instability of the rhenium carbon bond (Re–R, R = alkyl > CH₃).²⁴ Moreover, in solution an intramolecular β-hydride elimination pathway is observed at the higher alkyl-homologues (MTO bears no β-hydrides). Due to the very strong rhenium carbon bond MTO is, in an organometallic point of view, extraordinarily stable, but UV irradiation results in (photo)homolysis to •CH₃ and •ReO₃ radicals. The strength of the Re–C bond is reflected by the bond distance, and de facto the bond length in MTO is significantly shorter (206 pm) than in the less stable ethyltrioxorhenium derivative (210 pm). Moreover, chemists were interested in the existence of α-agostic interaction (Re...H–C bond) since they would reveal further decomposition pathways.

Those interactions are usually revealed by means of X-ray crystallography; however, a suitable single X-ray structure of MTO with satisfactory R values could never be obtained. As a reason of failure, the instability of the crystal in the X-ray beam was stated.^{25,26} Instead, the structure was determined via DFT calculations,² gas phase electron diffraction,²⁶ and powder neutron diffraction of the heavy derivative CD₃ReO₃.²⁵ In none of the obtained structures α-agostic interactions were found. In the structure the rhenium atom is located in the centre of an almost ideal tetrahedron formed by the methyl group and the three oxides. The methyl group nearly satisfies C₃ symmetry and is arranged staggered with respect to the ReO₃ fragment.

In order to gain an in-depth understanding of alcohol rhenium interactions, this work aimed at preparing and isolating MTO-alcohol adducts from concentrated alcoholic solutions of MTO (methanol, ethanol, 1-propanol, 2-propanol, but also acetonitrile), stored at 4 °C. The

dissolution of MTO in alcohols produces yellow solutions, indicating the desired rhenium alcohol coordination (since solutions in non-coordinating solvents usually are colourless); however, from all latter solutions colourless crystals grew. A ^1H NMR analysis revealed the crystals consisting of non-coordinated MTO. In contrast to crystals obtained via sublimation or ordinary crystallisation, not needles but cuboids formed. A single X-ray crystallographic analysis discloses the first single X-ray crystallographic structure of MTO with satisfactory R values as depicted in Figure 4-2.

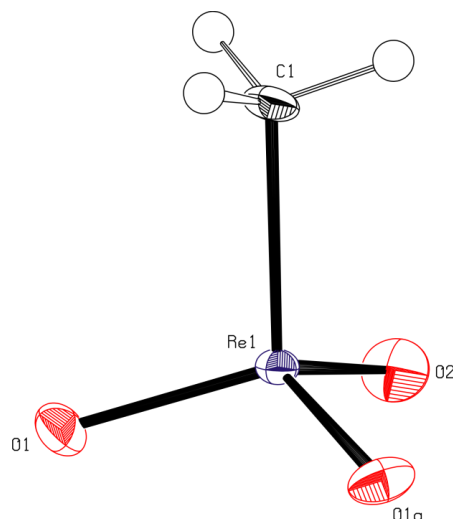


Figure 4-2. ORTEP style plot of MTO. Ellipsoids are shown at 50% probability level. Bond lengths (Å) and angles (deg): Re1–C1 2.060, Re1–O1 1.705, Re1–O1a 1.705, Re1–O2 1.691, O2–Re1–O1 112.3, O1–Re1–O1a 113.3, C1–Re1–O1 106.3, C1–Re1–O2 105.7.

Table 4-3. Crystallographic data/parameters of MTO

refined composition	$\text{CH}_3\text{O}_3\text{Re}$
M_r [g/mol]	249.24
T [K]	120(3)
λ [pm]	71.073
crystal system	monoclin
space group	$Cmc2_1$
a [pm]	743.93 (4)
b [pm]	1034.44 (6)
c [pm]	503.25 (3)
$\alpha = \beta = \gamma$ [°]	90
V [10^6 pm 3]	387.277
Z	4
crystal size [mm]	0.144 x 0.264 x 0.347
parameter refined/restrictions	30/2
R1 [$I > 4\sigma(I)$]	0.0267
R1 (all data)	0.0272
$\Delta\rho_{\text{min}}$ (max/min) [$\text{e}\cdot\text{\AA}^{-3}$]	5.899/ -3.267

A comparison with previously published data (bond lengths, angles) shows only marginal alterations, (see Table 4-4) underlining alternative methods to be very eligible for structure determination. As previously determined, within the structure, rhenium is located in an almost ideal tetrahedron, formed by the methyl group and the oxo-ligand. The methyl group again

nearly satisfies C_3 symmetry and is arranged staggered with respect to the ReO_3 fragment. The tetrahedron is not distorted; therefore any α -agostic interactions of any hydrogen atoms with the rhenium centre are excluded. Furthermore, it is unlikely that an improved refinement of the residual electron density $\Delta\rho_{fin}$ (last entry Table 4-3) will result in any surprising changes of the observed structural values.

Table 4-4. Comparison of the crystallographic data of MTO obtained via single crystal X-ray diffraction, powder neutron diffraction,²⁵ and gas phase electron diffraction.²⁶

Diffraction method	Re1–C1 [pm]	Re1–O1 [pm]	Re1–O2 [pm]	O2–Re1–O1 [°]	O1–Re1–O1 [°]	C1–Re1–O1 [°]	C1–Re1–O2 [°]
single X-ray	206.0	170.5	169.1	112.3	113.3	106.3	105.7
powder neutron ^a	206.3(2)	170.2(1)	170.2(2)	112.8(1)	113.2(1)	105.9(1)	105.4(1)
gas phase electron	206.0(9)	170.9(3)	n.a. ^b	113.0(3)	n.a. ^b	106.0(2)	n.a. ^b

a) Deuterium isomer CD_3ReO_3 b) degeneracy of Re–O bonds and angles due to identical O-atoms.

In summary, the single X-ray crystallographic structure of MTO was obtained with a very high R value finishing a more than 20 years lasting endeavour. The crystallographic data again proves the eligibility of alternative methods for determination of the crystal structure. Not surprisingly, only marginal alterations to the data, obtained via DFT calculations, powder neutron diffraction, and gas phase electron diffraction, are found. Furthermore, the short rhenium carbon bonding of 206 pm and the absence of any α -agostic interactions, which are excluded by the observed nearly perfect undistorted tetrahedral structure, again explain MTO's stability. Moreover, the obtained structure disproves the myth of MTO decomposition in X-ray beams.

4.4 References in Chapter 4

1. R. G. Harms, I. I. E. Markovits, M. Drees, W. A. Herrmann, M. Cokoja and F. E. Kühn, *ChemSusChem*, 2014, **7**, 429-434.
2. S. Köstlmeier, V. A. Nasluzov, W. A. Herrmann and N. Rösch, *Organometallics*, 1997, **16**, 1786-1792.
3. W. A. Herrmann, J. K. Felixberger, J. G. Kuchler and E. Herdtweck, *Z. Naturforsch.*, 1990, **45b**, 876-886.
4. J. K. Felixberger, J. G. Kuchler, E. Herdtweck, R. A. Paciello and W. A. Herrmann, *Angew. Chem.*, 1988, **100**, 975-978; *Angew. Chem. Int. Ed.*, 1988, **27**, 946-948.
5. W. A. Herrmann, P. W. Roesky, M. Wang and W. Scherer, *Organometallics*, 1994, **13**, 4531-4535.
6. C. Crestini, M. C. Caponi, D. S. Argyropoulos and R. Saladino, *Biorg. Med. Chem.*, 2006, **14**, 5292-5302.
7. C. Crestini, P. Pro, V. Neri and R. Saladino, *Biorg. Med. Chem.*, 2005, **13**, 2569-2578.
8. A. G. Sergeev and J. F. Hartwig, *Science*, 2011, **332**, 439-443.
9. Y. Ren, M. Yan, J. Wang, Z. C. Zhang and K. Yao, *Angew. Chem.*, 2013, **125**, 12906-12910; *Angew. Chem. Int. Ed.*, 2013, **52**, 12674-12678.
10. H. Lange, S. Decina and C. Crestini, *Eur. Polym. J.*, 2013, **49**, 1151-1173.
11. J. M. Nichols, L. M. Bishop, R. G. Bergman and J. A. Ellman, *J. Am. Chem. Soc.*, 2010, **132**, 12554-12555.
12. T. vom Stein, T. Weigand, C. Merkens, J. Klankermayer and W. Leitner, *ChemCatChem*, 2013, **5**, 439-441.
13. A. Wu, B. O. Patrick, E. Chung and B. R. James, *Dalton Trans.*, 2012, **41**, 11093-11106.
14. M. Aoyama, C.-L. Chen and D. Robert, *J. Chin. Chem. Soc.*, 1991, **38**, 77-84.
15. M. R. Sturgeon, S. Kim, K. Lawrence, R. S. Paton, S. C. Chmely, M. Nimlos, T. D. Foust and G. T. Beckham, *ACS Sus. Chem. Eng.*, 2014, **2**, 472-485.
16. K. Lundquist and R. Lundgren, *Acta Chem. Scand.*, 1972, **26**, 2005-2023.
17. T. J. Korstanje, E. F. de Waard, J. T. B. H. Jastrzebski and R. J. M. K. Gebbink, *ACS Catal.*, 2012, **2**, 2173-2181.
18. T. J. Korstanje, J. T. B. H. Jastrzebski and R. J. M. K. Gebbink, *ChemSusChem*, 2010, **3**, 695-697.
19. T. J. Korstanje, J. T. B. H. Jastrzebski and R. J. M. Klein Gebbink, *Chem. Eur. J.*, 2013, **19**, 13224-13234.
20. W. A. Herrmann, J. G. Kuchler, J. K. Felixberger, E. Herdtweck and W. Wagner, *Angew. Chem.*, 1988, **100**, 420-422; *Angew. Chem. Int. Ed.*, 1988, **27**, 394-396.

21. W. A. Herrmann and F. E. Kühn, *Acc. Chem. Res.*, 1997, **30**, 169-180.
22. C. C. Romão, F. E. Kühn and W. A. Herrmann, *Chem. Rev.*, 1997, **97**, 3197-3246.
23. W. A. Herrmann, R. W. Fischer, W. Scherer and M. U. Rauch, *Angew. Chem.*, 1993, **105**, 1209-1212; *Angew. Chem. Int. Ed.*, 1993, **32**, 1157-1160.
24. F. E. Kühn, Ph.D. thesis, Technische Universität München, 1994.
25. W. A. Herrmann, W. Scherer, R. W. Fischer, J. Bluemel, M. Kleine, W. Mertin, R. Gruehn, J. Mink and H. Boysen, *J. Am. Chem. Soc.*, 1995, **117**, 3231-3243.
26. W. A. Herrmann, P. Kiprof, K. Rypdal, J. Tremmel, R. Blom, R. Alberto, J. Behm, R. W. Albach and H. Bock, *J. Am. Chem. Soc.*, 1991, **113**, 6527-6537.

“Renewable biomass presents tremendous opportunities to produce chemicals. As a consequence, new methods and materials based on biomass refining are emerging for the chemical industry to use as feedstock.”

— Simon R. Collinson, 2010

5. Summary and Conclusion

Focus of this research project was the development of novel rhenium based catalysts for the degradation of lignin. For an efficient depolymerisation application of a catalyst competent cleaving the most abundant motif in native lignin, the β -O-4 linkage, is required. In this work all studies were conducted on model compound **1**, a simplified organic construct of the β -O-4 contained in native lignin (see Figure 5-1).

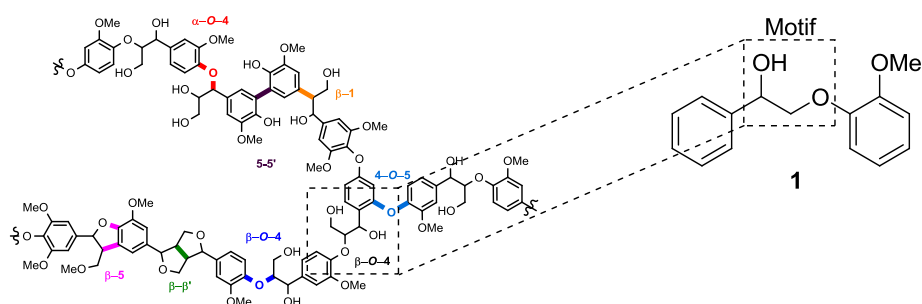
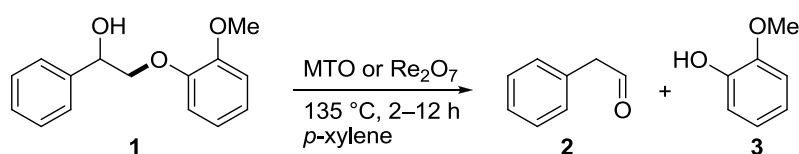


Figure 5-1. The “standard” model compound **1** is used to develop and benchmark degradation catalysts.

Previously, Crestini and Saladino *et al.* (please refer Chapter 2) reported the oxidative MTO-catalysed degradation of lignin model compounds. However, under the reported reaction conditions (20 mol% MTO, H_2O_2 , acetic acid, r.t.) no cleavage of **1** could be obtained, rendering MTO/ H_2O_2 unsuitable for the depolymerisation of native lignin. Variations of the reaction conditions (solvents, temperature, reaction time, catalysts loading, *N*-base addition) resulted in no improvement.

In this research study, MTO has been discovered to catalyse the desired C–O cleavage of **1** when the reaction is conducted under redox-neutral conditions, in hydrocarbon solvents, and at elevated temperatures (see Scheme 5-1).



Scheme 5-1. MTO and rhenium heptoxide catalyse the C–O bond cleavage of the standard lignin model compound **1** yielding phenylacetaldehyd (**2**) and guaiacol (**3**) in quantitative yields.

Reaction of 5 mol% MTO with **1** in *p*-xylene at 135 °C yields in quantitative formation of phenylacetaldehyde (**2**) and guaiacol (**3**) without addition of any co-catalysts or reagents.

Indeed, it was established that the actual catalyst is methylidioxorhenium (MDO) which is formed *in situ* from MTO. In accordance with cited works (refer to Chapter 2), MTO undergoes redox reaction with the secondary alcohol group of the substrate at higher temperatures, forming MDO and a ketone.

This is the first example of rhenium to catalyse the selective C–O bond cleavage in β -O-4 model compounds. The catalytic system is very stable in homogeneous phase and the same catalyst loading can be used for at least five consecutive runs. The obtained catalyst activity is rather low, which reveals a turnover frequency of $\text{TOF} = 8 \text{ h}^{-1}$ and a turnover number of $\text{TON} = 100$. Furthermore, it could be shown that MTO can be applied on a variety of β -O-4 linkage model compounds.

In a follow-up project it has been discovered that rhenium heptoxide too catalyses the highly selective C–O bond cleavage of **1**. The reaction is conducted under the same conditions, but in contrast only 0.1 mol% catalyst loading and 2 h reaction time are necessary to obtain complete conversion to **2** and **3**, thus Re_2O_7 is superior to MTO/MDO. Moreover, the kinetic reaction profile shows that Re_2O_7 remains unchanged in the heterogeneous phase and catalyses the cleavage reaction remarkably efficient. The observed kinetic data revealed that rhenium heptoxide is 300 times more active than MTO bearing a turnover frequency of $\text{TOF} = 2400$ and number of $\text{TON} = 2200$. *Nota bene*, rhenium heptoxide is the most active catalyst for the cleavage of model compound **1** which has been reported so far.

The high discrepancy in activity between MTO and Re_2O_7 is explained due to the fact that the catalysts follow fundamental different mechanism pathways. MTO/MDO obeys a molecular mechanism. Once MDO is formed, it reacts with **1** to an acoholate followed by elimination/dehydration. Subsequently, the methylrhenium (dihydroxy)monoxide (MDO hydrate) add formally to the enol ether double bond and forms a rhenium acetal. Liberation of MDO then yields in C–O cleavage. DFT calculations reveal an only slightly exergonic reaction profile, however, the cleavage remains disfavoured kinetically due to high energies found in the transition states.

In contrast rhenium heptoxide is a Lewis acid catalyst which shows inhibition upon addition of Lewis bases. Here, all mechanistic steps are similar to a sequence of Brønsted acid-catalysed dehydration and enol ether hydrolysis. Rapid acid/base reaction explains the high catalyst activity. Apparently, MTO's Lewis acidity is too low for an acid-catalysed reaction pathway, which is exposed clearly in the observed kinetic profile and the long induction period.

In a side project, the interaction of MTO with alcohols and coordinating solvents such as methanol, ethanol, or acetonitrile was investigated. We were interested to evidence the

coordination of alcohols to MTO, which is indicated by the change of colour in alcoholic solutions. Although no adducts could be crystallised from a concentrated solution, single X-ray crystallographic suitable crystals were obtained (see Figure 5-2). The obtained structure shows only marginal alteration to the previously published data obtained via DFT calculations, powder neutron diffraction, and gas phase electron diffraction. As expected, the non-distorted almost ideal tetrahedral structure excludes the existence of any α -agostic rhenium–hydrogen interaction, which is in agreement with the published data. Moreover, the latter results prove that exposure of MTO to X-ray beams do not result in significant decomposition.

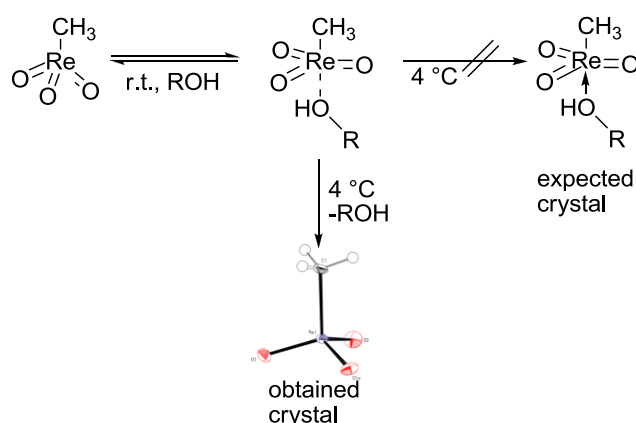


Figure 5-2. Proposed coordination of alcohols to MTO. Alcohol-MTO adducts cannot be crystallised from concentrated solutions, however, instead pure MTO crystals eligible for X-ray crystallographic single structure determination grow.

In summary, two novel rhenium based catalytic systems for the C–O cleavage of **1** were developed. An entirely new reactivity of MDO was found and the rudimentary mechanism was elucidated. Moreover, the catalytic activity observed using rhenium heptoxides set the benchmark to the community.

In future work the catalysts will be studied on model polymers. The low solubility of the polymers is an apparent obstacle, thus a reaction medium, in which the catalyst remains active but nevertheless dissolves the polymers, needs to be investigated.

The latter results are promising and might assist the pulp and paper industry to develop more efficient and sustainable processes. Highly active β -hydroxy aryl ether depolymerisation catalysts can be applied to permit the down-cycling of epoxy resins.

Furthermore, for the first time the single X-ray crystallographic structure of MTO was determined.

6. Bibliographic Details and Reprint Permissions

6.1 Bibliographic Details for Complete Publications

This chapter is devoted to provide the reader with bibliographic details of the publications summarised in Chapter 4 of this dissertation to allow for retrieval of the original manuscript and supplementary.

6.1.1 Organorhenium Dioxides as Oxygen Transfer Systems: Synthesis, Reactivity and Applications

Reentje G. Harms^a, Prof. Dr. Dr. h.c. mult. Wolfgang A. Herrmann^{b,*} and Prof. Dr. Fritz E. Kühn^{a,b,**}

^a Molecular Catalysis, Department of Chemistry and Catalysis Research Center, Technische Universität München, Lichtenbergstr. 4, 85747 Garching bei München, Germany

^b Chair of Inorganic Chemistry, Department of Chemistry and Catalysis Research Center, Technische Universität München, Lichtenbergstr. 4, 85747 Garching bei München, Germany

[*] Corresponding author. Tel.: +49 89 289 13096; fax: +49 89 289 13473.

[**] Corresponding author at: Molecular Catalysis, Department of Chemistry and Catalysis Research Center, Technische Universität München, Lichtenbergstr. 4, 85747 Garching bei München, Germany. Tel.: +49 89 289 13096; fax: +49 89 289 13473.

E-mail addresses: wolfgangherrmann@ch.tum.de (W.A. Herrmann), fritz.kuehn@ch.tum.de (F.E. Kühn).

Coord.Chem.Rev. **2015**, 296, 1–23. <http://dx.doi.org/10.1016/j.ccr.2015.03.015>

6.1.2 Cleavage of C–O Bonds in Lignin Model Compounds Catalyzed by Methyldioxorhenium in Homogeneous Phase

Reentje G. Harms, Iulius I. E. Markovits, Dr. Markus Drees, Prof. Dr. Dr. h.c. mult. Wolfgang A. Herrmann, Dr. Mirza Cokoja* and Prof. Dr. Fritz E. Kühn^{a,*}

^a Chair of Inorganic Chemistry/Molecular Catalysis, Catalysis Research Center, Technische Universität München, Ernst-Otto-Fischer-Str. 1, 85747 Garching bei München (Germany)

[*] Corresponding author Tel.: +49 89 289 13096; fax: +49 89 289 13473.

E-mail addresses: fritz.kuehn@ch.tum.de (F. E. Kühn), mirza.cokoja@ch.tum.de (M. Cokoja)

ChemSusChem **2014**, 7, 429–434, doi: 10.1002/cssc.201300918.

6.1.3 Re_2O_7 in C–O bond cleavage of a β –O–4 lignin model linkage: A highly active Lewis acidic catalyst

Reentje G. Harms^{†a}, Dr. Lilian Graser^{†b}, S. Schwaminger^c, Prof. Dr. Dr. h.c. mult. Wolfgang A. Herrmann^{a,*} and Prof. Dr. Fritz E. Kühn^{a,b,*}

^a Chair of Inorganic Chemistry, Catalysis Research Centre and Faculty of Chemistry, Technische Universität München, Lichtenbergstr. 4, D-85747 Garching bei München (Germany)

^b Molecular Catalysis, Catalysis Research Centre and Faculty of Chemistry, Technische Universität München, Lichtenbergstr. 4, D-85747 Garching bei München (Germany)

^c Faculty of Mechanical Engineering, Bioseparation Engineering Group, Technische Universität München, Boltzmannstr. 15, D-85748 Garching bei München (Germany).

[*] Corresponding author Tel.: +49 89 289 13096; fax: +49 89 289 13473.

† Equally contributing co-authors.

E-mail addresses: wolgangherrmann@ch.tum.de (W.A. Herrmann), fritz.kuehn@ch.tum.de (F.E. Kühn).

In preperation

6.2 Permissions for Reuse of Publications

6.2.1 Wiley Journals

JOHN WILEY AND SONS LICENSE TERMS AND CONDITIONS

Aug 25, 2014

This is a License Agreement between Reentje G Harms ("You") and John Wiley and Sons ("John Wiley and Sons") provided by Copyright Clearance Center ("CCC"). The license consists of your order details, the terms and conditions provided by John Wiley and Sons, and the payment terms and conditions.

All payments must be made in full to CCC. For payment instructions, please see information listed at the bottom of this form.

License Number	3455830510810
License date	Aug 25, 2014
Licensed content publisher	John Wiley and Sons
Licensed content publication	ChemSusChem
Licensed content title	Cleavage of C–O Bonds in Lignin Model Compounds Catalyzed by Methylidioxorhenium in Homogeneous Phase
Licensed copyright line	Copyright © 2014 WILEY-VCH Verlag GmbH & Co. KGaA, Weinheim
Licensed content author	Reentje G. Harms, Iulius I. E. Markovits, Markus Drees, h.c. mult. Wolfgang A. Herrmann, Mirza Cokoja, Fritz E. Kühn
Licensed content date	Jan 21, 2014
Start page	429
End page	434
Type of use	Dissertation/Thesis
Requestor type	Author of this Wiley article
Format	Print and electronic
Portion	Full article
Will you be translating?	No
Order reference number	Wiley CSSC
Title of your thesis / dissertation	Rhenium in Biomass Refining – Catalyst Development and Mechanistic Studies on the Rhenium Oxide-Catalysed C–O Bond Cleavage of Lignin Model Compounds
Expected completion date	Oct 2014
Expected size (number of pages)	260
Total	0.00 EUR
Terms and Conditions	

TERMS AND CONDITIONS

This copyrighted material is owned by or exclusively licensed to John Wiley & Sons, Inc. or one of its group companies (each a "Wiley Company") or handled on behalf of a society with which a Wiley Company has exclusive publishing rights in relation to a particular work (collectively "WILEY"). By clicking "accept" in connection with completing this licensing transaction, you agree that the following terms and conditions apply to this transaction (along with the billing and payment terms and conditions established by the Copyright Clearance Center Inc., ("CCC's Billing and Payment terms and conditions"), at the time that you opened your Rightslink account (these are available at any time at <http://myaccount.copyright.com>).

Terms and Conditions

- The materials you have requested permission to reproduce or reuse (the "Wiley Materials") are protected by copyright.
- You are hereby granted a personal, non-exclusive, non-sub licensable (on a stand-alone basis), non-transferable, worldwide, limited license to reproduce the Wiley Materials for the purpose specified in the licensing process. This license is for a one-time use only and limited to any maximum distribution number specified in the license. The first instance of republication or reuse granted by this licence must be completed within two years of the date of the grant of this licence (although copies prepared before the end date may be distributed thereafter). The Wiley Materials shall not be used in any other manner or for any other purpose, beyond what is granted in the license. Permission is granted subject to an appropriate acknowledgement given to the author, title of the material/book/journal and the publisher. You shall also duplicate the copyright notice that appears in the Wiley publication in your use of the Wiley Material. Permission is also granted on the understanding that nowhere in the text is a previously published source acknowledged for all or part of this Wiley Material. Any third party content is expressly excluded from this permission.
- With respect to the Wiley Materials, all rights are reserved. Except as expressly granted by the terms of the license, no part of the Wiley Materials may be copied, modified, adapted (except for minor reformatting required by the new Publication), translated, reproduced, transferred or distributed, in any form or by any means, and no derivative works may be made based on the Wiley Materials without the prior permission of the respective copyright owner. You may not alter, remove or suppress in any manner any copyright, trademark or other notices displayed by the Wiley Materials. You may not license, rent, sell, loan, lease, pledge, offer as security, transfer or assign the Wiley Materials on a stand-alone basis, or any of the rights granted to you hereunder to any other person.
- The Wiley Materials and all of the intellectual property rights therein shall at all times remain the exclusive property of John Wiley & Sons Inc, the Wiley Companies, or their respective licensors, and your interest therein is only that of having possession of and the right to reproduce the Wiley Materials pursuant to Section 2 herein during the continuance of this Agreement. You agree that you own no right, title or interest in or to the Wiley Materials or any of the intellectual property rights therein. You shall have no rights hereunder other than the license as provided for above in Section 2. No right, license or interest to any trademark, trade name, service mark or other branding ("Marks") of WILEY or its licensors is granted hereunder, and you agree that you shall not assert any such right, license or interest with respect thereto.
- NEITHER WILEY NOR ITS LICENSORS MAKES ANY WARRANTY OR REPRESENTATION OF ANY KIND TO YOU OR ANY THIRD PARTY, EXPRESS,

IMPLIED OR STATUTORY, WITH RESPECT TO THE MATERIALS OR THE ACCURACY OF ANY INFORMATION CONTAINED IN THE MATERIALS, INCLUDING, WITHOUT LIMITATION, ANY IMPLIED WARRANTY OF MERCHANTABILITY, ACCURACY, SATISFACTORY QUALITY, FITNESS FOR A PARTICULAR PURPOSE, USABILITY, INTEGRATION OR NON-INFRINGEMENT AND ALL SUCH WARRANTIES ARE HEREBY EXCLUDED BY WILEY AND ITS LICENSORS AND WAIVED BY YOU

- WILEY shall have the right to terminate this Agreement immediately upon breach of this Agreement by you.
- You shall indemnify, defend and hold harmless WILEY, its Licensors and their respective directors, officers, agents and employees, from and against any actual or threatened claims, demands, causes of action or proceedings arising from any breach of this Agreement by you.
- IN NO EVENT SHALL WILEY OR ITS LICENSORS BE LIABLE TO YOU OR ANY OTHER PARTY OR ANY OTHER PERSON OR ENTITY FOR ANY SPECIAL, CONSEQUENTIAL, INCIDENTAL, INDIRECT, EXEMPLARY OR PUNITIVE DAMAGES, HOWEVER CAUSED, ARISING OUT OF OR IN CONNECTION WITH THE DOWNLOADING, PROVISIONING, VIEWING OR USE OF THE MATERIALS REGARDLESS OF THE FORM OF ACTION, WHETHER FOR BREACH OF CONTRACT, BREACH OF WARRANTY, TORT, NEGLIGENCE, INFRINGEMENT OR OTHERWISE (INCLUDING, WITHOUT LIMITATION, DAMAGES BASED ON LOSS OF PROFITS, DATA, FILES, USE, BUSINESS OPPORTUNITY OR CLAIMS OF THIRD PARTIES), AND WHETHER OR NOT THE PARTY HAS BEEN ADVISED OF THE POSSIBILITY OF SUCH DAMAGES. THIS LIMITATION SHALL APPLY NOTWITHSTANDING ANY FAILURE OF ESSENTIAL PURPOSE OF ANY LIMITED REMEDY PROVIDED HEREIN.
- Should any provision of this Agreement be held by a court of competent jurisdiction to be illegal, invalid, or unenforceable, that provision shall be deemed amended to achieve as nearly as possible the same economic effect as the original provision, and the legality, validity and enforceability of the remaining provisions of this Agreement shall not be affected or impaired thereby.
- The failure of either party to enforce any term or condition of this Agreement shall not constitute a waiver of either party's right to enforce each and every term and condition of this Agreement. No breach under this agreement shall be deemed waived or excused by either party unless such waiver or consent is in writing signed by the party granting such waiver or consent. The waiver by or consent of a party to a breach of any provision of this Agreement shall not operate or be construed as a waiver of or consent to any other or subsequent breach by such other party.
- This Agreement may not be assigned (including by operation of law or otherwise) by you without WILEY's prior written consent.
- Any fee required for this permission shall be non-refundable after thirty (30) days from receipt by the CCC.
- These terms and conditions together with CCC's Billing and Payment terms and conditions (which are incorporated herein) form the entire agreement between you and WILEY concerning this licensing transaction and (in the absence of fraud) supersedes all prior agreements and representations of the parties, oral or written. This Agreement may not be amended except in writing signed by both parties. This Agreement shall be binding upon and inure to the benefit of the parties' successors, legal representatives, and authorized assigns.
- In the event of any conflict between your obligations established by these terms and conditions and those established by CCC's Billing and Payment terms and conditions, these terms and conditions shall prevail.
- WILEY expressly reserves all rights not specifically granted in the combination of (i) the license details provided by you and accepted in the course of this licensing transaction, (ii) these terms and conditions and (iii) CCC's Billing and Payment

terms and conditions.

- This Agreement will be void if the Type of Use, Format, Circulation, or Requestor Type was misrepresented during the licensing process.
- This Agreement shall be governed by and construed in accordance with the laws of the State of New York, USA, without regards to such state's conflict of law rules. Any legal action, suit or proceeding arising out of or relating to these Terms and Conditions or the breach thereof shall be instituted in a court of competent jurisdiction in New York County in the State of New York in the United States of America and each party hereby consents and submits to the personal jurisdiction of such court, waives any objection to venue in such court and consents to service of process by registered or certified mail, return receipt requested, at the last known address of such party.

WILEY OPEN ACCESS TERMS AND CONDITIONS

Wiley Publishes Open Access Articles in fully Open Access Journals and in Subscription journals offering Online Open. Although most of the fully Open Access journals publish open access articles under the terms of the Creative Commons Attribution (CC BY) License only, the subscription journals and a few of the Open Access Journals offer a choice of Creative Commons Licenses:: Creative Commons Attribution (CC-BY) license Creative Commons Attribution Non-Commercial (CC-BY-NC) license and Creative Commons Attribution Non-Commercial-NoDerivs (CC-BY-NC-ND) License. The license type is clearly identified on the article.

Copyright in any research article in a journal published as Open Access under a Creative Commons License is retained by the author(s). Authors grant Wiley a license to publish the article and identify itself as the original publisher. Authors also grant any third party the right to use the article freely as long as its integrity is maintained and its original authors, citation details and publisher are identified as follows: [Title of Article/Author/Journal Title and Volume/Issue. Copyright (c) [year] [copyright owner as specified in the Journal]. Links to the final article on Wiley's website are encouraged where applicable.

The Creative Commons Attribution License

The Creative Commons Attribution License (CC-BY) allows users to copy, distribute and transmit an article, adapt the article and make commercial use of the article. The CC-BY license permits commercial and non-commercial re-use of an open access article, as long as the author is properly attributed.

The Creative Commons Attribution License does not affect the moral rights of authors, including without limitation the right not to have their work subjected to derogatory treatment. It also does not affect any other rights held by authors or third parties in the article, including without limitation the rights of privacy and publicity. Use of the article must not assert or imply, whether implicitly or explicitly, any connection with, endorsement or sponsorship of such use by the author, publisher or any other party associated with the article.

For any reuse or distribution, users must include the copyright notice and make clear to others that the article is made available under a Creative Commons Attribution license, linking to the relevant Creative Commons web page.

To the fullest extent permitted by applicable law, the article is made available as is and without representation or warranties of any kind whether express, implied, statutory or otherwise and including, without limitation, warranties of title, merchantability, fitness for a particular purpose, non-infringement, absence of defects, accuracy, or the presence or absence of errors.

Creative Commons Attribution Non-Commercial License

The Creative Commons Attribution Non-Commercial (CC-BY-NC) License permits use, distribution and reproduction in any medium, provided the original work is properly cited and is not used for commercial purposes.(see below)

Creative Commons Attribution-Non-Commercial-NoDerivs License

The Creative Commons Attribution Non-Commercial-NoDerivs License (CC-BY-NC-ND) permits use, distribution and reproduction in any medium, provided the original work is properly cited, is not used for commercial purposes and no modifications or adaptations are made. (see below)

Use by non-commercial users

For non-commercial and non-promotional purposes, individual users may access, download, copy, display and redistribute to colleagues Wiley Open Access articles, as well as adapt, translate, text- and data-mine the content subject to the following conditions:

- The authors' moral rights are not compromised. These rights include the right of "paternity" (also known as "attribution" - the right for the author to be identified as such) and "integrity" (the right for the author not to have the work altered in such a way that the author's reputation or integrity may be impugned).
- Where content in the article is identified as belonging to a third party, it is the obligation of the user to ensure that any reuse complies with the copyright policies of the owner of that content.
- If article content is copied, downloaded or otherwise reused for non-commercial research and education purposes, a link to the appropriate bibliographic citation (authors, journal, article title, volume, issue, page numbers, DOI and the link to the definitive published version on **Wiley Online Library**) should be maintained. Copyright notices and disclaimers must not be deleted.
- Any translations, for which a prior translation agreement with Wiley has not been agreed, must prominently display the statement: "This is an unofficial translation of an article that appeared in a Wiley publication. The publisher has not endorsed this translation."

Use by commercial "for-profit" organisations

Use of Wiley Open Access articles for commercial, promotional, or marketing purposes requires further explicit permission from Wiley and will be subject to a fee.

Commercial purposes include:

- Copying or downloading of articles, or linking to such articles for further redistribution, sale or licensing;
- Copying, downloading or posting by a site or service that incorporates advertising with such content;
- The inclusion or incorporation of article content in other works or services (other than normal quotations with an appropriate citation) that is then available for sale or licensing, for a fee (for example, a compilation produced for marketing purposes, inclusion in a sales pack)
- Use of article content (other than normal quotations with appropriate citation) by for-profit organisations for promotional purposes
- Linking to article content in e-mails redistributed for promotional, marketing or educational purposes;
- Use for the purposes of monetary reward by means of sale, resale, licence, loan, transfer or other form of commercial exploitation such as marketing products
- Print reprints of Wiley Open Access articles can be purchased from: corporatesales@wiley.com

Further details can be found on Wiley Online Library
<http://olabout.wiley.com/WileyCDA/Section/id-410895.html>

Other Terms and Conditions:

v1.9

You will be invoiced within 48 hours of this transaction date. You may pay your invoice by credit card upon receipt of the invoice for this transaction. Please follow instructions provided at that time. To pay for this transaction now; please remit a copy of this document along with your payment. Payment should be in the form of a check or money order referencing your account number and this invoice number RLNK501385322. Make payments to "COPYRIGHT CLEARANCE CENTER" and send to:

**Copyright Clearance Center
Dept 001
P.O. Box 843006
Boston, MA 02284-3006**

Please disregard electronic and mailed copies if you remit payment in advance.

Questions? customercare@copyright.com or +1-855-239-3415 (toll free in the US) or +1-978-646-2777.

Gratis licenses (referencing \$0 in the Total field) are free. Please retain this printable license for your reference. No payment is required.

6.2.2 Elsevier Journals

**ELSEVIER LICENSE
TERMS AND CONDITIONS**

Oct 05, 2015

This is a License Agreement between Reentje Harms ("You") and Elsevier ("Elsevier") provided by Copyright Clearance Center ("CCC"). The license consists of your order details, the terms and conditions provided by Elsevier, and the payment terms and conditions.

All payments must be made in full to CCC. For payment instructions, please see information listed at the bottom of this form.

Supplier	Elsevier Limited The Boulevard, Langford Lane Kidlington, Oxford, OX5 1GB, UK
Registered Company Number	1982084
Customer name	Reentje Harms
Customer address	Sprengelstr. 42 Berlin, 13353
License number	3722510688093
License date	Oct 05, 2015
Licensed content publisher	Elsevier
Licensed content publication	Coordination Chemistry Reviews
Licensed content title	Organorhenium dioxides as oxygen transfer systems: Synthesis, reactivity, and applications
Licensed content author	Reentje G. Harms, Wolfgang A. Herrmann, Fritz E. Kühn
Licensed content date	15 July 2015
Licensed content volume number	296
Licensed content issue number	n/a
Number of pages	23
Start Page	1
End Page	23
Type of Use	reuse in a thesis/dissertation
Portion	full article
Format	both print and electronic
Are you the author of this Elsevier article?	Yes
Will you be translating?	No
Title of your thesis/dissertation	Rhenium in Biomass Refining - Catalyst Development and Mechanistic Studies on the Rhenium Oxide-Catalysed C-O Bond Cleavage of Lignin Model Compounds
Expected completion date	Oct 2015
Estimated size (number of pages)	120
Elsevier VAT number	GB 494 6272 12
Permissions price	0.00 EUR

VAT/Local Sales Tax	0.00 EUR / 0.00 GBP
Total	0.00 EUR
Terms and Conditions	

INTRODUCTION

1. The publisher for this copyrighted material is Elsevier. By clicking "accept" in connection with completing this licensing transaction, you agree that the following terms and conditions apply to this transaction (along with the Billing and Payment terms and conditions established by Copyright Clearance Center, Inc. ("CCC"), at the time that you opened your Rightslink account and that are available at any time at <http://myaccount.copyright.com>).

GENERAL TERMS

2. Elsevier hereby grants you permission to reproduce the aforementioned material subject to the terms and conditions indicated.
3. Acknowledgement: If any part of the material to be used (for example, figures) has appeared in our publication with credit or acknowledgement to another source, permission must also be sought from that source. If such permission is not obtained then that material may not be included in your publication/copies. Suitable acknowledgement to the source must be made, either as a footnote or in a reference list at the end of your publication, as follows:
"Reprinted from Publication title, Vol /edition number, Author(s), Title of article / title of chapter, Pages No., Copyright (Year), with permission from Elsevier [OR APPLICABLE SOCIETY COPYRIGHT OWNER]." Also Lancet special credit - "Reprinted from The Lancet, Vol. number, Author(s), Title of article, Pages No., Copyright (Year), with permission from Elsevier."
4. Reproduction of this material is confined to the purpose and/or media for which permission is hereby given.
5. Altering/Modifying Material: Not Permitted. However figures and illustrations may be altered/adapted minimally to serve your work. Any other abbreviations, additions, deletions and/or any other alterations shall be made only with prior written authorization of Elsevier Ltd. (Please contact Elsevier at permissions@elsevier.com)
6. If the permission fee for the requested use of our material is waived in this instance, please be advised that your future requests for Elsevier materials may attract a fee.
7. Reservation of Rights: Publisher reserves all rights not specifically granted in the combination of (i) the license details provided by you and accepted in the course of this licensing transaction, (ii) these terms and conditions and (iii) CCC's Billing and Payment terms and conditions.
8. License Contingent Upon Payment: While you may exercise the rights licensed immediately upon issuance of the license at the end of the licensing process for the transaction, provided that you have disclosed complete and accurate details of your proposed use, no license is finally effective unless and until full payment is received from you (either by publisher or by CCC) as provided in CCC's Billing and Payment terms and conditions. If full payment is not received on a timely basis, then any license preliminarily granted shall be deemed automatically revoked and shall be void as if never granted. Further, in the event that you breach any of these terms and conditions or any of CCC's Billing and Payment terms and conditions, the license is automatically revoked and shall be void as if never granted. Use of materials as described in a revoked license, as well as any use of the materials beyond the scope of an unrevoked license, may constitute copyright infringement and publisher reserves the right to take any and all action to protect its copyright in the materials.
9. Warranties: Publisher makes no representations or warranties with respect to the

licensed material.

10. **Indemnity:** You hereby indemnify and agree to hold harmless publisher and CCC, and their respective officers, directors, employees and agents, from and against any and all claims arising out of your use of the licensed material other than as specifically authorized pursuant to this license.

11. **No Transfer of License:** This license is personal to you and may not be sublicensed, assigned, or transferred by you to any other person without publisher's written permission.

12. **No Amendment Except in Writing:** This license may not be amended except in a writing signed by both parties (or, in the case of publisher, by CCC on publisher's behalf).

13. **Objection to Contrary Terms:** Publisher hereby objects to any terms contained in any purchase order, acknowledgment, check endorsement or other writing prepared by you, which terms are inconsistent with these terms and conditions or CCC's Billing and Payment terms and conditions. These terms and conditions, together with CCC's Billing and Payment terms and conditions (which are incorporated herein), comprise the entire agreement between you and publisher (and CCC) concerning this licensing transaction. In the event of any conflict between your obligations established by these terms and conditions and those established by CCC's Billing and Payment terms and conditions, these terms and conditions shall control.

14. **Revocation:** Elsevier or Copyright Clearance Center may deny the permissions described in this License at their sole discretion, for any reason or no reason, with a full refund payable to you. Notice of such denial will be made using the contact information provided by you. Failure to receive such notice will not alter or invalidate the denial. In no event will Elsevier or Copyright Clearance Center be responsible or liable for any costs, expenses or damage incurred by you as a result of a denial of your permission request, other than a refund of the amount(s) paid by you to Elsevier and/or Copyright Clearance Center for denied permissions.

LIMITED LICENSE

The following terms and conditions apply only to specific license types:

15. **Translation:** This permission is granted for non-exclusive world **English** rights only unless your license was granted for translation rights. If you licensed translation rights you may only translate this content into the languages you requested. A professional translator must perform all translations and reproduce the content word for word preserving the integrity of the article.

16. **Posting licensed content on any Website:** The following terms and conditions apply as follows: Licensing material from an Elsevier journal: All content posted to the web site must maintain the copyright information line on the bottom of each image; A hyper-text must be included to the Homepage of the journal from which you are licensing at <http://www.sciencedirect.com/science/journal/xxxxx> or the Elsevier homepage for books at <http://www.elsevier.com>; Central Storage: This license does not include permission for a scanned version of the material to be stored in a central repository such as that provided by Heron/XanEdu.

Licensing material from an Elsevier book: A hyper-text link must be included to the Elsevier homepage at <http://www.elsevier.com>. All content posted to the web site must maintain the copyright information line on the bottom of each image.

Posting licensed content on Electronic reserve: In addition to the above the following clauses are applicable: The web site must be password-protected and made available only to bona fide students registered on a relevant course. This permission is granted for 1 year only. You may obtain a new license for future website posting.

17. **For journal authors:** the following clauses are applicable in addition to the above:

Preprints:

A preprint is an author's own write-up of research results and analysis, it has not been peer-reviewed, nor has it had any other value added to it by a publisher (such as formatting, copyright, technical enhancement etc.).

Authors can share their preprints anywhere at any time. Preprints should not be added to or enhanced in any way in order to appear more like, or to substitute for, the final versions of articles however authors can update their preprints on arXiv or RePEc with their Accepted Author Manuscript (see below).

If accepted for publication, we encourage authors to link from the preprint to their formal publication via its DOI. Millions of researchers have access to the formal publications on ScienceDirect, and so links will help users to find, access, cite and use the best available version. Please note that Cell Press, The Lancet and some society-owned have different preprint policies. Information on these policies is available on the journal homepage.

Accepted Author Manuscripts: An accepted author manuscript is the manuscript of an article that has been accepted for publication and which typically includes author-incorporated changes suggested during submission, peer review and editor-author communications.

Authors can share their accepted author manuscript:

- immediately
 - via their non-commercial person homepage or blog
 - by updating a preprint in arXiv or RePEc with the accepted manuscript
 - via their research institute or institutional repository for internal institutional uses or as part of an invitation-only research collaboration work-group
 - directly by providing copies to their students or to research collaborators for their personal use
 - for private scholarly sharing as part of an invitation-only work group on commercial sites with which Elsevier has an agreement
- after the embargo period
 - via non-commercial hosting platforms such as their institutional repository
 - via commercial sites with which Elsevier has an agreement

In all cases accepted manuscripts should:

- link to the formal publication via its DOI
- bear a CC-BY-NC-ND license - this is easy to do
- if aggregated with other manuscripts, for example in a repository or other site, be shared in alignment with our hosting policy not be added to or enhanced in any way to appear more like, or to substitute for, the published journal article.

Published journal article (JPA): A published journal article (PJA) is the definitive final record of published research that appears or will appear in the journal and embodies all value-adding publishing activities including peer review co-ordination, copy-editing, formatting, (if relevant) pagination and online enrichment.

Policies for sharing publishing journal articles differ for subscription and gold open access articles:

Subscription Articles: If you are an author, please share a link to your article rather than the full-text. Millions of researchers have access to the formal publications on ScienceDirect, and so links will help your users to find, access, cite, and use the best available version.

Theses and dissertations which contain embedded PJAs as part of the formal submission

can be posted publicly by the awarding institution with DOI links back to the formal publications on ScienceDirect.

If you are affiliated with a library that subscribes to ScienceDirect you have additional private sharing rights for others' research accessed under that agreement. This includes use for classroom teaching and internal training at the institution (including use in course packs and courseware programs), and inclusion of the article for grant funding purposes.

Gold Open Access Articles: May be shared according to the author-selected end-user license and should contain a [CrossMark logo](#), the end user license, and a DOI link to the formal publication on ScienceDirect.

Please refer to Elsevier's [posting policy](#) for further information.

18. **For book authors** the following clauses are applicable in addition to the above:

Authors are permitted to place a brief summary of their work online only. You are not allowed to download and post the published electronic version of your chapter, nor may you scan the printed edition to create an electronic version. **Posting to a repository:** Authors are permitted to post a summary of their chapter only in their institution's repository.

19. **Thesis/Dissertation:** If your license is for use in a thesis/dissertation your thesis may be submitted to your institution in either print or electronic form. Should your thesis be published commercially, please reapply for permission. These requirements include permission for the Library and Archives of Canada to supply single copies, on demand, of the complete thesis and include permission for Proquest/UMI to supply single copies, on demand, of the complete thesis. Should your thesis be published commercially, please reapply for permission. Theses and dissertations which contain embedded PJAs as part of the formal submission can be posted publicly by the awarding institution with DOI links back to the formal publications on ScienceDirect.

Elsevier Open Access Terms and Conditions

You can publish open access with Elsevier in hundreds of open access journals or in nearly 2000 established subscription journals that support open access publishing.

Permitted third party re-use of these open access articles is defined by the author's choice of Creative Commons user license. See our [open access license policy](#) for more information.

Terms & Conditions applicable to all Open Access articles published with Elsevier:

Any reuse of the article must not represent the author as endorsing the adaptation of the article nor should the article be modified in such a way as to damage the author's honour or reputation. If any changes have been made, such changes must be clearly indicated.

The author(s) must be appropriately credited and we ask that you include the end user license and a DOI link to the formal publication on ScienceDirect.

If any part of the material to be used (for example, figures) has appeared in our publication with credit or acknowledgement to another source it is the responsibility of the user to ensure their reuse complies with the terms and conditions determined by the rights holder.

Additional Terms & Conditions applicable to each Creative Commons user license:

CC BY: The CC-BY license allows users to copy, to create extracts, abstracts and new works from the Article, to alter and revise the Article and to make commercial use of the Article (including reuse and/or resale of the Article by commercial entities), provided the user gives appropriate credit (with a link to the formal publication through the relevant DOI), provides a link to the license, indicates if changes were made and the licensor is not represented as endorsing the use made of the work. The full details of the license are available at <http://creativecommons.org/licenses/by/4.0>.

CC BY NC SA: The CC BY-NC-SA license allows users to copy, to create extracts, abstracts and new works from the Article, to alter and revise the Article, provided this is not done for commercial purposes, and that the user gives appropriate credit (with a link to the formal publication through the relevant DOI), provides a link to the license, indicates if changes were made and the licensor is not represented as endorsing the use made of the work. Further, any new works must be made available on the same conditions. The full details of the license are available at <http://creativecommons.org/licenses/by-nc-sa/4.0>.

CC BY NC ND: The CC BY-NC-ND license allows users to copy and distribute the Article, provided this is not done for commercial purposes and further does not permit distribution of the Article if it is changed or edited in any way, and provided the user gives appropriate credit (with a link to the formal publication through the relevant DOI), provides a link to the license, and that the licensor is not represented as endorsing the use made of the work. The full details of the license are available at <http://creativecommons.org/licenses/by-nc-nd/4.0>. Any commercial reuse of Open Access articles published with a CC BY NC SA or CC BY NC ND license requires permission from Elsevier and will be subject to a fee.

Commercial reuse includes:

- Associating advertising with the full text of the Article
- Charging fees for document delivery or access
- Article aggregation
- Systematic distribution via e-mail lists or share buttons

Posting or linking by commercial companies for use by customers of those companies.

20. Other Conditions:

v1.8

Questions? customer@copyright.com or +1-855-239-3415 (toll free in the US) or +1-978-646-2777.

7. Appendix

7.1 Unpublished Manuscripts used within this Thesis

Reentje G. Harms, Lilian Graser, S. Schwaminger, Prof. Dr. Wolfgang A. Herrmann and Prof. Dr. Fritz E. Kühn

“Re₂O₇ in C–O bond cleavage of a β–O–4 lignin model linkage: A highly active Lewis acidic catalyst in heterogeneous phase”

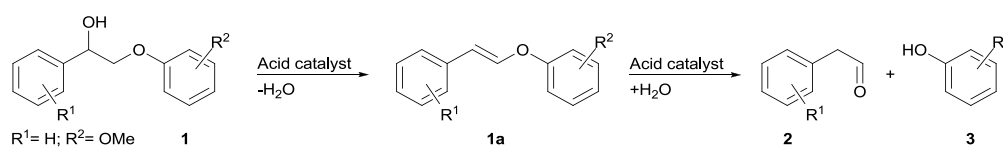
Abstract: A Lewis acid highly active in catalysing the C–O bond cleavage reaction of the β-hydroxy aryl ether lignin model compound 2-(2-methoxyphenoxy)phenylethanol (**1**) is presented. A systematic screening of various Lewis acids revealed rhenium heptoxide as the most active catalyst which results in quantitative substrate conversion and excellent selectivity towards two cleavage products. With a TOF of 2400 h⁻¹, this is the most active catalyst for the C–O cleavage of model compound **1** reported so far. Furthermore, Re₂O₇ is more active in heterogeneous (apolar media) than in homogeneous (coordinating solvents) phase. The catalyst deactivation has been studied by means of TEM, XPS and Raman spectroscopy. Based on the observed intermediate and the kinetic reaction profile a mechanism close to Brønsted acid-catalysed C–O bond cleavages is discussed.

Introduction: The worldwide increasing demand for energy and material sources is faced with dwindling fossil resources. The depletion of crude oil is accompanied with a dramatic sevenfold increase of the oil price during the past 15 years,¹ which underlines the ecological and economical need for replacement of conventional oil resources. Biomass is currently considered as alternative resource and growing research efforts are ventured to find sustainable pathways for the production of petrochemicals, energy and fuels.²⁻⁴ Here, the effort of the inefficient and thermodynamically highly disfavoured reduction of CO₂ carbon atom has already been done by nature. Many routes have been developed for the refining of biomass-derived feedstocks such as carbohydrates (cellulose, starch) to value added fine chemicals;⁵⁻⁹ however, next to naphtha lignin is the only direct and economical valuable feedstock for the production of bulk aromatic compounds. The pyrolysis or hydrodeoxygenation of lignin into bio-oils are promising candidates for the renewable fuel production. In contrast, genesis of bulk chemical compounds demands more specific functional group transformations.^{10, 11} Lignin is a very complex phenolate based

heterogeneous polymer, which inhibits so far its efficient degradation and application as chemical carbon feedstock.

In natural lignin the β -O-4 bond – simply described by a β -hydroxy aryl ether bond – is the predominant intermonomer linkage between the aromatic units (up to 50%).⁹⁻¹² Hence, that linkage presents a promising target in fundamental C–O bond cleavage studies and heterogeneous (zeolites, supported transition metals, nanoparticles)¹³⁻²⁰ and homogeneous (acidic, alkaline or transition metal)²⁰⁻²⁹ catalysts have been investigated.

Recently, the methyldioxorhenium(V)-catalysed C–O bond cleavage of several non-phenolic lignin model compounds at mild reaction conditions (110–135 °C) was reported.³⁰ The active catalyst is generated *in situ* by deoxygenative reduction of the precursor compound methyltrioxorhenium (MTO). The C–O cleavage proceeds via a stable enol ether intermediate, which is the formal dehydration product of the secondary alcohol group containing the β -hydroxy model compound.



Scheme 1. The general acid-catalysed C–O bond cleavage occurs in a sequence of two reaction steps a) via formation of enol ether as intermediate, which is the formal dehydration product of the β -hydroxy aryl ether, and b) subsequent hydrolysis which yields in C–O cleavage to phenylacetaldehyde and phenol derivatives.

This intermediate is observed also in the Brønsted acid-catalysed cleavage of lignin model compounds as depicted in Scheme 1. Matsumoto et al. investigated the acidolysis (acid-catalysed cleavage) of dimeric β -O-4 model compounds in water/dioxane mixtures using a range of mineral acids such as HBr, HCl, H₂SO₄ and isolated the latter enol ether intermediate.³¹⁻³³ The subsequent acid-catalysed hydrolysis of the enol ether yields in the desired C–O bond cleavage. Lundquist and Lundgren discussed in a seminal work from the 1970s an ionic cleavage mechanism of the sulphuric acid-catalysed degradation of lignin and lignin model compounds.³⁴

In a recent catalytic and computational study by Sturgeon et al. the ionic mechanism and the observed enol ether intermediate was confirmed for a variety of phenolic and non-phenolic β -hydroxy aryl ether compounds.³⁵ Notably, not only Brønsted but Lewis acids are capable for degradation of lignin model compounds and lignin.³⁶⁻³⁸ The cleavage of non-phenolic β -O-4 model dimers is conducted by treatment with aluminium-, ferric- or stannic chloride in diluted alcoholic solutions at 170 °C;³⁹ by application of group 3 and group 13 triflates hydrolysis of aryl-oxygen linkages is obtained at 250 °C.⁴⁰ Binder et al. found several metal chlorides and triflates suitable for model compound degradation in ionic liquid media.⁴¹ Technical lignin

degradation applying ZnCl_2 , FeCl_3 or AlCl_3 catalyst produces phenols in low yields at temperatures from 300 °C,^{41, 42} however, conversions of 30% are obtained when Alcell-derived lignin is reacted with NiCl_2 or FeCl_3 .⁴³ However, detailed studies regarding the reactivity towards functional groups are not available.

Since both Brønsted and Lewis acids catalyse the dehydration of secondary alcohols to olefins, the formation of intermediate enol ethers while treatment of β -hydroxy-aryl ethers is feasible.⁴⁴⁻⁴⁷ The dehydration of benzylic alcohols was extensively studied by Espenson et al. and Korstanje et al. applying strong acids such as *p*-toluenesulphonic acid and sulphuric acid or rhenium based compounds such as MTO, perrhenic acid and rhenium heptoxide.⁴⁸⁻⁵¹ Re_2O_7 is revealed to be the most efficient rhenium based dehydration catalyst for a broad range of benzylic alcohols in toluene at 100 °C. The catalyst allows quantitative conversions of the substrate with distinct olefin selectivity and a remarkable activity (TOF of 431 h^{-1} for 1-phenylethanol; >800 h^{-1} for 1,2,3,4-tetrahydronaphthol).

Although the latter results present a promising approach for the economical lignin refining, to our surprise, the recent impact on the scientific community is rather marginal. Herein, we present the application rhenium heptoxide as Lewis acidic catalyst for the efficient C–O bond cleavage of exceedingly stable 2-(2-methoxyphenoxy)phenylethanol (**1**) lignin model dimer at mild reaction conditions. The observed catalyst activity is, up to our knowledge, the highest that has ever been reported. Moreover, the reaction proceeds quantitatively with excellent product selectivity.

Results and discussion: In this work the Lewis acid-catalysed C–O bond cleavage of β -hydroxy aryl ether **1**, a frequently used lignin model dimer, to phenylacetaldehyd (**2**) and guaiacol (**3**) is reported (see Table 1). The catalytic activity of several in this context studied Lewis acids were applied to an aromatic hydrophobic reaction medium.^{39, 40} Toluene was previously proven to be an efficient reaction medium for the Brønsted and Lewis acid-catalysed dehydration reaction, however, *p*-xylene was used to realise significant higher reaction temperatures without utilisation of any special high pressure equipment.

Therefore, the Lewis acid was added to a solution of **1** in *p*-xylene under aerobic conditions and the reaction mixture was heated to 140 °C for 2 h. The screened Lewis acid catalysts are not soluble in *p*-xylene and stay in heterogeneous phases during catalysis. However, the liquid compounds TiCl_4 and SnCl_4 , and ethereal BF_3 were soluble and represent homogeneous Lewis acids. It was found that rhenium heptoxide, stannic chloride, scandium triflate, and titanium chloride are capable for complete conversion of model compound **1** (Table 1, entry 5-8). Using $\text{BF}_3 \cdot \text{Et}_2\text{O}$ and FeCl_3 yields moderate conversions of $\approx 70\%$ (entries 3 and 4). Nonetheless, the obtained product yields are rather low.

Table 1. Screening of various Lewis acids in the catalytic C–O bond cleavage of β -hydroxy aryl ether **1**.

Entry	Lewis acid catalyst	Conv. [%] ^a	Yield 2 [%] ^a	Yield 3 [%] ^a
1	AlCl ₃	16	0	4
2	Al ₂ (SO ₄) ₃ *18H ₂ O	21	0	0
3	BF ₃ *Et ₂ O	70	0	36
4	FeCl ₃	72	2	46
5	Re₂O₇	100	86	93
6	Sc(OTf) ₃	100	7	71
7	SnCl ₄	100	0	36
8	TiCl ₄	100	0	47

Reaction conditions: 100 mg 2-(2-methoxyphenoxy)phenylethanol (**1**); a) conversions and yields were determined by GC FID.

This is probably ascribed to the sensitivity of β -hydroxy aryl ether cleavage products under the applied acidic conditions which was previously described by Sturgeon et al.³⁵ In particular aldehydes are well known to be very reactive under acidic conditions. The polymerisation of various aldehydes at low temperatures is catalysed by both protic and Lewis acids such as FeCl₃ and BF₃ and was reported by Vogl et al. and later reviewed by Tsukamoto.⁵²⁻⁵⁴ Moreover, aldehydes are subjected to acetal formation at such acidic conditions. Several aluminium compounds merely showed conversion and no product yield within the GC method error. When **1** is subjected to 5 wt% Re₂O₇ quantitative conversions and an almost complete mass balance is observed. It seems that Re₂O₇ provides the best properties for the reaction meaning sufficient strong acidic to obtain substrate conversion, but also not to exceedingly strong to catalyse product decomposition.

Moreover, a significant influence of air and moisture on the conversion and product yields is not observed. Neither the use of with water saturated *p*-xylene (washed with water and phases were separated) nor application of Schlenk conditions and argon inert gas atmosphere has an influence on the reaction outcome. However, when 2 mL of water are added, no conversion is obtained. This is due to the formation of a two-phasic system, in which the aqueous phase extracts and retains the rhenium heptoxide catalyst as perrhenic acid.

Other critical parameters, such as the influence of temperature, reaction time, catalyst loading, and the reaction media was optimised after this suitable catalyst system has been identified (see Table 2).

Table 2. Optimisation of the reaction parameters of the Re₂O₇-catalysed C–O cleavage of **1**.

Entry	Cat. conc. [mol%]	Medium	Temp [°C]	Conv. [%] ^a	Yield 2 [%] ^a	Yield 3 [%] ^a
1	2.5	<i>p</i> -xylene	140	100	86	93
2	0.5	<i>p</i> -xylene	140	100	92	96
3	0.1	<i>p</i>-xylene	140	100	96	97
4 ^b	0.1	<i>p</i> -xylene	140	100	51	93
5	0.1	THF	140	71	44	54
6	0.1	MeCN	140	23	7	11
7	0.1	<i>n</i> -decane	140	19	7	9
8	0.05	<i>p</i> -xylene	140	100	69 (83) ^c	77 (91) ^c
9	0	<i>p</i> -xylene	140	0	0	0

Reaction conditions: 100 mg **1**, 4 mL solvent, reaction time 2 h; a) conversions and yields were determined by GC FID; b) 16 h; c) 2.5 h.

The optimal reaction conditions were found at a low catalyst loading of 0.1 mol% (0.2 wt%; Table 2, entry 3). Applied under these reaction conditions the catalyst reaches a TOF of 2400 h⁻¹ after 10 minutes. The latter high activity in C–O bond cleavage of model compound **1** is, up to our knowledge, the highest reported so far.

A further decrease in the catalyst loading to 0.05 mol% yields in full conversion, but the obtained product yields are rather low (entry 8). However, a prolonged reaction time of 2.5 h results in an almost complete mass balance, indicating an unchanged catalyst activity. On the other hand, a decreasing product yield is perceivable at higher catalyst loadings (entries 1 and 2, see also the SI, Table S1). The reaction time of 2 h was found to be optimal at a catalyst loading of 0.1 mol%. A kinetic profile exhibits reasonable lower conversion at shorter reaction times than 2 h (please see the kinetic profile at the SI, Figure S3), however, an extended reaction time of 16 h results in complete conversion but decreased product yields, especially of **2** (entry 4). The negative influence of higher catalyst loading and extended reaction times is attributed to product sensitivity towards acidic conditions (vide supra and see the SI, Figure S2). A blank experiment without the catalyst shows no conversion (entry 9). Moreover, the used reaction medium shows a strong influence on the catalytic activity. Application of an aliphatic reaction medium (entry 7) results in a strong decline of conversion. Rhenium heptoxide is soluble in coordinating solvents, thus allowing the reaction to be conducted in homogeneous phase. However, the use of THF and acetonitrile results in a decline of conversion (entries 5 and 6) probably due to downgrading the catalyst's Lewis acidity. This is a rare example, where the catalyst is more active in suspension rather than in solution.^{55, 56}

Notably, lower reaction temperatures lead to significant lower conversions. The influence of the temperature on the conversion was studied for temperatures ranging from 140 °C,

100 °C, 80 °C and r.t. and is illustrated in Figure 1. At a reaction temperature of 100 °C both poor conversion and product yields are observed, and 80 °C yields only in a marginal conversion. At room temperature no conversion is observed (please see the SI, Table S1 for detailed conversions and yields).

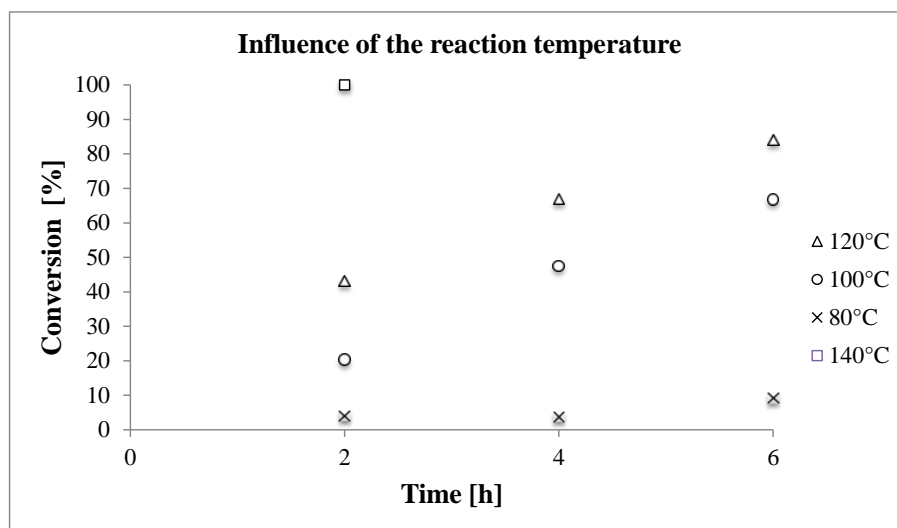


Figure 1. Influence of the reaction temperature in conversion of **1** using 0.1 mol% Re_2O_7 in *p*-xylene.

To elucidate if the C–O cleavage reaction is catalysed either due to the Lewis acidity of Re_2O_7 or due to in situ formation of a catalytically active metallic or oxidic rhenium compound, commercially available rhenium compounds in several oxidation states ranging from Re(0) to Re(VII) were tested (see Table 3).^{30, 49, 50, 57-61}

Table 3. Screening of different rhenium compounds from oxidation state Re(0) to Re(VII) under optimised catalytic reaction conditions.

Entry	Rhenium-compound	Conv. 1 [%] ^a	Yield 2 [%] ^a	Yield 3 [%] ^a
1	Re powder 325 mesh	7	2	3
2	$\text{Re}_2(\text{CO})_{10}$	24	11	13
3	ReO_2^{b}	0	0	0
4	ReO_3^{b}	0	0	0
5	AgReO_4	6	2	4
6	$\text{NH}_4\text{ReO}_4^{\text{c}}$	15	4	6
7	HReO_4	91	42	44

Reaction conditions: 0.1 mol% rhenium-compound, 4 mL *p*-xylene, 140°C, 2 h; a) conversions and yields were determined by GC FID; b) under argon atmosphere; c) aqueous stock solution precluded solubility issues.

Elemental rhenium is only poorly active and negligible conversion is observed (entry 1); however, rhenium decacarbonyl exhibits a higher but still low conversion of 24% (entry 2). Since $\text{Re}(\text{CO})_{10}$ is prone to aerobic oxidation,⁶² probably a small amount of catalytic active

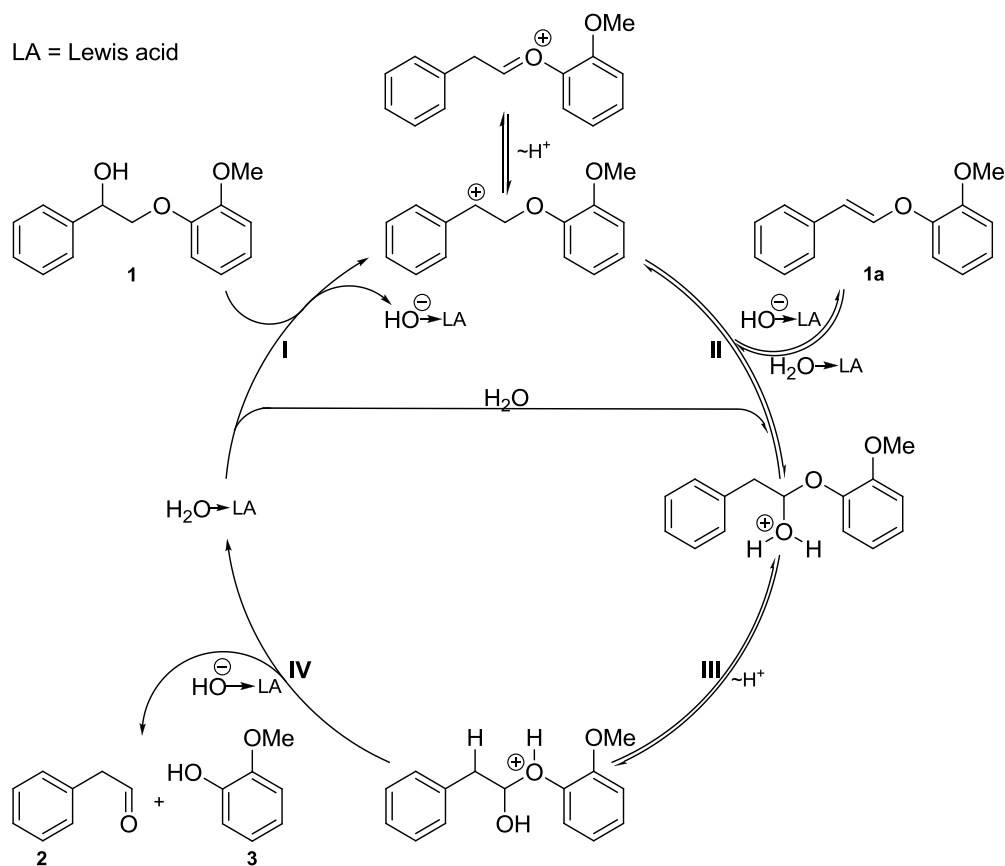
rhodium oxide has been formed. The formation of Re(IV) and Re(VI) oxides (entries 3 and 4) as active species is excluded because latter oxides showed no conversion of **1**.

This experiment was conducted under argon atmosphere to prevent aerobic oxidation. Rhenium heptoxide is known to decompose at elevated temperatures due to fragmentation into perrhenate ReO_4^- and cationic perrhenyl ReO_3^+ .^{63, 64} To investigate the catalytic ability of perrhenate, AgReO_4 and NH_4ReO_4 were tested (entries 5 and 6). When these were applied poor substrate conversions are observed, limiting its role as active catalyst species.

In contrast, the Brønsted acid HReO_4 shows very good conversion, but is less selective towards C–O cleavage (entry 7); the formation of non-volatile ethers of **1** is observed instead. In comparison of latter distinct results, Re_2O_7 outperforms all other rhenium compounds in both activity and product yield.

Mechanism

The mechanism of the acid-catalysed cleavage of β -hydroxy aryl ethers was discussed previously by Yokoyama et al.,³¹⁻³³ Lundquist et al.,³⁴ Sturgeon et al.,³⁵ and Aoyama et al.³⁹ Based on the latter findings the rhenium heptoxide catalysed C–O cleavage of **1** most probably follows the same reaction mechanism as depicted in Scheme 2.



Scheme 2. Proposed mechanism of the Lewis acid (LA) catalysed ionic C–O bond cleavage of β -hydroxy aryl ether **1** according to Yokoyama et al.,³¹⁻³³ Lundquist et al.,³⁴ Sturgeon et al.,³⁵ and Aoyama et al.³⁹

The observed intermediate **1a** (please see the SI for further details) and the reaction products **2** and **3** fit to an acid-catalysed reaction type which is consisting of a sequence from initial dehydration plus subsequent enol ether hydrolysis. Furthermore, the substrate conversion drastically declines if *n*-decane is used as reaction medium.

Apolar aprotic alkanes are less capable stabilising the ionic intermediates in absence of any coordinating agent, thus disfavouring the required hydroxide abstraction. In a first step the Lewis acid (LA) abstracts **1**'s secondary hydroxyl group and forms a benzylic carbocation (see Scheme 2, step I). Subsequent loss of a proton generates the observed intermediate **1a** (step II). Enol ethers are very sensitive towards hydrolysis which is catalysed by small amounts of acid (step III).^{65, 66} The Lewis acid–water adduct is sufficient acidic to catalyse the enol ether hydrolysis leaving **2** and **3** (step IV).

Several experiments revealed that Re_2O_7 is the active Lewis acid catalyst which stays unchanged in heterogeneous phase; the formation of other active species was verified to be unlikely. When the reaction mixture is filtered through a layer of Celite® (diatomaceous earth), no further conversion is observed after continued heating and stirring of the filtrate. However, if the reaction mixture has passed or syringe filter (0.45 μm pore size), a virtually unchanged catalyst activity (>95% conversion) in the filtrate is revealed. Hence, the catalyst stays as very small particles in heterogeneous phase and no formation of any active soluble compounds occurs. The formation of perrhenic acid as the catalytic active species is refuted because it is found to be both less catalytically active and selective than Re_2O_7 . Furthermore, the stable perrhenate fragment is catalytically inactive (vide supra), thus no heterolytic decomposition into ReO_3^+ and ReO_4^- occurs.

The aqueous extraction of the reaction mixture after quantitative conversion of **1** reveals intact rhenium heptoxide, which was elucidated by its unaltered chemical reactivity.

Since Re_2O_7 hydrolyses in excess water into two equiv. of perrhenic acid, the pH value provides information about the remaining rhenium amount. A measured value of pH = 4.1 indicates the presence of perrhenic acid. Considering HReO_4 as strong acid ($\text{p}K_{\text{a}} = -1.25$),⁶⁷ the obtained pH value of 4.1 is equivalent to an amount of ≈ 0.11 mg of Re_2O_7 which represents 55% of initial catalyst loading. Subsequent addition of silver nitrate gave a white precipitate of silver perrhenate which confirms the latter formation perrhenic acid. The remaining amount of Re_2O_7 explains the residual catalytic activity which is observed by the consecutive addition of a new substrate load. Herein, further conversion of 72% is obtained within 2 h at 140 °C.

The importance of the acidity was confirmed by addition of a Lewis base which inhibits the catalyst probably reducing its Lewis acidity. Similar reactivity was previously observed by Korstanje et al. when *N*-base addition resulted in inhibition of Re_2O_7 in the alcohol dehydration, a reaction known to be catalysed by Lewis acids.⁴⁸ The latter effect is applied

for the MTO-catalysed olefin epoxidation. Addition of *N*-bases decreases its acidity and increases the selectivity towards acid sensitive epoxides.^{68, 69} Moreover, the kinetic profile exhibits no induction period and first order behaviour (please see the SI, Figure S3). Thus, no preceding transformation to an active catalyst species occurs.

However, catalyst decomposition is observed limiting the catalysts turn over number to TON = 2200 (*vide infra*). During reaction a black, insoluble precipitate forms due to Re_2O_7 instability at such reaction conditions. Heating of Re_2O_7 in the reaction medium (all tested solvents as *p*-xylene, toluene, THF, 1,4-dioxane, MeCN) resulted in reasonable decomposition. Noteworthy, the isolated precipitate is catalytically not active.

Analysis of the decomposed catalyst (black precipitate)

The black material was separated from the supernatant solution and subsequently analysed. The very fine grained solid is insoluble in all commonly used laboratory solvents such as BTX aromatics, aliphatic hydrocarbons, halogenated alkanes, ethers, DMSO, CH_3CN , and pyridine. Thus, the precipitate can be washed with toluene and hexane and be dried in the high-vacuum. While latter procedure no change of the powder in shape and colour is observed. An elemental analysis revealed an unexpected high content in carbon of 18.8% and low rhenium percentage of 55.7%. Moreover, the high amount of carbon was confirmed by the energy dispersive X-ray spectroscopy (EDX, see the SI Figure S6). The related scanning electron microscopy (SEM) picture shows an overview of the decomposed catalyst. The powder is composed of small sized and equally distributed particles; however, a powder XRD analysis exhibited the amorphous character of the solid.

The surface of the powder was analysed by X-ray photoelectron spectroscopy (XPS) to gain insight about the elemental composition and present oxidation states. This spectroscopic method is very suitable for the determination of the oxidation state of rhenium compounds, since the binding energies of each oxidation state differs from $\text{Re}(0)$ to $\text{Re}(\text{VII})$ by 7 eV.⁷⁰⁻⁷³ The wide scan (survey) XPS spectrum of the washed solid (see Figure 2, a) shows reasonable intense signals of rhenium $\text{Re}4f$, $\text{Re}4d_{3/2}$, $\text{Re}4d_{5/2}$, oxygen $\text{O}1s$ and carbon $\text{C}1s$. The narrow scan of this sample over the $\text{Re}4f$ region illustrates the presence of multiple rhenium oxidation states due to the overlaid to $\text{Re}4f_{5/2}$ and $\text{Re}4f_{7/2}$ signals (see Figure 2, b). Deconvolution exhibits the $4f$ region to be consisted of the contributions of at least three $\text{Re}4f$ spin orbit coupling doublet components, which indicates that rhenium is present in at least three different oxidation states.

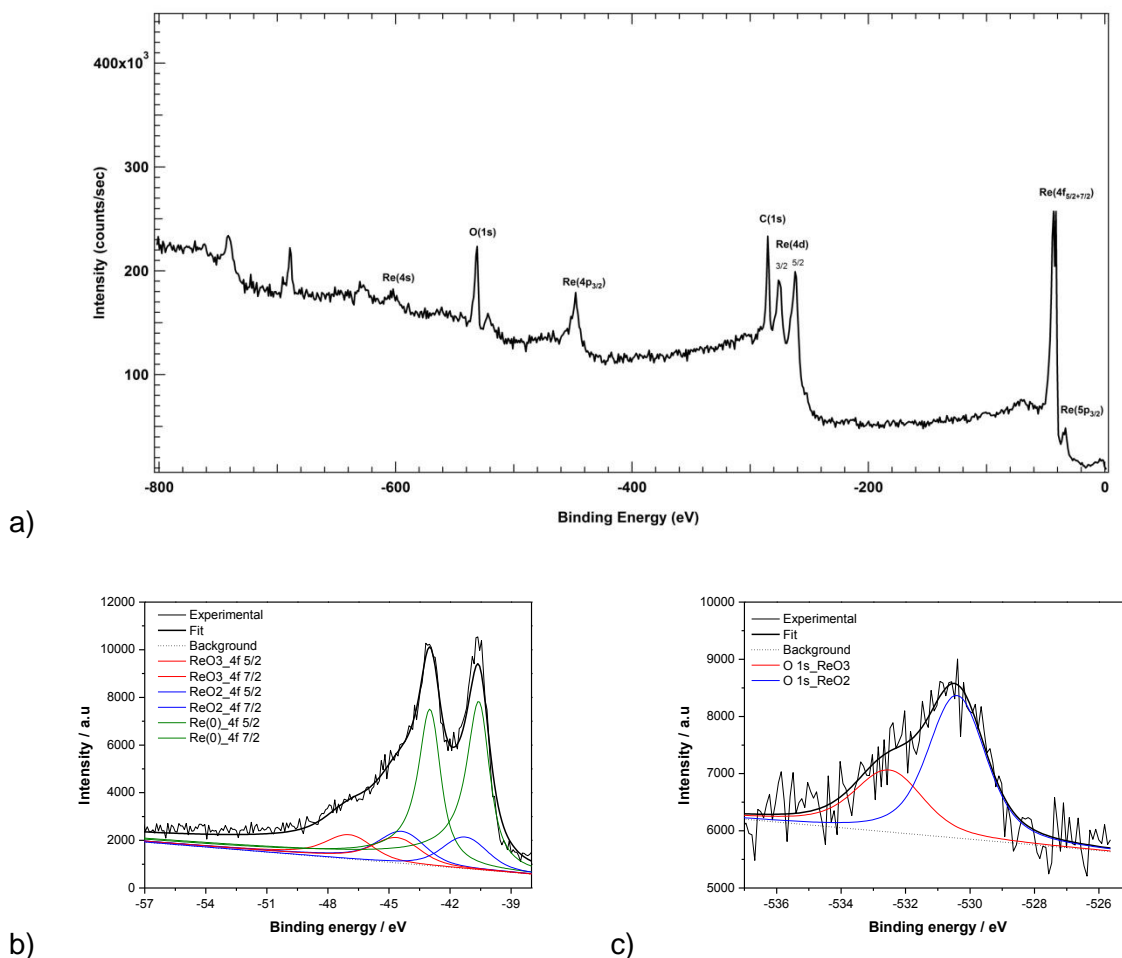


Figure 2. X-ray photoelectron spectra of the black precipitate: a) survey scan (b.e. -800 to 0 eV) with annotation of the corresponding orbital signal; b) narrow scan over the Re4f energy window (b.e. -58 to -38 eV) and deconvolution of the overlapped proportion; c) narrow scan over the O1s energy window (b.e. -537 to -526 eV) and deconvolution of two overlapped proportions.

The most intense peak of the Re $4f_{7/2,5/2}$ doublet pair is the lowest binding energy component. The binding energies of -40.7 – -43.1 eV are in agreement with the literature for elemental Re(0).⁷⁰⁻⁷⁴ The deconvolution in higher binding energy components proves the presence of higher oxidation states. In accordance to the literature, the existence of Re(IV) and Re(VI) is revealed by the pairs of peaks at binding energies of -42.5 – -44.8 eV and -44.5 – -46.8 eV respectively, in decreasing intensity.^{71, 73, 75} A narrow scan of the oxygen O1s region shows a broad, overlaid signal (see Figure 2, c). The deconvolution exposes two species of oxygen. The binding energies of -530.6 eV and -532.5 eV are in agreement with the literature values of oxygen found in ReO₂ and ReO₃, respectively.⁷⁵ The carbon C1s region shows only a single signal, which is in literature referred to graphite (see the SI for detailed spectra).⁷² These values prove that the black precipitate is consisted only of rhenium, carbon and oxygen. Furthermore, the contained rhenium is present in three different oxidation state, whereas the major ratio is contributed by rhenium(0) and in much diminished amounts by rhenium(IV) and rhenium(VI). The Re4d region exhibits a higher amount of Re(IV) than the

Re4f (see the SI). Since the photoelectron escape depth of 4d electron is lower, the Re4d regions exhibits more surface details than from the bulk material. Thus, the surface of the particles is more oxidised than the bulk material, pointing to the formation of Re(0) rather than the formation of a mixed oxide. Moreover, rhenium(VII) of the initially used Re_2O_7 is not present indicating a complete, reductive decomposition and no co-precipitation or adsorption on char.⁷¹⁻⁷⁵ The formation of elemental rhenium and its superficial oxidation is not surprising since the reduction of perrhenates to Re(0) in presence of alcohols was reported previously.^{57, 76} Furthermore, elemental jet-black rhenium clusters are known to undergo rapid oxidation to Re(III/IV) and Re(VI/VII) oxides in aerobic atmosphere,^{77, 78} and black Re(0) nanoparticles of 2 nm size are easily oxidised to ReO_2 .^{57, 76} The high carbon content found in elemental analysis is identified by XPS as graphite.

Further insight in the nature of the carbon and the rhenium oxide species was gained by Raman spectroscopy (see Figure 3).

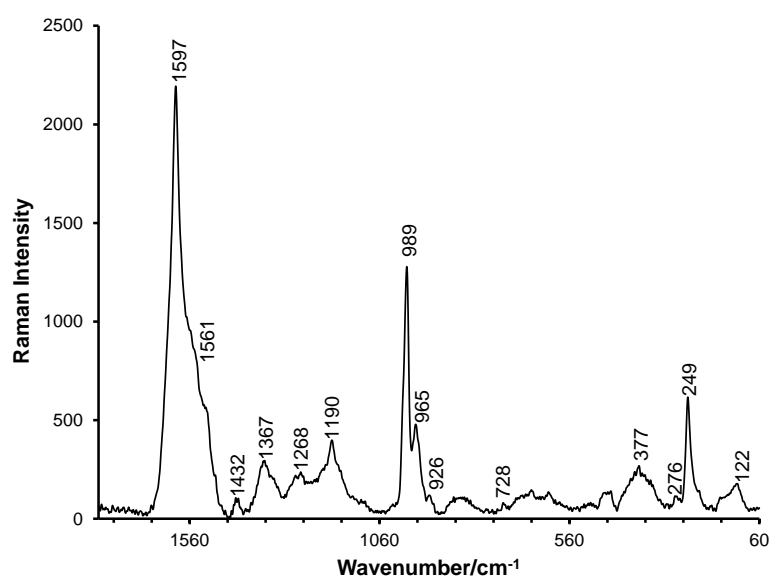


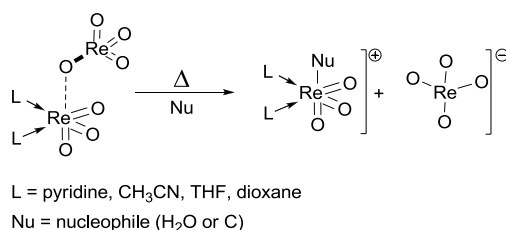
Figure 3. Raman spectrum of the black precipitate which forms during catalysis. The questioned composition is revealed by Raman spectroscopy as disordered graphite and ReO_2 .

A very strong and broad band at 1597 cm^{-1} indicates enormous amounts of sp^2 -hybridised carbon. The position and broadness of the latter band and the appearance of an additional band at 1367 cm^{-1} displays the possible formation of disordered graphite as observed by Reich et al.⁷⁹ The bands at 1367 cm^{-1} and 1597 cm^{-1} may also refer as D (diamond or disorder-induced) and G (graphite) bands respectively as observed in Raman spectra of carbon nanotubes.⁸⁰⁻⁸³ A comparison with the Raman spectra of authentic rhenium samples (ReO_2 , ReO_3 , NH_4ReO_4 , see the SI), identified the very strong bands at 989, 965, 377, and 249 cm^{-1} as ReO_2 . The strong and sharp bands at 989 cm^{-1} and 965 cm^{-1} show the presence

of Re–O vibrational modes which might also refer to the ν_s and ν_{as} vibration mode of ReO_3 units in Re_2O_7 . However, the Raman spectrum excludes the presence of rhenium heptoxide, because no signal originating from characteristic vibration of the Re–O–Re bonds is found in the region of $\approx 61 \text{ cm}^{-1}$.⁸⁴⁻⁸⁶ Moreover, only small amount of ReO_3 can be assigned to the absorption band at 728 and $\approx 340 \text{ cm}^{-1}$.^{87, 88} Although the high-frequency mode at 965 cm^{-1} could be derived from the Re–O stretching mode in ReO_4 tetrahedra in solid perrhenates,⁸⁹ characteristic bands at 914, 892, and 343 cm^{-1} are not present excluding the presence of any perrhenate (see the SI).

Consideration of rhenium heptoxide's reductive decomposition

As afore mentioned the decompositions of Re_2O_7 at the applied reaction conditions (100–140 °C) is independent of the presence of substrate. The decomposition rate depends on the used solvent and *N*-basic additives. In *O*-donor solvents as THF and 1,4-dioxane reasonable decomposition is observed at 80 °C and 100 °C, respectively (vide supra for solvent influence on the catalytic activity). Rhenium heptoxide is stable in CH_3CN at 80 °C, however, an elevated temperature to 140 °C leads to precipitation of a black solid. Addition of 1 equiv. pyridine per rhenium heptoxide to a *p*-xylene mixture slows down the decomposition process at 140 °C, but addition of 10 equiv. completely inhibits both catalysis and catalyst decomposition. Small amounts of water or the presence of Lewis base *O*- or *N*-donor compounds (THF, 1,4-dioxane, CH_3CN , pyridine) result in formation of Lewis acid-base pairs in the type of $\text{L}_2\text{ReO}_3[\text{ReO}_4]$ (see Scheme 3). Two octahedral aligned ligands coordinate a single rhenium centre generating a perrhenyl and perrhenate centre, which in consequence weakens the Re–O–Re intramolecular bond (see Scheme 2).⁶³



Scheme 3. Lewis base coordination to Re_2O_7 weakens the Re–O bond and preforms a ReO_4^- fragment. Thus, the perrhenyl fragment becomes extremely sensitive to nucleophiles.

Coordination of two *O*-donor solvent molecules destabilises the rhenium heptoxide, thus the improved solubility may also effect accelerated decomposition. The increased stability in *N*-donor media or in presence of *N*-bases is explained by a reduced Lewis acidity of rhenium heptoxide itself which probably overwhelms the effect of destabilization due to *N*-base coordination.^{64, 90} Although Re_2O_7 forms stable Lewis base adducts, no alcohol adducts are observed and reductive decompositions in concentrated alcoholic solutions occurs instead.

By thermal treatment of an alcoholic solution of Re_2O_7 the reductive formation of nanoparticles (10–100 nm) was observed.⁹¹⁻⁹⁴ At similar reaction conditions, Biswas et al. reported the syntheses of red coloured ReO_3 nanoparticles by the thermal decomposition of Re_2O_7 -dioxanes adducts in toluene.^{93, 94} Since red rhenium(VI) oxide is known to form black aqua-adducts, the uncontrolled formation and growth of black ReO_3 nanoparticles is possible.⁹¹

Furthermore, Abu-Omar et al. observed black $\text{Re}(0)$ nanoparticles upon treatment of either MTO or ammonium perrhenate with secondary alcohols at similar reaction temperatures ranging from 140–180 °C.^{57, 95} The synthesis of nanostructured gray-black ReO_2 by reductive hydrolysis of MTO was reported by Fröba and Muth,⁹⁶ while Mucalo et al. obtained black $\text{Re}(0)$ particles upon reduction of Re(VI) halides.^{77, 78}

Formation of carbon

Amorphous sp^2 -hybridised carbon is probably generated by the catalytic ability of colloid $\text{Re}(0)$ particles. Ritschel et al. reported that magnesium oxide supported rhenium is capable to catalyse the growth of carbon nanotubes (CNT) by decomposition of methane.⁹⁷ Usually benzene or xylene is used as carbon source in CNT synthesis and Fe, Co or Ni nanoparticles are proven to be efficient catalysts. As Kumar and Ando stated in their recent review article any metal can catalyse the CNT growth, and just any carbon containing material can yield in CNT.⁹⁸

Moreover, the formation of black carbon is commonly considered as charring. The groups of Abu-Omar and Nicholas observed significant charring or formation of a black precipitate when MTO is exposed to similar reaction conditions (alcoholic substrates, higher temperature range).^{61, 95, 99} However, charring was previously observed also in absence of rhenium catalyst. Sturgeon et al. reported the charring of β -hydroxy aryl ether lignin model compounds in presence of 0.2 M sulphuric acid at 150 °C.³⁵ The authors stated the sensitivity of the cleavage products towards strong acidic treatment. The observed charring is also reflected in a decrease of the product yield after prolonged reaction times. The longer the heating of the reaction mixture is continued after full conversion and the higher the initial rhenium heptoxide loading, the lower the observed product yields (see the SI, Figure S2).

Conclusion: In summary, a new benchmark system for selective C–O bond cleavage of a very stable and commonly β -hydroxy aryl ether lignin model compound has been presented. The cleavage reaction is revealed to be Lewis acid-catalysed and Re_2O_7 proved to be both the most active and selective. The catalyst stays unchanged as fine, heterogeneous Re_2O_7 particles in the reaction medium and no preceding modification or formation of any further active species is observed. Based on first order kinetics and reactivity studies a mechanism

analogue to Brønsted acid-catalysed reactions is proposed. Up to our knowledge, this is the first example on the degradation of a β -O-4 lignin model linkage because of Lewis acidity of a rhenium compound. However, the catalytic system suffers from reductive decomposition due to the formation of catalytically inactive Re(0) under the applied reaction conditions. The deactivated catalyst was thoroughly analysed by means of elemental analysis, XPS, and Raman spectroscopy. The application of the latter promising results in the C–O bond cleavage of other lignin model compounds and the depolymerisation of β -hydroxy aryl ether macromolecules are currently under investigation. Moreover, solid non-precious Lewis acids exhibit comparable catalytic activity at the applied reaction conditions. Hence, this might be a promising concept for the catalytic C–O bond cleavage in unprocessed lignin.

Experimental: Typical procedure for the catalytic cleavage of 2-(2-methoxyphenoxy)phenylethanol (**1**): A solution of **1** (100 mg, 0.410 mmol) and *p*-xylene (4 mL) was added to Re₂O₇ (0.20 mg, 0.42 mmol, 0.1 mol%) and 1,2,4,5-tetramethylbenzene (ca. 20–40 mg as internal standard) in a 20 mL vial and heated under stirring for 2 h at 140 °C. Although full substrate conversions are observed at lower catalyst concentrations, a loading of 0.1 mol% allowed a more precise and convenient work routine.

During the reaction the initial colourless mixture changed to pale brown and subsequently the precipitation of a black solid is observed. After given reaction time, the reaction was stopped by cooling down using an external water bath. For GC FID analysis the reaction mixture was filtered to remove the black solid. An aliquot of 50 μ L was taken from the filtrate, diluted with 950 μ L toluene and 500 μ L external standards solution in toluene (see the SI for details). If different solvents were used, the procedure was not changed, however, using low boiling point solvents an ACE pressure tube was used instead as reaction vessel.

For the aqueous extraction the reaction mixture was passed through a Whatman® filter and the filtrate subsequently washed with 1 mL water. After separation of the two phases all further experiments were conducted from the aqueous phase.

Acknowledgements: RGH and LG are grateful to the TUM Graduate School for financial support. We also thank Prof. Dr. Sebastian Günther for providing the XPS system and Prof. Dr. Sonja Berensmeier for providing the Raman spectrometer. We appreciate helpful discussions with Prof. Dr. Richard W. Fisher and Dr. Mirza Cokoja.

References:

1. U.S. Energy Information Administration, monthly average Brent spot prices of 2004/Jan to 2014/Jan, conversion to February 2013 dollars uses US CPI for All Urban Consumers (CPI-U)
2. C. K. James M. Tour, Vicki L. Colvin, *Nature Materials*, 2010, **9**, 871-874.
3. S. R. Collinson and W. Thielemans, *Coord. Chem. Rev.*, 2010, **254**, 1854-1870.
4. D. R. Dodds and R. A. Gross, *Science*, 2007, **318**, 1250-1251.
5. D. M. Alonso, J. Q. Bond and J. A. Dumesic, *Green Chemistry*, 2010, **12**, 1493-1513.
6. H. Z. Tushar P. Vispute, Aimaro Sanna, Rui Xiao, George W. Huber, *Science*, 2010, **330**.
7. R. Rinaldi and F. Schuth, *Energy Environ. Sci.*, 2009, **2**, 610-626.
8. G. W. Huber and A. Corma, *Angew. Chem. Int. Ed.*, 2007, **46**, 7184-7201.
9. G. W. Huber, S. Iborra and A. Corma, *Chem. Rev.*, 2006, **106**, 4044-4098.
10. M. P. Pandey and C. S. Kim, *Chemical Engineering & Technology*, 2011, **34**, 29-41.
11. J. Zakzeski, P. C. A. Bruijninx, A. L. Jongerius and B. M. Weckhuysen, *Chem. Rev.*, 2010, **110**, 3552-3599.
12. W. Boerjan, J. Ralph and M. Baucher, *Annu. Rev. Plant Biol.*, 2003, **54**, 519.
13. Z. Strassberger, A. H. Alberts, M. J. Louwse, S. Tanase and G. Rothenberg, *Green Chemistry*, 2013, **15**, 768-774.
14. M. R. Sturgeon, M. H. O'Brien, P. N. Ciesielski, R. Katahira, J. S. Kruger, S. C. Chmely, J. Hamlin, K. Lawrence, G. B. Hunsinger, T. D. Foust, R. M. Baldwin, M. J. Bidy and G. T. Beckham, *Green Chemistry*, 2014, **16**, 824-835.
15. J. C. Hicks, *J. Phys. Chem. Lett.*, 2011, **2**, 2280.
16. C. Zhao and J. A. Lercher, *ChemCatChem*, 2012, **4**, 64-68.
17. A. G. Sergeev, J. D. Webb and J. F. Hartwig, *J. Am. Chem. Soc.*, 2012, **134**, 20226-20229.
18. T. H. Parsell, B. C. Owen, I. Klein, T. M. Jarrell, C. L. Marcum, L. J. Hauptert, L. M. Amundson, H. I. Kenttamaa, F. Ribeiro, J. T. Miller and M. M. Abu-Omar, *Chemical Science*, 2013, **4**, 806-813.
19. Y. Ren, M. Yan, J. Wang, Z. C. Zhang and K. Yao, *Angew. Chem. Int. Ed.*, 2013, **52**, 12674-12678.
20. H. Wang, M. Tucker and Y. Ji, *Journal of Applied Chemistry*, 2013, **2013**, 9.
21. V. M. Roberts, V. Stein, T. Reiner, A. Lemonidou, X. Li and J. A. Lercher, *Chem. Eur. J.*, 2011, **17**, 5939-5948.
22. A. G. Sergeev and J. F. Hartwig, *Science*, 2011, **332**, 439-443.
23. S. Son and F. D. Toste, *Angew. Chem. Int. Ed.*, 2010, **49**, 3791-3794.
24. S. K. Hanson, R. T. Baker, J. C. Gordon, B. L. Scott and D. L. Thorn, *Inorg. Chem.*, 2010, **49**, 5611-5618.
25. S. K. Hanson, R. Wu and L. A. P. Silks, *Angew. Chem. Int. Ed.*, 2012, **51**, 3410-3413.
26. J. Zhang, Y. Liu, S. Chiba and T.-P. Loh, *Chem. Commun.*, 2013, **49**, 11439-11441.
27. J. M. Nichols, L. M. Bishop, R. G. Bergman and J. A. Ellman, *J. Am. Chem. Soc.*, 2010, **132**, 12554-12555.
28. T. vom Stein, T. Weigand, C. Merckens, J. Klankermayer and W. Leitner, *ChemCatChem*, 2013, **5**, 439-441.
29. B. Sedai, C. Díaz-Urrutia, R. T. Baker, R. Wu, L. A. P. Silks and S. K. Hanson, *ACS Catalysis*, 2011, **1**, 794-804.
30. R. G. Harms, I. I. E. Markovits, M. Drees, W. A. Herrmann, M. Cokoja and F. E. Kühn, *ChemSusChem*, 2014, **7**, 429-434.
31. T. Yokoyama and Y. Matsumoto, *Holzforschung*, 2008, **62**, 164.
32. H. Ito, T. Imai, K. Lundquist, T. Yokoyama and Y. Matsumoto, *J. Wood Chem. Technol.*, 2011, **31**, 172.
33. T. Yokoyama and Y. Matsumoto, *J. Wood Chem. Technol.*, 2010, **30**, 269.
34. K. Lundquist and R. Lundgren, *Acta Chem. Scand.*, 1972, **26**, 2005-2023.

35. M. R. Sturgeon, S. Kim, K. Lawrence, R. S. Paton, S. C. Chmely, M. Nimlos, T. D. Foust and G. T. Beckham, *ACS Sustainable Chemistry & Engineering*, 2014, **2**, 472-485.
36. S. W. Eachus and C. W. Dence, in *Holzforschung - International Journal of the Biology, Chemistry, Physics and Technology of Wood*, 1975, vol. 29, p. 41.
37. F. Davoudzadeh, B. Smith, E. Avni and W. Coughlin Robert, in *Holzforschung - International Journal of the Biology, Chemistry, Physics and Technology of Wood*, 1985, vol. 39, p. 159.
38. A. Vuori and M. Niemelä, in *Holzforschung - International Journal of the Biology, Chemistry, Physics and Technology of Wood*, 1988, vol. 42, p. 327.
39. M. Aoyama, C.-L. Chen and D. Robert, *J. Chin. Chem. Soc.*, 1991, **38**, 77-84.
40. L. Yang, Y. Li and P. E. Savage, *Industrial & Engineering Chemistry Research*, 2014, **53**, 2633-2639.
41. J. B. Binder, M. J. Gray, J. F. White, Z. C. Zhang and J. E. Holladay, *Biomass Bioenergy*, 2009, **33**, 1122-1130.
42. M. Kudsy and H. Kumazawa, *The Canadian Journal of Chemical Engineering*, 1999, **77**, 1176-1184.
43. M. M. Hepditch and R. W. Thring, *The Canadian Journal of Chemical Engineering*, 2000, **78**, 226-231.
44. A. Corma, *Chem. Rev.*, 1995, **95**, 559-614.
45. H. Pines and W. O. Haag, *J. Am. Chem. Soc.*, 1961, **83**, 2847-2852.
46. WO 2005035468 A1, 2005.
47. D. S. Noyce, D. R. Hartter and R. M. Pollack, *J. Am. Chem. Soc.*, 1968, **90**, 3791-3794.
48. T. J. Korstanje, J. T. B. H. Jastrzebski and R. J. M. Klein Gebbink, *Chem. Eur. J.*, 2013, **19**, 13224-13234.
49. T. J. Korstanje, E. F. de Waard, J. T. B. H. Jastrzebski and R. J. M. K. Gebbink, *Acs Catalysis*, 2012, **2**, 2173-2181.
50. T. J. Korstanje, J. T. B. H. Jastrzebski and R. J. M. K. Gebbink, *ChemSusChem*, 2010, **3**, 695-697.
51. Z. L. Zhu and J. H. Espenson, *J. Org. Chem.*, 1996, **61**, 324-328.
52. O. Vogl, *Journal of Macromolecular Science: Part A - Chemistry*, 1967, **1**, 243-266.
53. O. Vogl and W. M. D. Bryant, *J. Polym. Sci., Part A: Gen. Pap.*, 1964, **2**, 4633-4645.
54. A. Tsukamoto and O. Vogl, *Prog. Polym. Sci.*, 1971, **3**, 199-279.
55. A. Behr and P. Neubert, *Applied Homogeneous Catalysis*, Wiley, 2012.
56. B. Cornils and W. A. Herrmann, *Applied homogeneous catalysis with organometallic compounds: Developments*, Wiley-VCH, 2002.
57. J. Yi, J. T. Miller, D. Y. Zemlyanov, R. Zhang, P. J. Dietrich, F. H. Ribeiro, S. Suslov and M. M. Abu-Omar, *Angew. Chem. Int. Ed.*, 2014, **53**, 833-836.
58. A. L. Denning, H. Dang, Z. Liu, K. M. Nicholas and F. C. Jentoft, *ChemCatChem*, 2013, **5**, 3567-3570.
59. J. Yi, S. Liu and M. M. Abu-Omar, *ChemSusChem*, 2012, **5**, 1401-1404.
60. M. Shiramizu and F. D. Toste, *Angew. Chem. Int. Ed.*, 2012, **51**, 8082-8086.
61. I. Ahmad, G. Chapman and K. M. Nicholas, *Organometallics*, 2011, **30**, 2810-2818.
62. E. Arceo, J. A. Ellman and R. G. Bergman, *J. Am. Chem. Soc.*, 2010, **132**, 11408-11409.
63. C. C. Romão, F. E. Kühn and W. A. Herrmann, *Chem. Rev.*, 1997, **97**, 3197-3246.
64. W. A. Herrmann, P. W. Roesky, F. E. Kühn, W. Scherer and M. Kleine, *Angew. Chem. Int. Ed. Engl.*, 1993, **32**, 1714-1716.
65. J. Clayden, N. Greeves and S. Warren, *Organic Chemistry*, Oxford University Press, Oxford, New York, 2012.
66. M. B. Smith and J. March, *March's Advanced Organic Chemistry: Reactions, Mechanisms, and Structure*, Wiley, Hoboken, New Jersey, 2007.
67. G. Rouschias, *Chem. Rev.*, 1974, **74**, 531-566.

68. F. E. Kühn, A. M. Santos, I. S. Gonçalves, C. C. Romão and A. D. Lopes, *Appl. Organomet. Chem.*, 2001, **15**, 43-50.
69. S. A. Hauser, M. Cokoja and F. E. Kuhn, *Catalysis Science & Technology*, 2013, **3**, 552-561.
70. L. P. Bevy, ed., *Focus on Catalysis Research* Nova Science Publishers, New York, 2006.
71. A. Cimino, B. A. De Angelis, D. Gazzoli and M. Valigi, *Z. Anorg. Allg. Chem.*, 1980, **460**, 86-98.
72. C. D. Wagner, W. M. Riggs, L. E. Davis and J. F. Moulder, ed. G. E. Muilenberg, Perkin-Elmer Corporation, Eden Praire, Minnesota, 1979.
73. J. Okal, W. Tylus and L. Kępiński, *J. Catal.*, 2004, **225**, 498-509.
74. Y. Fukuda, F. Honda and J. Wayne Rabalais, *Surf. Sci.*, 1980, **93**, 338-350.
75. E. Brockawik, J. Haber and L. Ungier, *J. Phys. Chem. Solids*, 1981, **42**, 203-208.
76. J. Yi, J. T. Miller, D. Y. Zemlyanov, R. Zhang, P. J. Dietrich, F. H. Ribeiro, S. Suslov and M. M. Abu-Omar, *Angew. Chem.*, 2014, **126**, 852-855.
77. K. M. Babu and M. R. Mucalo, *J. Mater. Sci. Lett.*, 2003, **22**, 1755-1757.
78. M. R. Mucalo and C. R. Bullen, *J. Colloid Interface Sci.*, 2001, **239**, 71-77.
79. S. Reich and C. Thomsen, *Philosophical Transactions of the Royal Society of London. Series A: Mathematical, Physical and Engineering Sciences*, 2004, **362**, 2271-2288.
80. F. Adar, *Spectroscopy*, 2009, **24**, 28-39.
81. J. Hodkiewicz, Thermo Fisher Scientific, Madison, WI, USA, 2010.
82. M. S. Dresselhaus and P. C. Eklund, *Advances in Physics*, 2000, **49**, 705-814.
83. M. S. Dresselhaus, A. Jorio, M. Hofmann, G. Dresselhaus and R. Saito, *Nano Lett.*, 2010, **10**, 751-758.
84. R. A. Nyquist, C. L. Putzig and M. A. Leugers, *Handbook of Infrared and Raman Spectra of Inorganic Compounds and Salts*, Academic Press, New York, 1997.
85. I. R. Beattie, T. R. Gilson and P. J. Jones, *Inorg. Chem.*, 1996, **35**, 1301-1304.
86. I. R. Beattie and G. A. Ozin, *Journal of the Chemical Society A: Inorganic, Physical, Theoretical*, 1969, 2615-2619.
87. E. Cazzanelli, M. Castriota, S. Marino, N. Scaramuzza, J. Purans, A. Kuzmin, R. Kalendarev, G. Mariotto and G. Das, *J. Appl. Phys.*, 2009, **105**, -.
88. J. Purans, A. Kuzmin, E. Cazzanelli and G. Mariotto, *J. Phys.: Condens. Matter*, 2007, **19**, 226206.
89. P. L. Gassman, J. S. McCloy, C. Z. Soderquist and M. J. Schweiger, *Journal of Raman Spectroscopy*, 2014, **45**, 139-147.
90. W. A. Herrmann, P. W. Roesky, F. E. Kuehn, M. Elison, G. Artus, W. Scherer, C. C. Romao, A. Lopes and J.-M. Basset, *Inorg. Chem.*, 1995, **34**, 4701-4707.
91. D. E. Emel'yanov, Y. Y. Gukova, Y. V. Karyakin and M. I. Ermolaev, *Russian Journal of Inorganic Chemistry*, 1968, **13**, 89-90.
92. *Japan Pat.*, JP 09142846 and JP 3956400, 1997.
93. K. Biswas and C. N. R. Rao, *The Journal of Physical Chemistry B*, 2006, **110**, 842-845.
94. S. Ghosh, K. Biswas and C. N. R. Rao, *J. Mater. Chem.*, 2007, **17**, 2412-2417.
95. S. Liu, A. Senocak, J. L. Smeltz, L. Yang, B. Wegenhart, J. Yi, H. I. Kenttämä, E. A. Ison and M. M. Abu-Omar, *Organometallics*, 2013, **32**, 3210-3219.
96. M. Fröba and O. Muth, *Adv. Mater.*, 1999, **11**, 564-567.
97. M. Ritschel, A. Leonhardt, D. Elefant, S. Oswald and B. Büchner, *The Journal of Physical Chemistry C*, 2007, **111**, 8414-8417.
98. M. Kumar and Y. Ando, *Journal of Nanoscience and Nanotechnology*, 2010, **10**, 3739-3758.
99. J. E. Ziegler, M. J. Zdilla, A. J. Evans and M. M. Abu-Omar, *Inorg. Chem.*, 2009, **48**, 9998-10000.

Supporting Information

Table of Contents

C-1 General	103
C-1.1 Material and methods	103
C-1.2 Instruments	103
C-2 Catalysis	104
C-2.1 Typical GC analysis at optimised reaction conditions	104
C-2.2 Optimisation of reaction conditions	105
C-2.2.1 Influence of temperature, catalyst loading and reaction time	105
C-2.2.2 Solvent influence	106
C-3 Mechanistic investigations	107
C-3.1 Kinetic data	107
C-3.2 Formation of the enol ether intermediate (1a)	108
C-4 Analysis of the inactive decomposed catalyst	110
C-4.1 EDX Spectra and SEM picture	110
C-4.2 Raman Spectra	110
C-4.3 XPS	112
C-5 Product identification and NMR spectra	117
C-5.1 Retention times and NMR data	117
C-5.2 Selected NMR spectra	118
C-6 References	119

C-1 General

C-1.1 Material and methods

The NMR solvents *p*-Xylene- d_{10} (Sigma-Aldrich) and chloroform- d_3 (Deutero GmbH) were used without further purification. Rhenium heptoxide was provided from Enovik Industries AG (former Degussa AG) or prepared according to a literature procedure.¹ 2-(2-methoxyphenoxy)phenylethanol was synthesised according to a literature procedure.^{2, 3} All other reagents were purchased from commercial suppliers (Sigma-Aldrich and ABCR, Karlsruhe) and used without further purification.

Catalytic reactions were carried out in a 20 mL vial. When the reaction was conducted under argon atmosphere a Schlenk tube was used instead. If reaction temperature exceeded the boiling point of the solvent, ACE pressure tubes were used as reaction vessel.

C-1.2 Instruments

Catalytic runs were monitored by using GC methods on a Hewlett–Packard HP 6890 Series GC System equipped with a FID and using Standard ChemStation G1701AA Version A.03.00 as software. Integrals have been quantified using internal (1,2,4,5-tetramethylbenzene; TMB) and external (3-methylanisol, diphenylether, 4-methylacetophenone) standards. NMR spectra were recorded on a Bruker Avance DPX 400 (293 K, $^1\text{H-NMR}$, 400.1 MHz;) and chemical shifts are reported relative to the residual signal of the deuterated solvent (*p*-xylene- d_{10} was prior referred to tetramethylsilane $\delta = 6.90, 2.12$ ppm).

C-2 Catalysis

C-2.1 Typical GC analysis at optimised reaction conditions

The formation of phenylacetaldehyd (2) and guaiacol (3) was observed via GC FID. The data are in agreement with an authentic sample. GC FID showed an identical retention time. Signals at retention time of 5.077, 7.994, and 8.638 min originate from solvent impurities as revealed by a blank test.

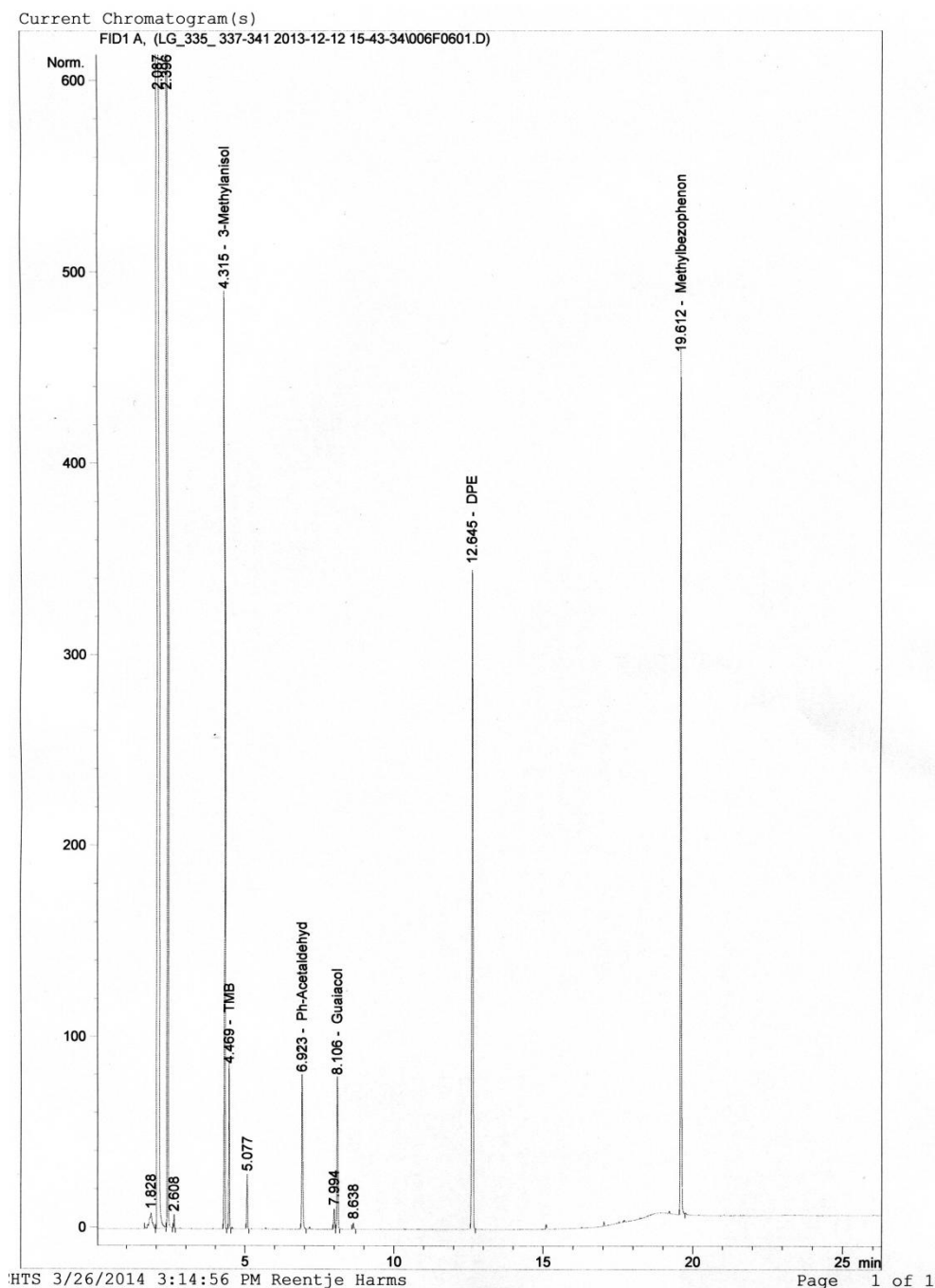


Figure S1. GC FID spectrum after a standard catalysis run (2 h at 140 °C; TMB = 1,2,4,5-tetramethylbenzene).

C-2.2 Optimisation of reaction conditions

C-2.2.1 Influence of temperature, catalyst loading and reaction time

The influence of catalyst loading and reaction time was determined. An increase of catalyst concentration resulted in an aggravated mass balance. Extended reaction times gave full conversions, however, the product yields decreased.

Table S1. Effect of catalyst concentration in the Re_2O_7 catalysed C–O cleavage of **1**.

Entry	Cat. conc. [mol%]	Temp.	Conv. 1 [%]	Yield 2 [%]	Yield 3 [%]
1	5	140	100	52	63
2	2.5	140	100	86	93
3	0.5	140	100	92	96
4	0.1	140	100	96	97
5	0.1	120	43	20	22
6	0.1	100	20	18	15
7	0.1	80	4	0	0
8	0.1	r.t.	0	0	0
9	0.05	140	100	69	77
10	0.025	140	41	34	37
11	0	140	0	0	0

Conversion and yields were determined by GC FID.

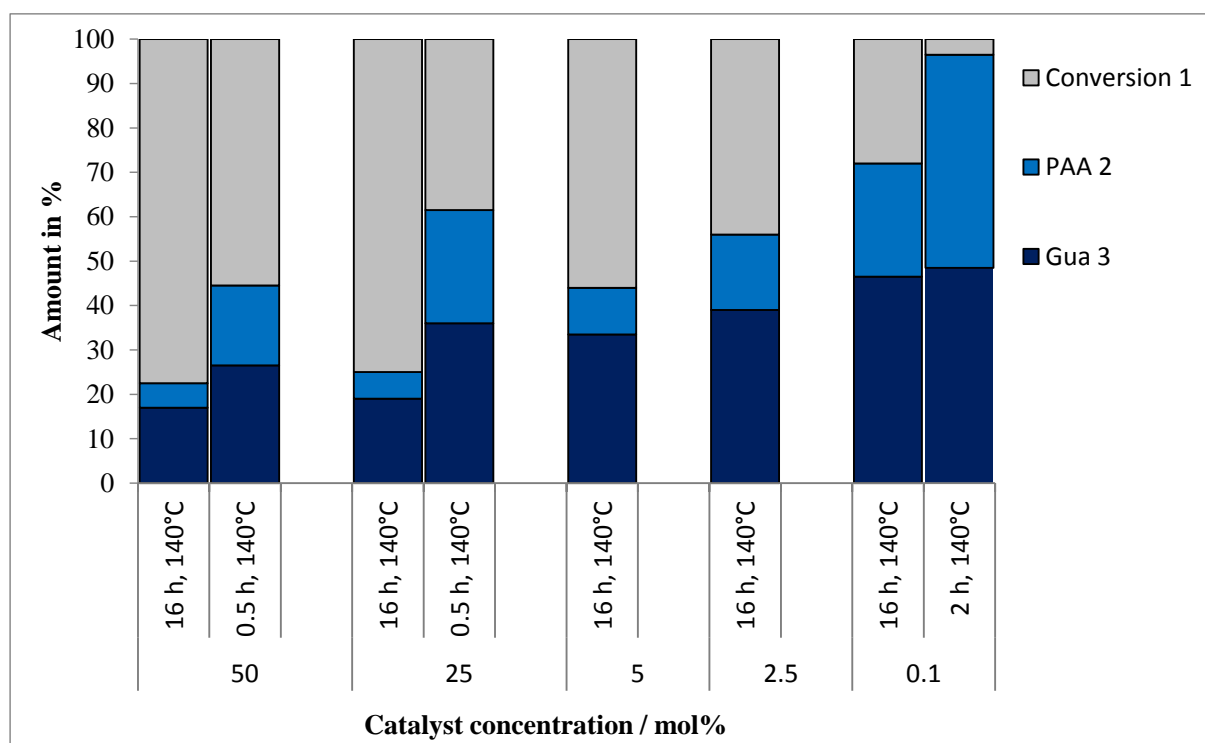


Figure S2. Influence of the catalyst loading (mol%) and reaction time (h).

C-2.2.2 Solvent influence

Table S2. Effect of different solvents on the catalytic activity and product yield.

Entry	Solvent/Medium ^a	Temp. [°C]	Conv. 1 [%]	Yield 2 [%]	Yield 3 [%]
1	THF ^b	140	71	44	54
2	THF ^b	100	55	25	27
3	THF ^b	80	32	12	15
4	MeCN ^c	140	23	7	11
5	MeCN ^c	80	9	0	0
6	MeCN ^d	80	22	32	3
7	MeCN ^e	80	41	38	13
8	Dioxane ^b	80	86	47	65
9	<i>n</i> -decane ^c	140	19	7	9
10	CH ₃ COOH ^c	140	65	43	44
11	CH ₃ COOH ^c	110	13	0	7

a) 4 mL solvent; b) 5 mol% Re₂O₇, 2 h; c) 0.1 mol% Re₂O₇, 2 h; d) 0.1 mol% Re₂O₇, 16 h; e) 0.1 mol% Re₂O₇, 24h.

C-3 Mechanistic investigations

C-3.1 Kinetic data

The kinetic behaviour of the catalytic reaction was determined. For every data point an individual reaction mixture was prepared with a catalyst loading of 0.1 mol% Re_2O_7 in 4 mL *p*-xylene and heated for the corresponding reaction time to 140°C. After given reaction time, the reaction mixture was quickly cooled down by means of an external water bath. The samples were taken following the standard catalytic procedure (see experimental section). The conversion was determined by GC FID.

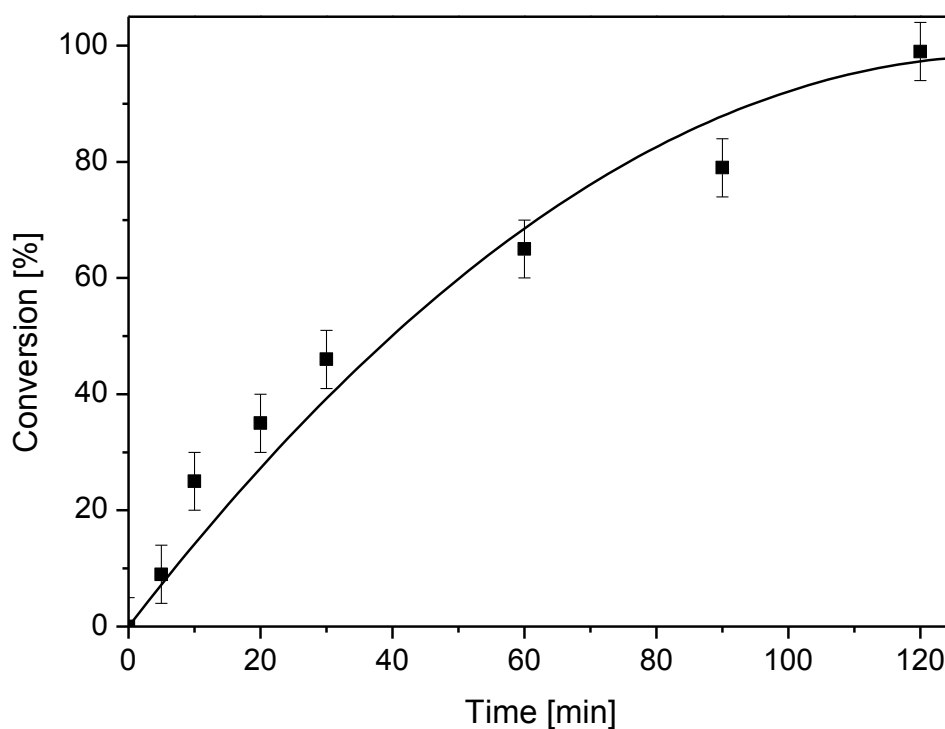
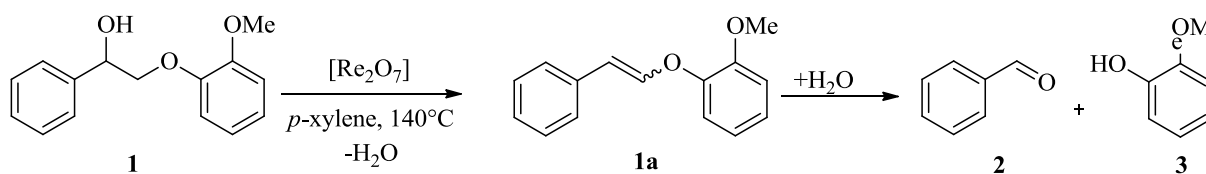


Figure S3. Kinetic profile of the Re_2O_7 -catalysed C–O cleavage reaction of **1**.

C-3.2 Formation of the enol ether intermediate (1a)

Scheme S1: Formation of the enol ether intermediate **1a** during catalysis.

During the reaction of **1** to cleavage products **2** and **3** at 140°C formation and subsequent depletion of an isomeric mixture of olefins (6.64 and 6.62 ppm, *Z*-isomer; 5.72 and 5.77 ppm, *E*-isomer) is observed. The ^1H NMR and GC FID spectra (*vide infra*) was recorded after 30 min reaction time. The identical intermediate **1a** was already isolated and characterised by a recently published work.⁴

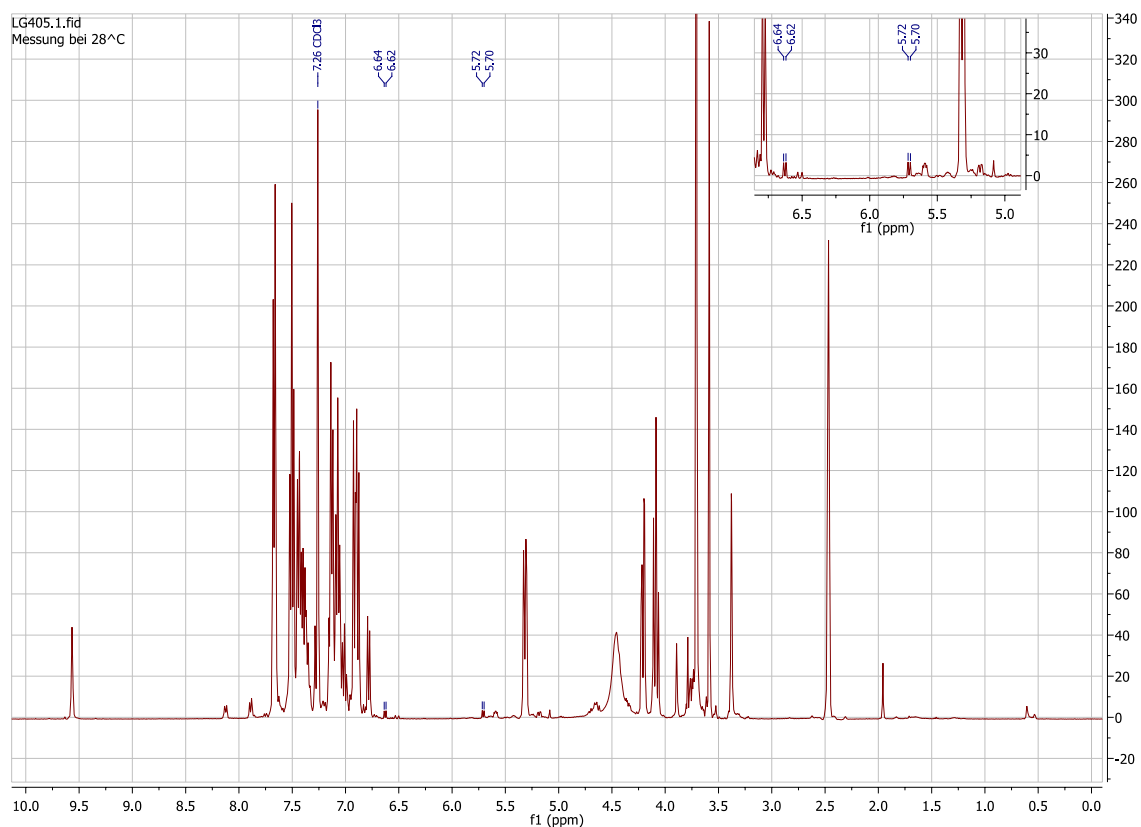


Figure S4. ^1H NMR spectrum (in *p*-xylene- d_{10}) during the catalytic C–O cleavage reaction of **1** measured after 30 min reaction time. The zoom box shows the olefinic signals of **1a**.

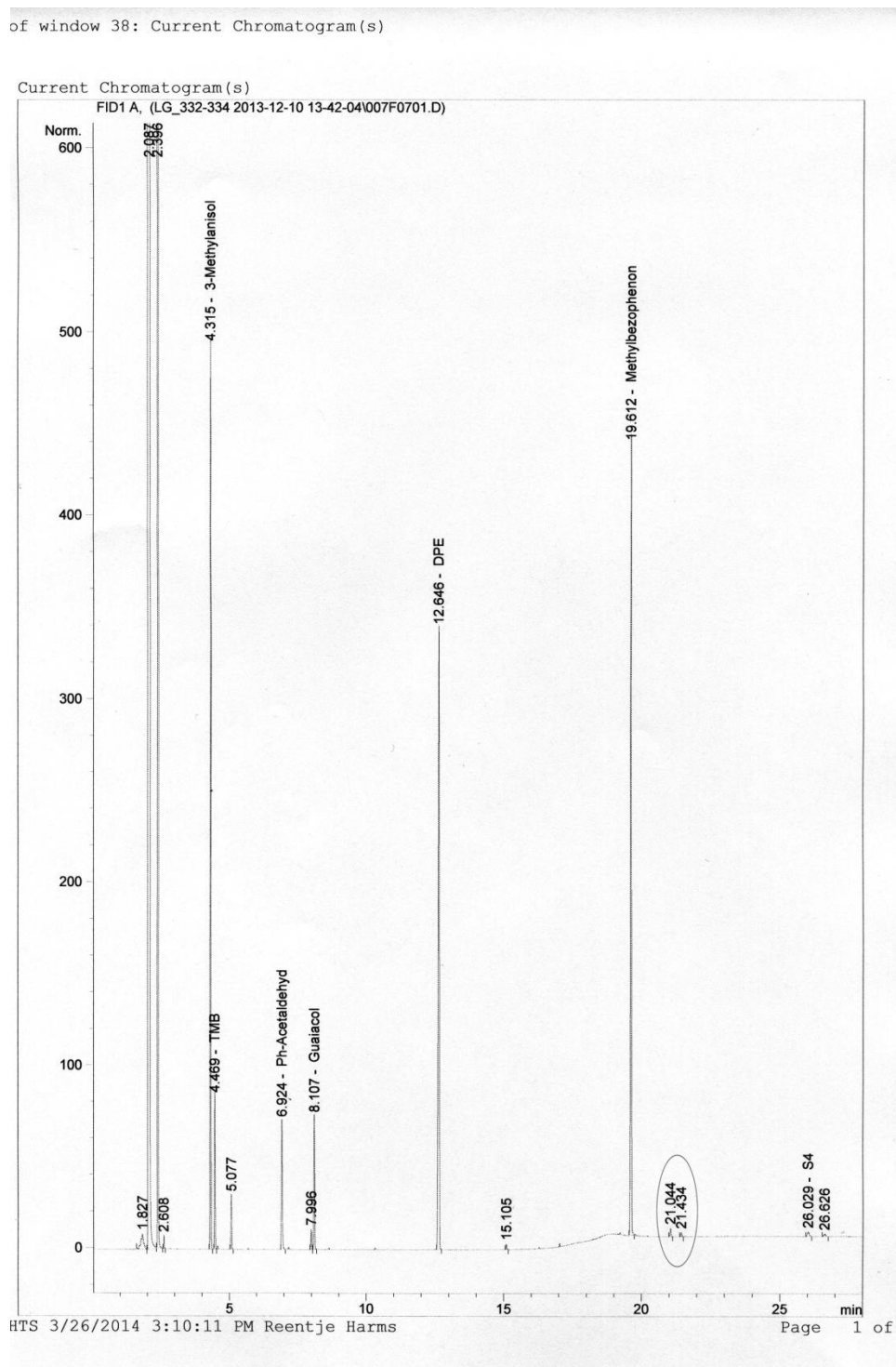


Figure S5. GC FID spectrum shows the olefins at the retention time of 21.04 min and 21.43 min which formed after 30 min reaction time. S4 (26.03 min) represents unconverted substrate **1**.

C-4 Analysis of the inactive decomposed catalyst

C-4.1 EDX Spectra and SEM picture

The related scanning electron microscopy (SEM) picture was recorded on a CamScan CS24 (Compact) and shows an overview of the decomposed catalyst. The black powder is composed by small sized and equally distributed particles; however, a powder XRD analysis exhibited the amorphous character of the solid. The chemical compositions was recorded by energy dispersive X-ray spectroscopy (EDX) using an Oxford Instruments Swift ED.

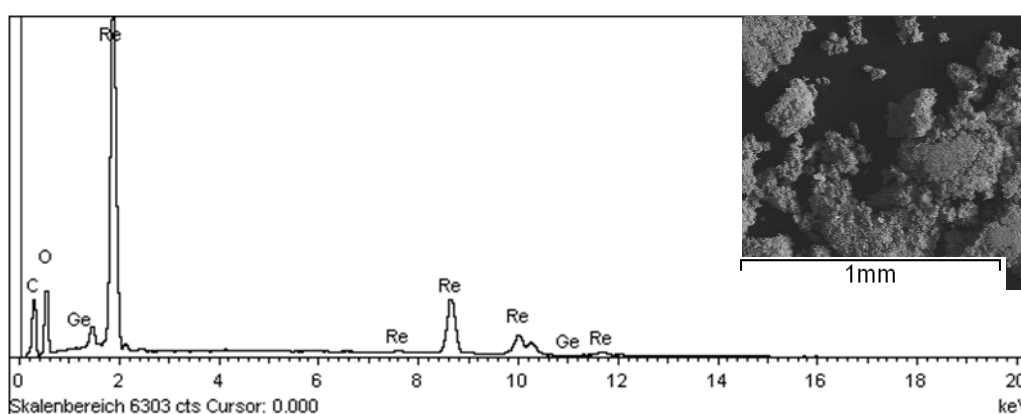


Figure S6. EDX spectrum and SEM picture of the black precipitate, which is obtained as amorphous powder. Analysis data: Re: 54.5%; C: 14.2%; O: 30.8%.

C-4.2 Raman Spectra

The chemical composition was determined by Raman spectroscopy. A Senterra Raman spectrometer (Bruker Corporation, USA), equipped with a 488 nm laser, was used for the analysis of particles produced. A laser power of 1 mW and an integration time of 30 s were chosen for each sample analysis. A baseline correction was accomplished, using the rubber band method, with the software OPUS for each spectrum measured by Raman spectroscopy. Although Re(0) has no active Raman vibration modes, it was measured to exhibit any oxidation of the surface which was found identical with ReO_2 .

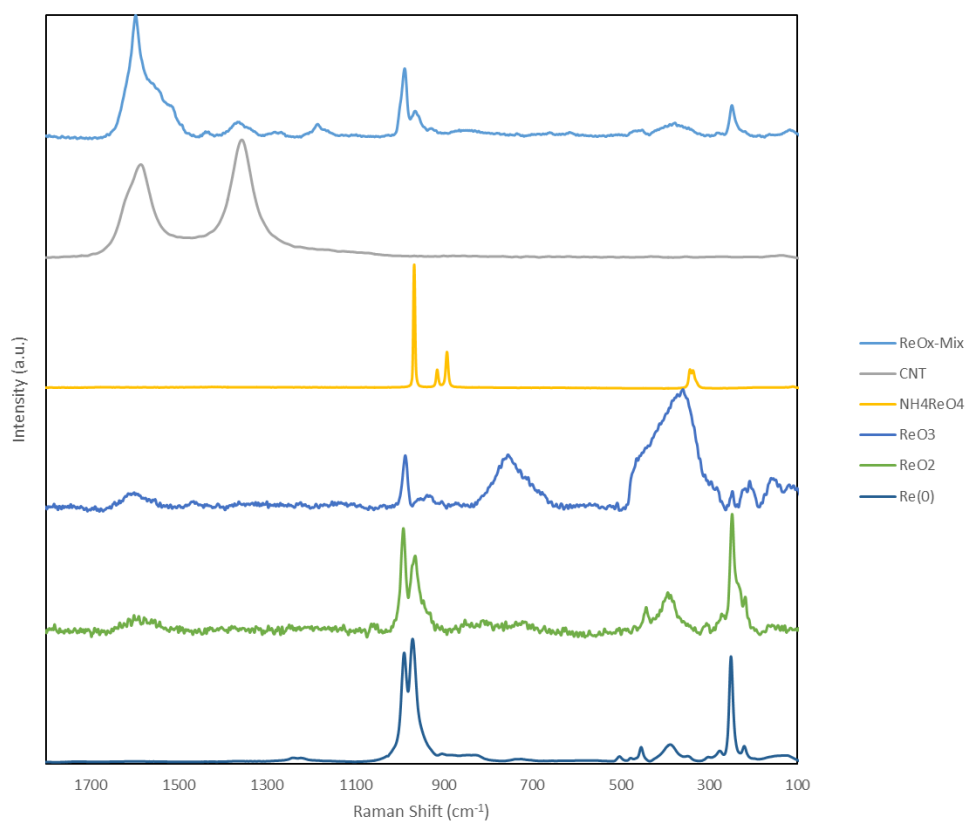


Figure S7. Waterfall diagram of the Raman spectra of the black rhenium precipitate (deactivated catalyst) and the authentic samples of carbon nano tubes (CNT, sp² hybridised), ammonium perrhenate, Re(VI) oxide, Re(IV) oxide and rhenium powder (surficial oxidised).

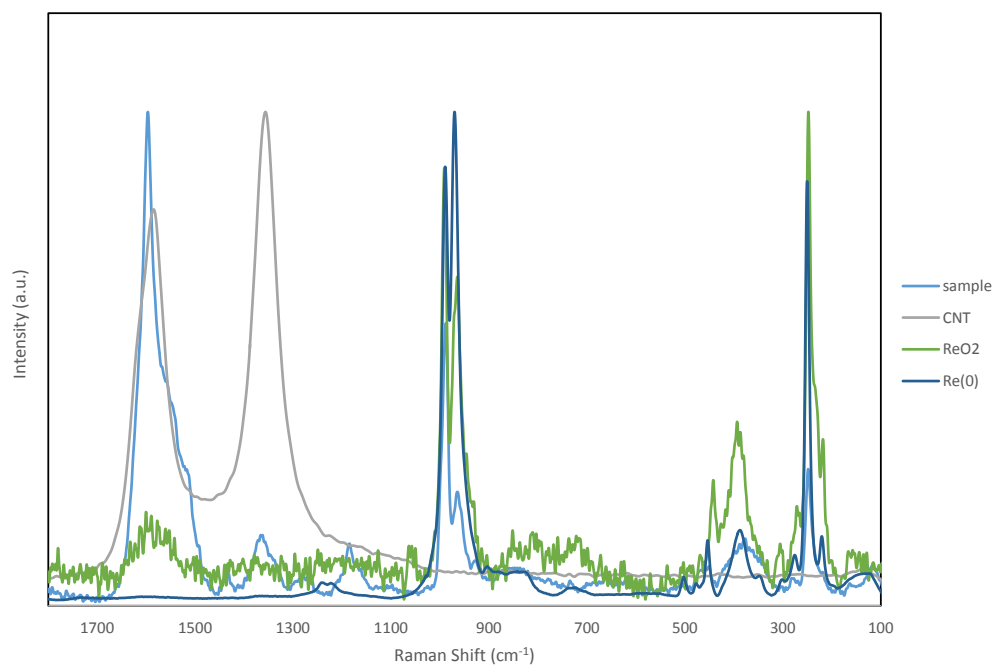


Figure S8. Overlaid Raman spectra of the black rhenium sample, CNT, rhenium(IV) oxide and rhenium powder (surficial oxidised to ReO₄).

C-4.3 XPS

Chemical analysis was accomplished by XPS with a Leybold-Heraeus LHS 10 XPS chamber in ultra-high vacuum (UHV). A non-monochromatized MgK α -source (1253.6 eV) was used to investigate the rhenium precipitate pellets. The samples were sputtered with argon ions to remove the surface layer before measuring at a pressure below 2×10^{-8} mbar. The survey spectrum was recorded with a pass energy of 100 eV, a stepsize of 1 eV and a dwelltime of 0.1 s while the regions of interest were recorded with a pass energy of 20 eV, a stepsize of 0.1 eV and a dwelltime of 0.1 s. As a reference the C1s (-284.5 eV) peak was used and the spectra corrected to compensate charge effects. Since the presence of sp^2 -hybridized carbon was revealed by Raman spectroscopy, the C1s signal was referenced on the literature value of graphite C=C. The Spectra of the Re4d region show significantly higher amounts of rhenium oxides due to the lower escape depth of electrons in this energy range. So a more surfacial insight to the samples chemical composition is given by the scans in the Re4d region compared to the Re4f region.

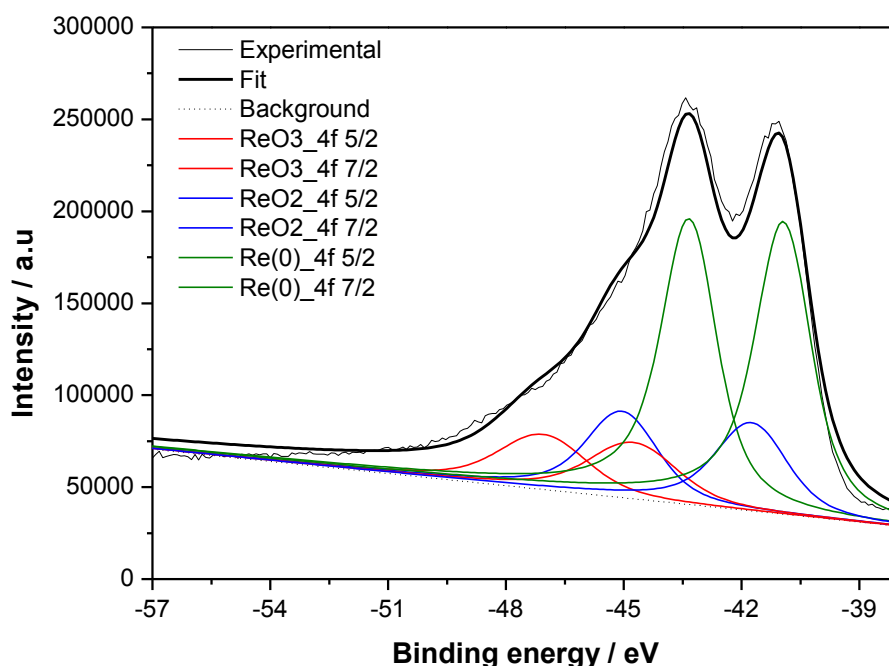


Figure S9. Re4f region narrow scan, fit and deconvolution in three compartments; PE100.

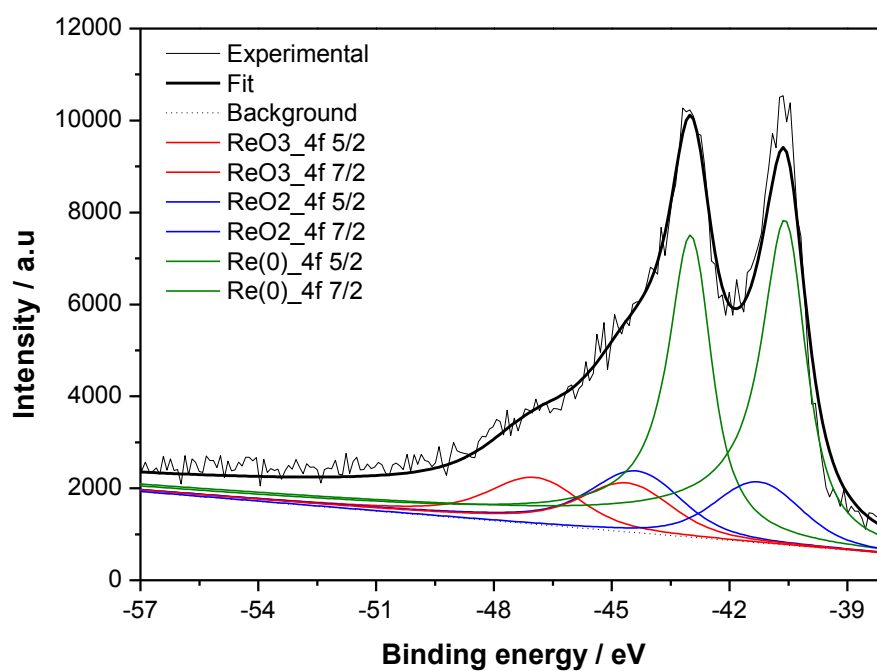


Figure S10. Re4f region narrow scan, fit and deconvolution in three compartments; PE20.

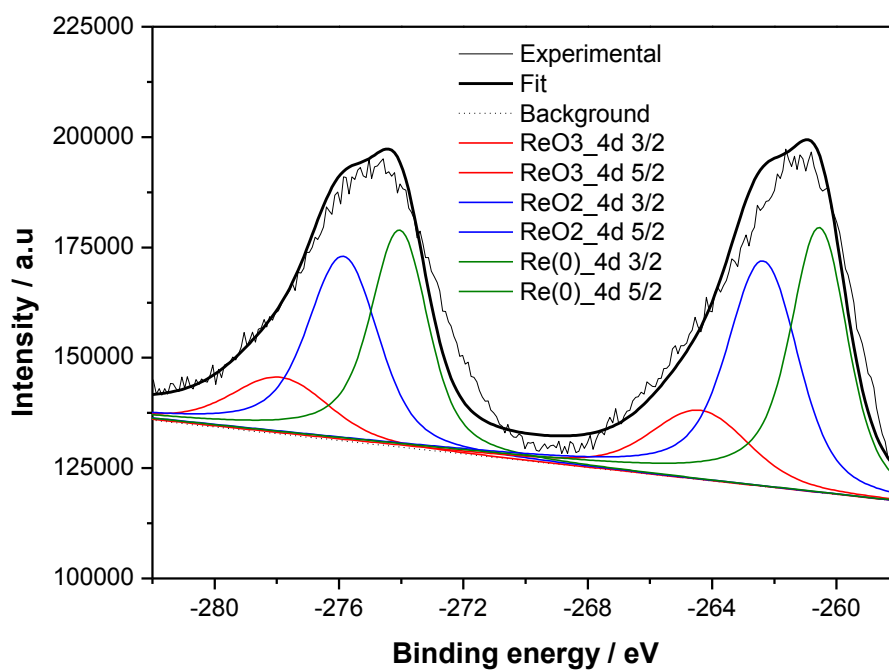


Figure S11. Re4d region narrow scan, fit and deconvolution; PE100.

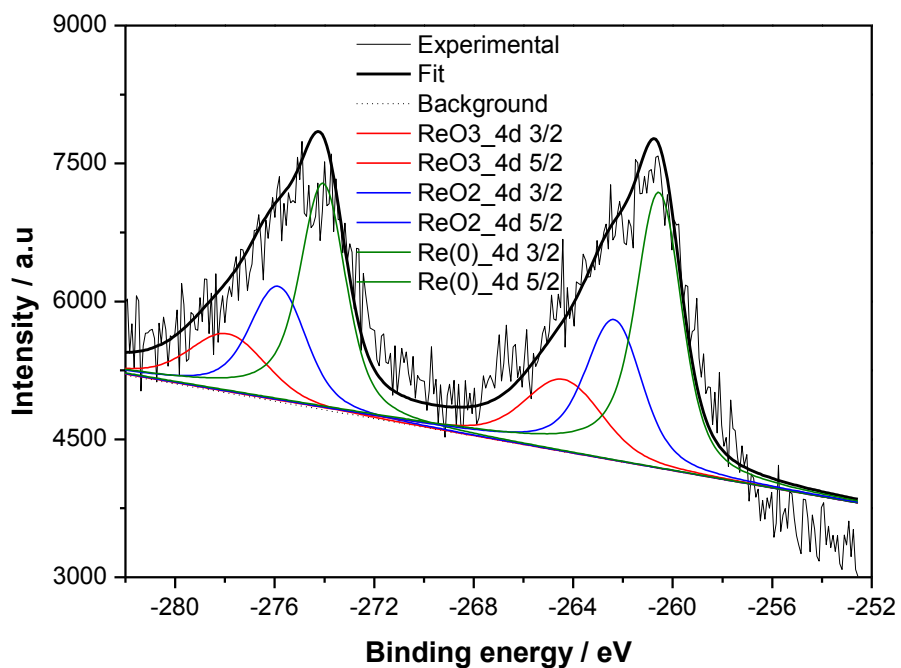


Figure S12. Re4d region narrow scan, fit and deconvolution; PE20.

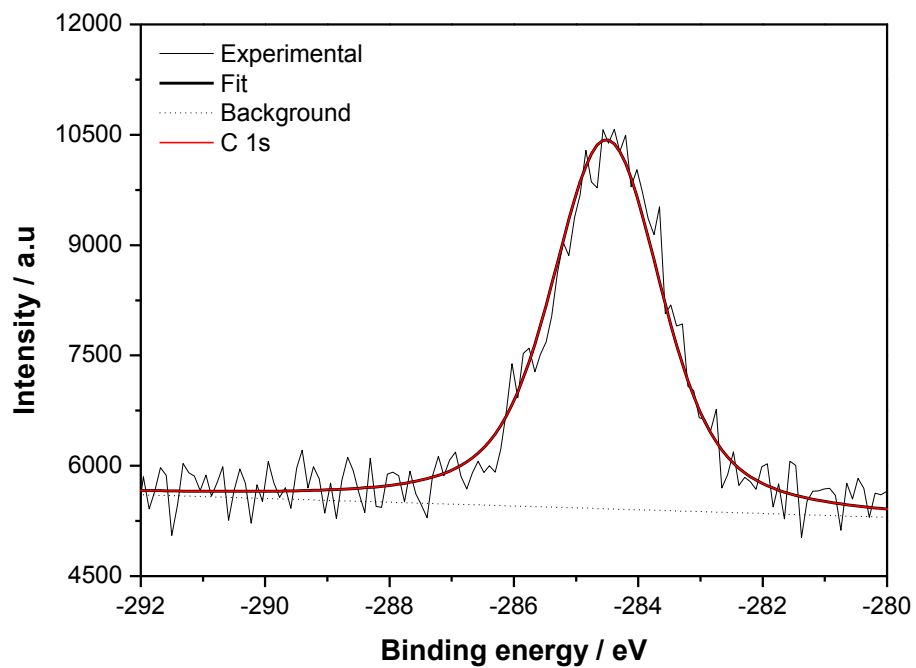


Figure S13. C1s region narrow scan, fit and deconvolution; PE20.

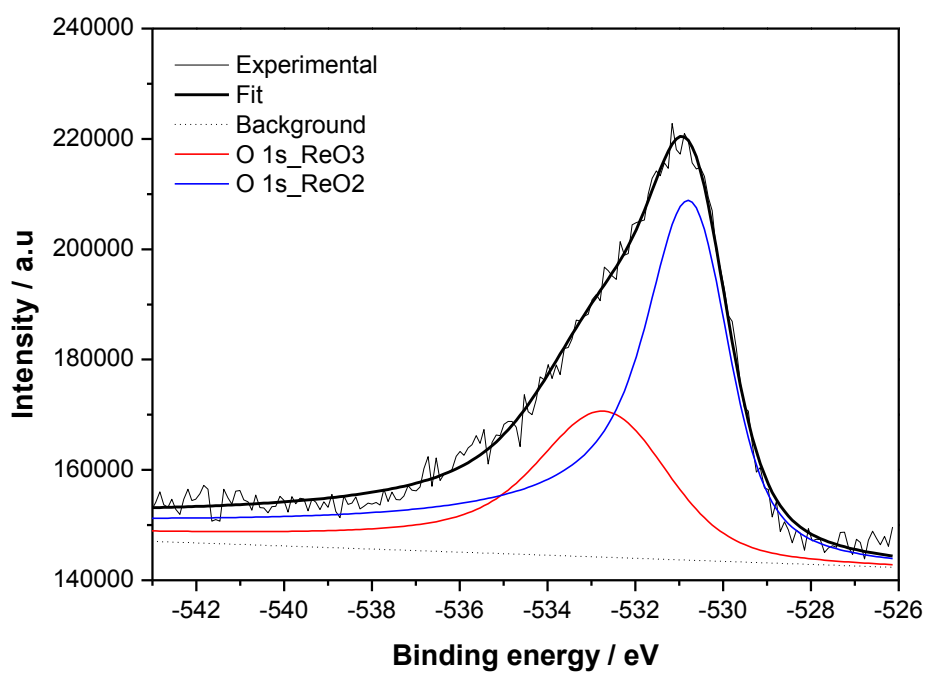


Figure S14. O1s region narrow scan, fit and deconvolution; PE100.

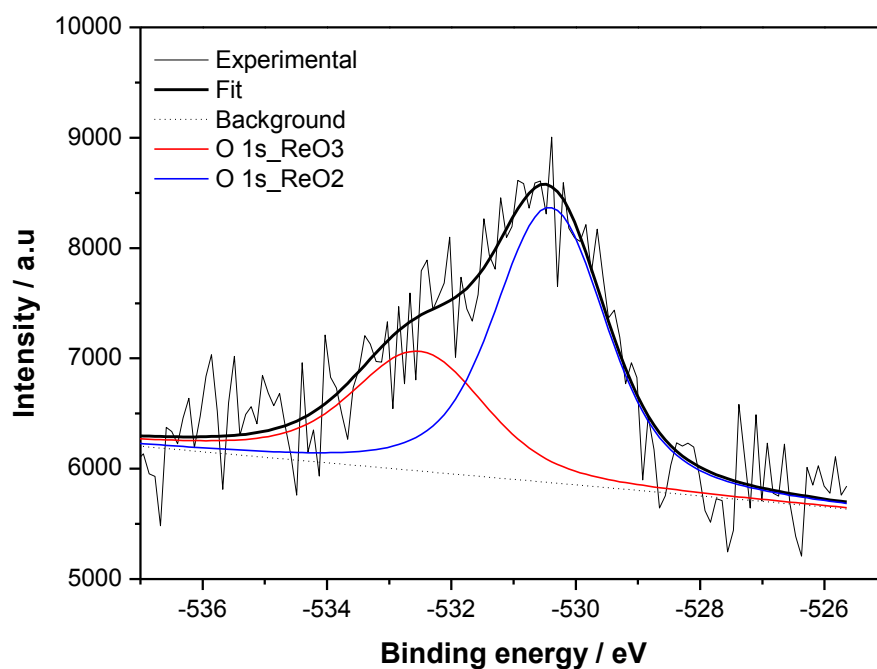


Figure S15. O1s region narrow scan, fit and deconvolution; PE20.

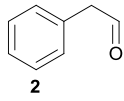
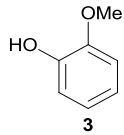
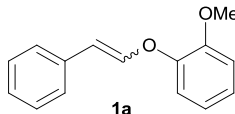
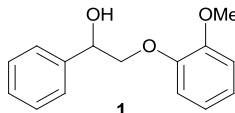
Table S3. Mathematic data sets of all fits, deconvolutions, and peak areas of the Re4f, Re4d, C1s and O1s windows in resolutions of P100 and PE20.

Re4f 100PE												
Peak_Nr	start_E	stop_E	Distance	Incline	Lorentzian	asym	Gaussian	height	energy_pos	area_int	area_rel	area_ges
0	-54.91	-38.13	48605.4	-2196.35	1	0.05	2	58650	-47	101575	0.082	1.24E+06
1	-54.91	-38.13	48605.4	-2196.35	1	0.05	1.5	78200	-45	136910	0.11	1.24E+06
2	-54.91	-38.13	48605.4	-2196.35	1	0.05	2	60000	-44.7	105116	0.085	1.24E+06
3	-54.91	-38.13	48605.4	-2196.35	1	0.05	1	214950	-43.3	377573	0.304	1.24E+06
4	-54.91	-38.13	48605.4	-2196.35	1	0.05	1.5	80000	-41.7	139726	0.112	1.24E+06
5	-54.91	-38.13	48605.4	-2196.35	1	0.05	1	220000	-40.9	381229	0.307	1.24E+06
Re4f 20PE												
Peak_Nr	start_E	stop_E	Distance	Incline	Lorentzian	asym	Gaussian	height	energy_pos	area_int	area_rel	area_ges
0	-53.41	-37.63	1208.93	-70.5949	1	0.1	2	1900	-46.83	3911.29	0.076	51329.1
1	-53.41	-37.63	1208.93	-70.5949	1	0.1	2	2500	-44.24	5243.06	0.102	51329.1
2	-53.41	-37.63	1208.93	-70.5949	1	0.1	2	1982.43	-44.49	4151.75	0.081	51329.1
3	-53.41	-37.63	1208.93	-70.5949	1	0.1	0.5	7327.98	-42.94	15460	0.301	51329.1
4	-53.41	-37.63	1208.93	-70.5949	1	0.01	2	2692.32	-41.26	4135.6	0.081	51329.1
5	-53.41	-37.63	1208.93	-70.5949	1	0.133	0.5	7800.5	-40.52	18427.4	0.359	51329.1
Re4d 100PE												
Peak_Nr	start_E	stop_E	Distance	Incline	Lorentzian	asym	Gaussian	height	energy_pos	area_int	area_rel	area_ges
0	-281.88	-258.07	132626.3	-762.5619	1	0.05	3	32800	-277.8	54025.93	0.071	765900.8
1	-281.88	-258.07	132626.3	-762.5619	1	0.05	2	81900	-275.8	140326.5	0.183	765900.8
2	-281.88	-258.07	132626.3	-762.5619	1	0.05	3	40000	-264.3	72400.14	0.095	765900.8
3	-281.88	-258.07	132626.3	-762.5619	1	0.05	1.5	81900	-274	142990.8	0.187	765900.8
4	-281.88	-258.07	132626.3	-762.5619	1	0.05	2	100000	-262.3	180112.3	0.235	765900.8
5	-281.88	-258.07	132626.3	-762.5619	1	0.05	1.5	100000	-260.5	176045.2	0.23	765900.8
Re4d 20PE												
Peak_Nr	start_E	stop_E	Distance	Incline	Lorentzian	asym	Gaussian	height	energy_pos	area_int	area_rel	area_ges
0	-281.38	-254.47	4999.184	-47.20811	1	0.05	3	1640	-277.8	2659.023	0.082	32272.16
1	-281.38	-254.47	4999.184	-47.20811	1	0.05	2	2460	-275.8	4192.755	0.13	32272.16
2	-281.38	-254.47	4999.184	-47.20811	1	0.05	3	2000	-264.3	3647.952	0.113	32272.16
3	-281.38	-254.47	4999.184	-47.20811	1	0.05	1.5	4100	-274	7138.463	0.221	32272.16
4	-281.38	-254.47	4999.184	-47.20811	1	0.05	2	3000	-262.3	5488.208	0.17	32272.16
5	-281.38	-254.47	4999.184	-47.20811	1	0.05	1.5	5000	-260.5	9145.761	0.283	32272.16
C1s 20PE												
Peak_Nr	start_E	stop_E	Distance	Incline	Lorentzian	asym	Gaussian	height	energy_pos	area_int	area_rel	area_ges
0	-292.6	-281.38	5415.09	-25.5675	1	0.01	1.464	8495.35	-284.5	12732.4	1	12732.4
O1s 100PE												
Peak_Nr	start_E	stop_E	Abstand	Steigung	Lorentzian	asym	Gaussian	height	energy_pos	area_int	area_rel	area_ges
0	-543.11	-526.14	144121	-278.643	1	0.136	2.665	56004.7	-532.5	127186	0.333	382021
1	-543.11	-526.14	144121	-278.643	1	0.187	1.399	94200.7	-530.6	254834	0.667	382021
O1s 20PE												
Peak_Nr	start_E	stop_E	Distance	Incline	Lorentzian	asym	Gaussian	height	energy_pos	area_int	area_rel	area_ges
0	-537.59	-525.64	5976.68	-50.0007	1	0.05	1.856	-2031.48	-532.46	3381.36	0.345	9796.54
1	-537.59	-525.64	5976.68	-50.0007	1	0	1.512	-4327.74	-530.41	6415.18	0.655	9796.54

C-5 Product identification and NMR spectra

C-5.1 Retention times and NMR data

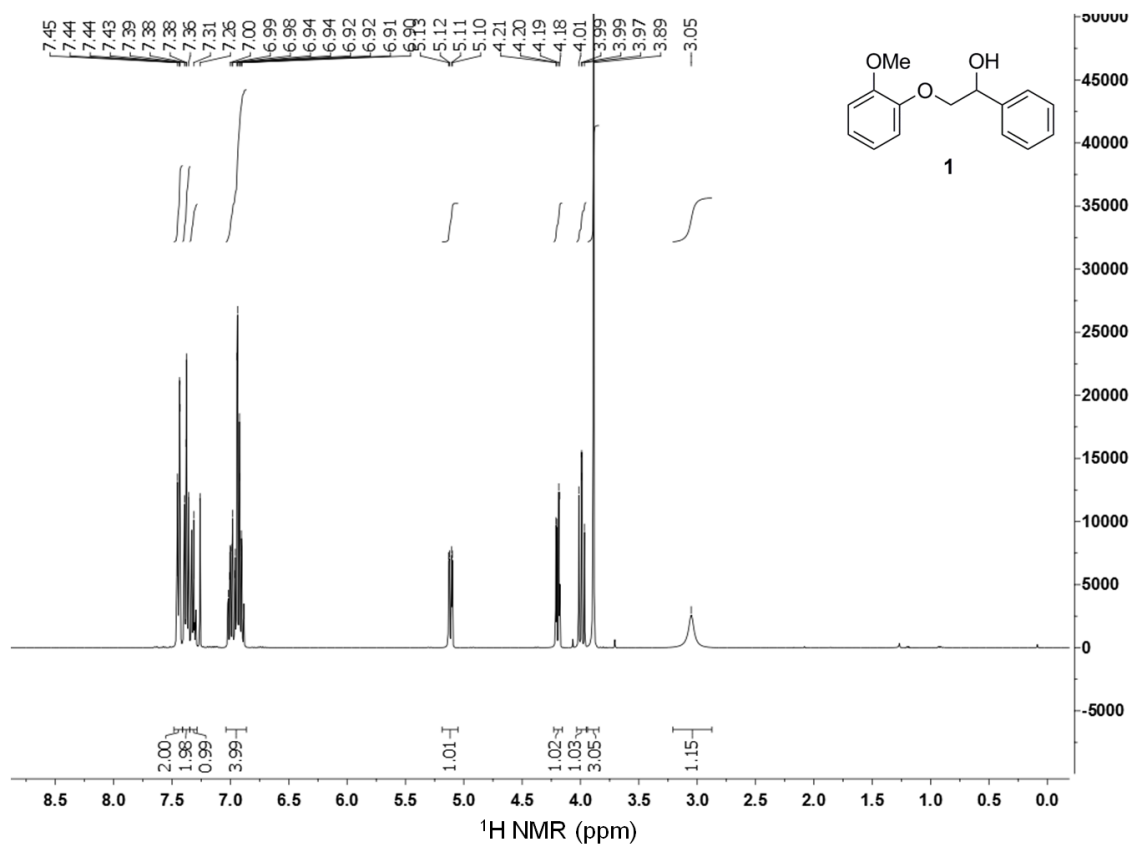
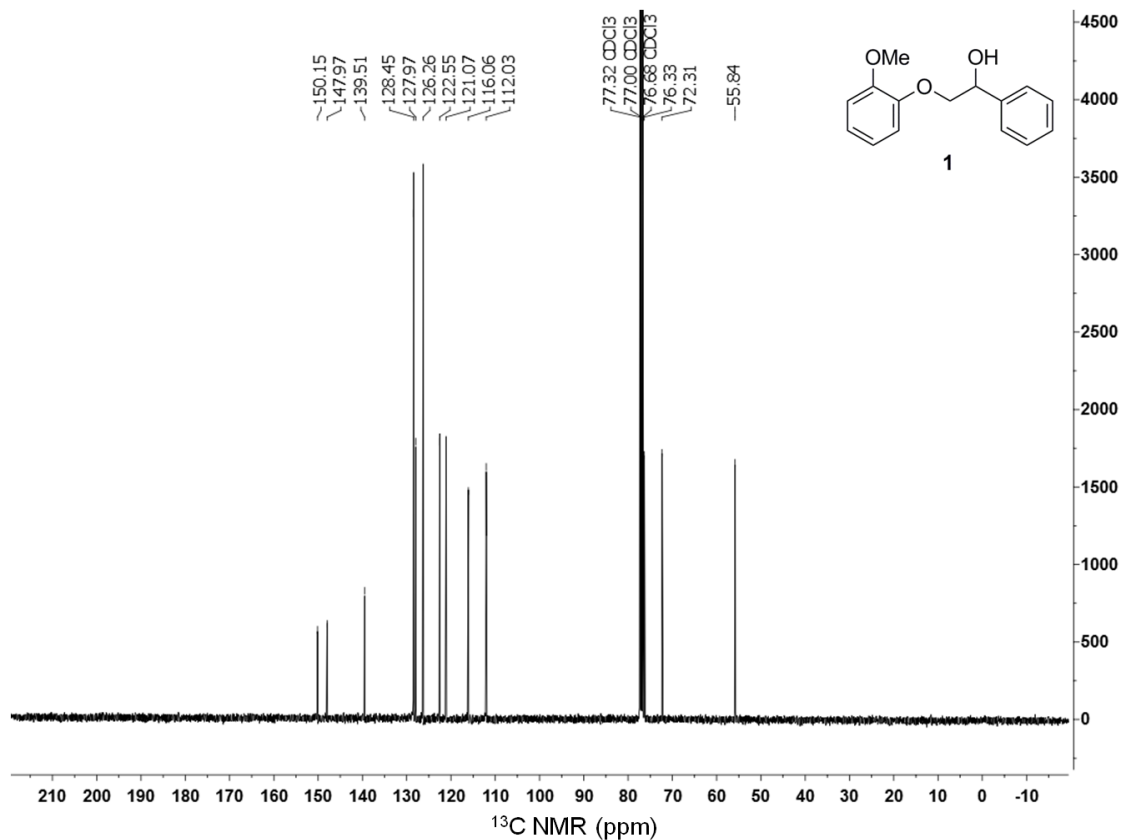
Table S4. Analytical data of observed cleavage products

Product	Structure	GC retention time [min]	NMR data	Other analysis
Phenylacet-aldehyde		6.92	¹ H-NMR (400 MHz, <i>p</i> -xylene-d ₁₀) δ (ppm) = 9.22 (t, ³ J = 2.4 Hz; 1H), 7.08–6.98 (m, 3H), 6.80–6.78 (m, 2H), 3.02 (d, ³ J = 2.4 Hz; 2H).	A, B
Guaiacol		8.11	¹ H-NMR (400 MHz, CDCl ₃) δ (ppm) = 6.98–6.84 (m, 4H), 5.61 (s, 1H), 3.89 (s, 3H). ¹ H-NMR (400 MHz, <i>p</i> -xylene-d ₁₀) δ (ppm) = 6.93–6.89 (m, 1H), 6.73 (ddd, ³ J = 7.8 Hz, ⁴ J = 1.5 Hz; 1H), 6.65 (ddd, ³ J = 7.8 Hz, ⁴ J = 1.5 Hz; 1H), 6.42 (d, ³ J = 8.0 Hz; 1H), 5.40 (d, 1H), 3.23 (s, 3H).	A, B
(<i>E/Z</i>)-1-Methoxy-2-(styroloxy)-benzene		21.04 / 21.43	¹ H-NMR (400 MHz, CDCl ₃) δ (ppm) = 7.75–7.70 (m, 2 H, (<i>Z</i> -isomer)), 7.36– 7.26 (m, 3H), 7.23–7.05 (m, 4H), 7.01–6.91 (m, 3H), 6.54 (d, ³ J = 6.9 Hz; 1 H, (<i>Z</i> -isomer)), 6.32 (d, ³ J = 12.4 Hz; 0.3 H, (<i>E</i> -isomer)), 5.58 (d, ³ J = 6.9 Hz; 1 H, (<i>Z</i> -isomer)), 3.90 (s, 4 H, (<i>Z</i> - and <i>E</i> -isomer)). ¹ H-NMR (400 MHz, <i>p</i> -xylene-d ₁₀) δ (ppm) = 7.78 (m, 2H), 6.28 (d, ³ J = 6.9 Hz; 1 H, (<i>Z</i> -isomer)), 6.17 (d, ³ J = 12.4 Hz; 1 H, (<i>E</i> -isomer)), 5.36 (d, ³ J = 6.9 Hz; 1 H, (<i>Z</i> -isomer)).	A, B
2-Phenoxy-phenylethanol		26.03	¹ H-NMR (400 MHz, <i>p</i> -xylene-d ₁₀) δ (ppm) = 7.37–7.30 (m, 2H), 7.20–7.12 (m, 2H), 7.12–7.06 (m, 1H), 6.82–6.69 (m, 2H), 6.59–6.50 (m, 2H), 5.00 (dd, 3J = 9.0, 3.2 Hz; 1H), 4.11 (s, 1H), 3.86 (dd, 3J = 7.6 Hz, 2J = 9.6 Hz; 1H), 3.76 (m-dd, 3J = 9.0 Hz, 2J = 9.6 Hz; 1H), 3.34 (s, 3H).	A, B

A) GC-MS and GC-FID analysis (retention time, mass spectra) matched with the authentic sample.

B) The product peaks in ¹H-NMR spectrum of the reaction mixture were in agreement with the ¹H-NMR spectra of the authentic sample in CDCl₃ (literature value or sample prepared).

C-5.2 Selected NMR spectra

Figure S16. ¹H NMR spectrum of model compound 1 in CDCl₃.Figure S17. ¹³C NMR spectrum of model compound 1 in CDCl₃.

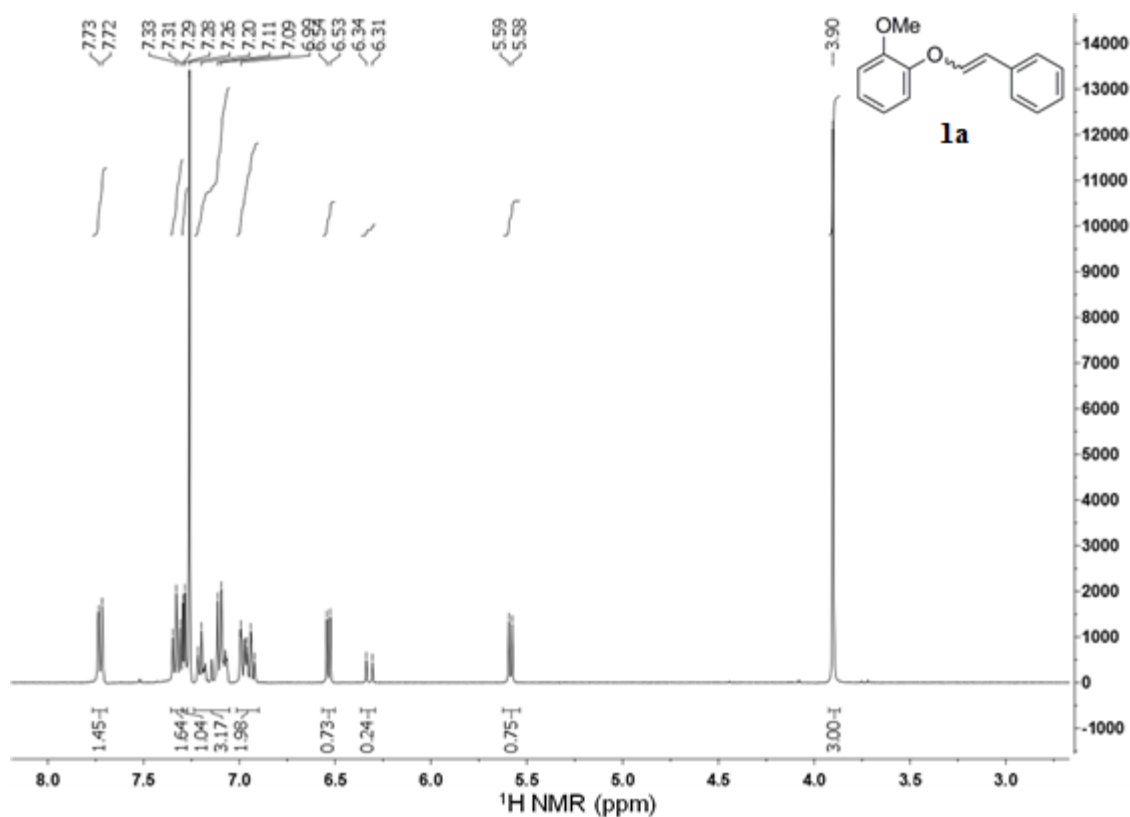


Figure S18. ^1H NMR spectrum of the isolated mixture of **1a** in CDCl_3 . The signals are shifted to low field compared to those sample measured in *p*-xylene.

C-6 References

1. G. Brauer, ed., *Handbuch der präparativen anorganischen Chemie*, F. Enke Verlag, Stuttgart, 1978.
2. J. M. Nichols, L. M. Bishop, R. G. Bergman and J. A. Ellman, *J. Am. Chem. Soc.*, 2010, **132**, 12554-12555.
3. P. H. Kandanarachchi, T. Autrey and J. A. Franz, *J. Org. Chem.*, 2002, **67**, 7937-7945.
4. R. G. Harms, I. I. E. Markovits, M. Drees, W. A. Herrmann, M. Cokoja and F. E. Kühn, *ChemSusChem*, 2014, **7**, 429-434.

8. List of Publications, Talks and Poster Presentations

Talks, Conferences and Poster Presentations

- April 2013 **245th American Chemical Society National Meeting & Exposition**
New Orleans, LA (USA)
Talk: „C–O Bond Cleavage in Lignin Model Compounds in Homogeneous Phase”
- March 2013 **46th Annual Meeting of German Catalysis Experts**
Weimar (Germany)
Talk: “C–O bond cleavage in lignin model compounds by molecular catalysts“
- September 2012 **15th International Conference on Organometallic Chemistry**
Lisbon (Portugal)
Poster presentation and flash talk: „CNC Pincer Ruthenium Complexes“
- July 2012 **15th International Conference on Catalysis**
Munich (Germany)
Poster presentation “Rutheniumhydrides and application in C–O Bond Cleavage”
- March 2012 **45th Annual Meeting of German Catalysis**
Weimar (Germany)

Publications and Book Contributions

- 1) **R. G. Harms**, L. Graser, S. Schwaminger, W. A. Herrmann, F. E. Kühn, "*Re₂O₇ in C–O bond cleavage of a β–O–4 lignin model linkage: A highly active Lewis acidic catalyst in heterogeneous phase*", in preparation.
- 2) M. Rahmel, **R. G. Harms**, "The '3 Rs' in homogeneous catalysis", *SpecChemOnline* **2015**, February
- 2) **R. G. Harms**, W. A. Herrmann, F. E. Kühn, "Organorhenium Dioxides as Oxygen Transfer Systems: Synthesis, Reactivity and Applications", *Coord. Chem. Rev.* **2015**, 296, 1–23. <http://dx.doi.org/10.1016/j.ccr.2015.03.015>
- 3) **R. G. Harms**, I. I. E. Markovits, M. Drees, W. A. Herrmann, M. Cokoja, F. E. Kühn, "Cleavage of C–O Bonds in Lignin Model Compounds Catalyzed by Methyl-dioxorhenium in Homogeneous Phase", *ChemSusChem* **2014**, 7, 429–434. <http://dx.doi.org/10.1002/cssc.201300918>.
- 4) Book Contribution in: "*Catalysis from A to Z: A concise Encyclopedia*", eds. W. A. Herrmann and B. Cornils, 4th edition **2013**, Wiley-VCH: Weinheim.